The role of Hmgcs2-mediated ketogenesis in non-alcoholic fatty liver disease development and treatment

By: Shaza Asif

A thesis submitted to the Faculty of Graduate and Postdoctoral Studies as a requirement for the MSc degree in Cellular and Molecular Medicine

Department of Cellular and Molecular Medicine

Faculty of Medicine

University of Ottawa

ABSTRACT

Non-alcoholic fatty liver disease (NAFLD), described by the build-up of excess fat in the liver, is the most prevalent chronic liver condition globally. One of the essential metabolic functions of the liver is the production of ketone bodies, a process called, ketogenesis. Ketone bodies serve as alternative fat-derived sources of fuel for tissues under conditions of nutrient deficit (i.e., fasting). Interestingly, recent studies have found that ketogenesis is dysregulated in NAFLD patients. Similarly, we also found that high-fat diet-induced NAFLD mice exhibited diminished fasting-induced ketogenesis with reduced expression of liver Hmgcs2, the rate-limiting enzyme of ketogenesis. To understand the role of ketogenesis in NAFLD pathogenesis and treatment, we generated mouse models of ketogenic insufficiency and activation through *Hmgcs2* loss- and gain-of-function, respectively. Notably, a change in dietary environment rescued the fatty liver phenotype of *Hmgcs2* knockout mice and increased ketogenic function through *HMGCS2* overexpression improved NAFLD-associated metabolic dysfunction and hepatosteatosis in adult mice. Furthermore, an untargeted metabolomics approach provided a comprehensive metabolic view underlying *HMGCS2* overexpression-mediated NAFLD improvement, suggesting that hepatic ketogenesis impacts liver metabolism via regulation of other metabolic pathways. Together, our study adds new knowledge to the field of ketone body metabolism and suggests a viable therapeutic strategy involving ketogenesis activation in the prevention and treatment of NAFLD.

ACKNOWLEDGEMENTS

I would like to begin by conveying my sincerest gratitude to my supervisor Dr. Kyoung-Han Kim for allowing me to purse an MSc in his lab and for supporting and mentoring my work throughout the years. Thank you for the extraordinary learning experience and opportunity to grow and develop my knowledge and skills as a scientist. To that end, I would like to thank the past and present members of the lab with whom I had the absolute pleasure of working with: Nia Kang, Elayna Tian, Matthew Lynn, Woosol Yoo, Saif Dababneh, Hyejin Lee, Thet Fatica, Yena Oh and Dr. Riyoun Kim. Thank you for providing an enjoyable environment to conduct research in. I would like to specifically thank Yena Oh for always being on hand to help and answer any lab-related questions and for being a great support throughout the course of my degree. Thank you for the laughter, fun and memories. I would also like to extend special acknowledgements to Dr. Riyoun Kim, for her indispensable guidance and training on this project, without whom this project would not have been possible.

I wish to acknowledge my wonderful thesis advisory committee members Dr. Erin Mulvihill, Dr. Morgan Fullerton, and Dr. Ryan Russell for providing valuable direction and feedback on the development of my project.

Lastly, and most importantly, I would like to extend my deepest appreciation to my parents, Rubina Asif and Asif Mehmood; sister, Sara Asif; brother, Abdullah Asif, grandparents and extended family in Pakistan, and friends for their unwavering love and support. Thank you for always believing in me and my work, and for encouraging me to stay positive when times were hard.

Without the acknowledged, this thesis would not have been possible – thank you for everything.

TABLE OF CONTENTS

LIST OF ABBREVIATIONS

AcAc: Acetoacetate

ACS: Acyl-CoA synthase

ANOVA: Analysis of variance

ASO: Antisense oligonucleotide

AUC: Area under the curve

BDH1: D-3-hydroxybutyrate dehydrogenase 1

β-OHB: β-hydroxybutyrate

CAT: Carnitine acetyltransferase

CoA: Coenzyme A

COT: Carnitine octanoyltransferase

CPT: Carnitine palmitoyltransferase

DNL: *de novo* lipogenesis

ER: Endoplasmic reticulum

FAO: Fatty acid oxidation

FFA: Free fatty acids

FOXA2: Forkhead box A2

GTT: Glucose tolerance test

H&E: Hematoxylin & Eosin

HCC: Hepatocellular carcinoma

HET: Heterozygous

HFD: High-fat diet

HMGCS2: 3-hydroxymethylglutaryl-CoA synthase 2

HMGCL: HMG-CoA lyase

IF: Intermittent fasting

ITT: Insulin tolerance test

KO: Knockout

LCFA: Long-chain fatty acid

LC-MS: Liquid chromatography mass spectrometry

MCFA: Medium-chain fatty acid

mHS: Mitochondrial HMGCS2 deficiency

mHL: Mitochondrial HMGCL deficiency

NAFLD: Non-alcoholic fatty liver disease

NASH: Non-alcoholic steatohepatitis

OE: Overexpression

P: Postnatal day

PBS: Phospho-buffered saline

PLIN2: Perilipin 2

PNPLA3: Patatin-like phospholipase domain-containing 3

PPAR: Peroxisome proliferator-activated receptor

PPP: Pentose phosphate pathway

PSR: Picrosirius red

qPCR: Quantitative polymerase chain reaction

ROS: Reactive oxygen species

RT: Room temperature

RXR: Retinoid X receptor

SCFA: Short-chain fatty acid

SCOT: Succinyl-CoA:3-oxacid CoA transferase

T2D: Type 2 diabetes

TCA: Tricarboxylic acid

TM6SF2: Transmembrane 6 superfamily member 2

VLCFA: Very long-chain fatty acid

VLDL: Very low-density lipoproteins

WT: Wild-type

LIST OF FIGURES

LIST OF TABLES

INTRODUCTION

1.1. Non-alcohol fatty liver disease (NAFLD)

1.1.1. NAFLD Characteristics

Non-alcoholic fatty liver disease (NAFLD) is pathologically characterized by the abnormal and excessive accumulation of intracellular lipids in hepatocytes, in the absence of excessive alcohol consumption. NAFLD is driven by multiple factors, including lifestyle, genetics (i.e., PNPLA3) and other metabolic conditions (i.e., diabetes, obesity). If not managed or treated, NAFLD can rapidly progress to a more severe form of non-alcoholic steatohepatitis (NASH), associated with increased metabolic dysfunction, inflammation, fibrosis, and a greater risk of progression to the irreversible stages of cirrhosis, liver failure, and hepatocellular carcinoma (HCC). Whereas NAFLD is mainly characterized by simple steatosis, NASH is identified by severe hepatic cell injury[1]. NAFLD often presents with other metabolic complications, including obesity, hypertension, hyperglycemia, and dyslipidemia, which serve as risk factors in the development of cardiovascular disease, stroke and type 2 diabetes (T2D)[2].

NAFLD is the most common chronic liver condition in the world, with an approximate global prevalence of 25%[3,4]. Specifically, the incidence of NAFLD has been reported to be 20-30% in western countries and 5-18% in Asian countries. NAFLD is also more prevalent in the male population, in which its occurrence increases from youth to middle age, with a decline after the age of 50. While, the opposite is seen in the female population, in which the incidence only begins to increase after the age of 50 and peaks at 60-69 years of age, indicating a protective pre-menopausal effect against NAFLD. NASH, however, presents more severely in females than in males. Interestingly, fatty liver can begin as early as in utero for infants born to obese mothers with gestational diabetes and continues to be the most common liver abnormality in children between the ages of 2-19 years, with one-third of obese children presenting with NAFLD[1].

The increase in dietary negligence and sedentary lifestyle promotes the rise in NAFLD cases every year. In particular, the western diet, high in fats, largely contributes to the development of metabolic syndromes and its progression to NAFLD. The presence of coexisting metabolic comorbidities (i.e., T2D, obesity) also increases the incidence of NAFLD within certain populations. Specifically, patients with T2D have a 2-4-fold higher risk of developing NAFLD[5], and in comparison, to non-diabetic individuals have ~80% greater liver fat content[6]. Additionally, one study showed the prevalence of NAFLD to be ~70% in the type 2 diabetic population[7]. While, in obese individuals, the incidence of NAFLD was found to be 10% greater in comparison to lean individuals[8]. This obese population showed varying manifestations of NAFLD, with approximately 60% presenting with steatosis, 20-25% with NASH, and 2-3% with cirrhosis[9]. However, this is not to say that in the absence of these metabolic abnormalities, NAFLD is nonexistent, as a substantial portion of non-obese or lean individuals are diagnosed with NAFLD and have been associated with a worse prognosis, despite having a healthier metabolic profile in comparison to obese NAFLD patients[10]. Interestingly, in contrast to the obese NAFLD patients, lean NAFLD patients are generally young and female, suggesting vast differences in their clinical manifestation and likely pathology[8]. The work of this thesis will focus on obesity-associated NAFLD.

1.1.2. NAFLD genetics

Various genome-wide association studies have revealed genetic components to the development of NAFLD. Genes associated with NAFLD have been classified into seven different categories; (1) hepatic lipid export and oxidation in steatosis (*PNPLA3*, *TM6SF2*, *NRqI2*, *PPARA*, *PEMT*, *MTTP*, *APOC3*, and *APOE*); (2) glucose metabolism and insulin resistance (*ENPP1*/*IRS1*, *GCKR*, *SLC2A1*, *GOAT*, *TCF7L2* and *PPARG*); (3) steatosis-hepatic lipid import or synthesis

(*SLC27A5*, *FADS1* and *LPIN1*); (4) steatohepatitis-oxidative stress (*HFE*, *GCLC*/*GCLM*, *ABCC2*, and *SOD2*); (5) steatohepatitis-endotoxin response (*TLR4* and *CD14*); (6) cytokines (*TNF* and *IL6*) and (7) fibrosis (*AGTR1* and *KLF6*)[1]. Specifically, small nucleotide polymorphisms (SNPs) of the patatin-like phospholipase domain-containing 3 (*PNPLA3*) and transmembrane 6 superfamily member 2 (*TM6SF2*) gene serve as the major genetic determinants of NAFLD susceptibility and progression and are involved in the regulation of liver fat metabolism[2,11].

1.1.3. NAFLD Pathogenesis

A two-hit hypothesis was initially proposed in the pathogenesis of NAFLD. The first hit was described as the intrahepatic build-up of lipids, which increased the liver's vulnerability to secondary hits, including insulin resistance, inflammation, and fibrosis. However, it was disputed whether inflammation and insulin resistance precede or succeed fat accumulation in NAFLD. Thus, the two-hit hypothesis has since been replaced by a multiple-hit hypothesis in which several factors act simultaneously rather than sequentially in the progression of NAFLD and involve extra-hepatic players, such as brain hormonal regulation, gut microbiome, adipose lipolysis and cytokine secretion[12].

Insulin resistance is a major contributor to the progression of NAFLD to NASH, promoting increased hepatic *de novo* lipogenesis (DNL) and decreased adipose tissue lipolysis and resulting in high levels of free fatty acids (FFAs) in the liver. Additionally, excess hepatic triglyceride content results in endoplasmic reticulum (ER) stress, mitochondrial dysfunction, and a build-up of reactive oxygen species (ROS). ER stress essentially leads to the development of insulin resistance, the turning point of NAFLD to NASH[1]. It is important to note that insulin resistance can present as increased circulating levels of insulin, increased hepatic

gluconeogenesis, impaired glucose uptake by muscle and/or increased release of FFAs and inflammatory cytokines from adipose tissue, all of which serve to promote the progression of hepatic steatosis[2].

Steatosis within NAFLD can take on two forms; macrovesicular steatosis in which large lipid droplets occupy the cytoplasm and often dislodge the nucleus to the periphery and microvesicular steatosis in which myriads of tiny, small lipid droplets form a patchy/foamy distribution within the cytoplasm and allow the nucleus to remain in its original central location within the cell[1]. Macrovesicular steatosis, the more prevalent form, has been associated with better long-term prognosis and rarely ever progresses to advanced stages of fibrosis and cirrhosis. On the other hand, microvesicular steatosis, marked by additional histological features, including hepatocyte ballooning, chronic inflammatory cell infiltrates and Mallory-Denk bodies, has been associated with the more advanced stages of NASH, indicating cellular injury, cytoskeletal damage and even fibrosis. The difference between macro- and microvesicular steatosis and their association with the early and later stages of NAFLD, respectively, may be attributable to increased oxidative stress and mitochondrial dysfunction[9]. Hepatic steatosis of 5% or more is considered to be the clinically significant mark of NAFLD. From this point, the pathological assessment of steatosis is divided into thirds with 5-13% being mild, 34-66% moderate and >66% as severe[1]. Additionally, there are several mechanisms by which hepatic steatosis can occur, such as an increase in fat source either from a high-fat diet or excess adipose lipolysis, a decrease in fat export in the form of very low-density lipoproteins (VLDL), a decrease in fatty acid β-oxidation, or an increase in DNL[2].

1.1.4. NAFLD diagnosis and treatment

Diagnosis of NAFLD. The most reliable way to diagnose patients with NAFLD is through a liver biopsy followed by histological analysis[13]. However, as a liver biopsy is an invasive procedure associated with limitations of cost and sampling error, it is often only performed after strong indications from screening of liver enzymes (i.e., AST, ALT) and imaging (i.e., ultrasonography, CT, MRI)[14-16]. Still, current methods of diagnosis are not ideal and may result in the under-recording and under-diagnosis of NAFLD[17].

Pharmacotherapeutics for the treatment of NAFLD. Several available drug-dependent therapeutic approaches to NAFLD have been tested, however, none serve to directly target the disease. These drugs have already been clinically approved for the treatment of other metabolic conditions and include two main groups; (1) drugs targeting dyslipidemia and insulin resistance, such as statins, GLP-1 agonists, DPP4-inhibitors, gliatazones and metformin, and (2) drugs targeting hepatic apoptosis, inflammation and fibrosis, such as PPAR-alpha/delta agonists, caspase inhibitors, FXR agonists, CCR2/CCL2 agonists[13]. Recently, SGLT2 inhibitors, commonly used in the treatment of diabetes, have shown metabolic improvements in the context of NAFLD[18,19] and indicate increased ketogenesis as a potential mechanism of action[20-22].

Dietary interventions for the treatment of NAFLD. Due to a lack of direct pharmacotherapies targeting NAFLD, lifestyle changes, such as exercise and diet restriction, remain the first line of therapy. Specifically, dietary interventions that stimulate a state of physiological ketosis, such as intermittent fasting (IF) and ketogenic diets, have shown promising results in NAFLD, including improvements in hyperglycemia and dyslipidemia[23-27]. Additionally, caloric restriction and IF have also been shown to prevent and alleviate the development of hepatic inflammation and fibrosis, associated with the more advanced condition of NASH[27-29].

1.2. Ketogenesis

1.2.1. Hepatic Ketogenesis

Ketogenesis, the breakdown of fatty acids for the production of ketone bodies, primarily occurs in the mitochondria of the liver where it is tightly regulated. This pathway provides alternative sources of fuel for extra-hepatic tissues (i.e., brain, skeletal muscle, adipose) and is activated in the presence of high fatty acid and low carbohydrate and/or at low circulating insulin concentrations[30], such as during neonatal development, pregnancy and under food-restricted (i.e., fasting, starvation), exercise-sustained, or diseased states (i.e., diabetes, aging, heart failure)[31-33].

Fatty acid oxidation (FAO). Hydrolysis of triglycerides in intrahepatic or extrahepatic fat stores (i.e., adipose tissues) releases free fatty acids that serve as substrates for oxidation in mitochondrial or peroxisomal compartments of the liver. Medium- (MCFA; C8 – C12) and short-chain fatty acids (SCFA; < C8) directly enter the mitochondrial matrix, where they are activated to their corresponding fatty acyl-CoA by acyl-CoA synthases (ACS). While very long (VLCFA; >C16) and long-chain fatty acids (LCFA; > C12) are esterified to fatty acyl-CoA by ACS on mitochondrial and peroxisomal membranes and require carnitine acyltransferase proteins for entry. Among the three carnitine acyltransferase proteins identified in the liver, carnitine palmitoyltransferase (CPT) is exclusively associated with the mitochondria, while carnitine octanoyltransferase (COT) is peroxisomal, and carnitine acetyltransferase (CAT) is both mitochondrial and peroxisomal. Specifically, carnitine palmitoyltransferase I (CPT1) and II (CPT2) are located on the outer and inner mitochondrial membranes, respectively. Once inside the mitochondria, fatty acyl-CoAs undergo repeated cycles of β-oxidation to yield acetyl-CoA. Incomplete β-oxidation of LCFA and VLCFA also occurs in peroxisomes, where the end products are SCFA- and MCFA-CoA. These fatty acyl-CoAs are then trans-esterified to fatty

acylcarnitines via peroxisomal CAT and COT proteins and are transported to the mitochondria, where they undergo complete β-oxidation to acetyl-CoA. ATP-binding cassette class D (ABCD) transporters allows for direct entry of VLCFA- and LCFA- into the peroxisome, without the requirement of carnitine acyltransferase proteins (**Fig. 1**) [34-39]. Another difference between mitochondrial and peroxisomal β-oxidation is the generation of hydrogen peroxide (H_2O_2) from the acyl-CoA oxidase in the first step of peroxisomal oxidation, playing a role in the detoxification of ROS[40]. Although, the majority of FAO occurs in the mitochondria, under conditions of excess fatty acid supply, such as during neonatal development, the number and activity of peroxisomal oxidation increases, but still only accounts for 10-15% of the total β-oxidation in the livers of newborns[39].

Ketogenesis. β-oxidation-derived acetyl-CoA can further undergo partial oxidation to energy-generating ketone bodies through ketogenesis. Mitochondrial 3-hydroxymethylglutaryl-CoA synthase 2 (HMGCS2) is the key rate-limiting enzyme of ketogenesis and catalyzes, the breakdown of acetyl-CoA and acetoacetyl-CoA (AcAc-CoA) to generate HMG-CoA and free CoA. HMG-CoA is cleaved by HMG-CoA lyase (HMGCL) to generate acetoacetate (AcAc), which is further reduced to β-hydroxybutyrate (β-OHB) through the enzymatic activity of D-3-hydroxybutyrate dehydrogenase 1 (BDH1)[31,32,41]. The ketone bodies, AcAc and β-OHB, are then released from the liver and circulate to extrahepatic tissues where they are terminally oxidized for fuel (**Fig. 1**). AcAc is also spontaneously decarboxylated to acetone, which is excreted or exhaled out. While the majority of circulating ketone bodies are produced from fatty acid β-oxidation derived acetyl-CoA, a very small portion of these ketone bodies are also produced from glucose metabolism (pyruvate decarboxylation) and the catabolism of branched-chain (leucine, isoleucine, valine) and ketogenic (lysine, phenylalanine, tyrosine, tryptophan) amino acids[32,42].

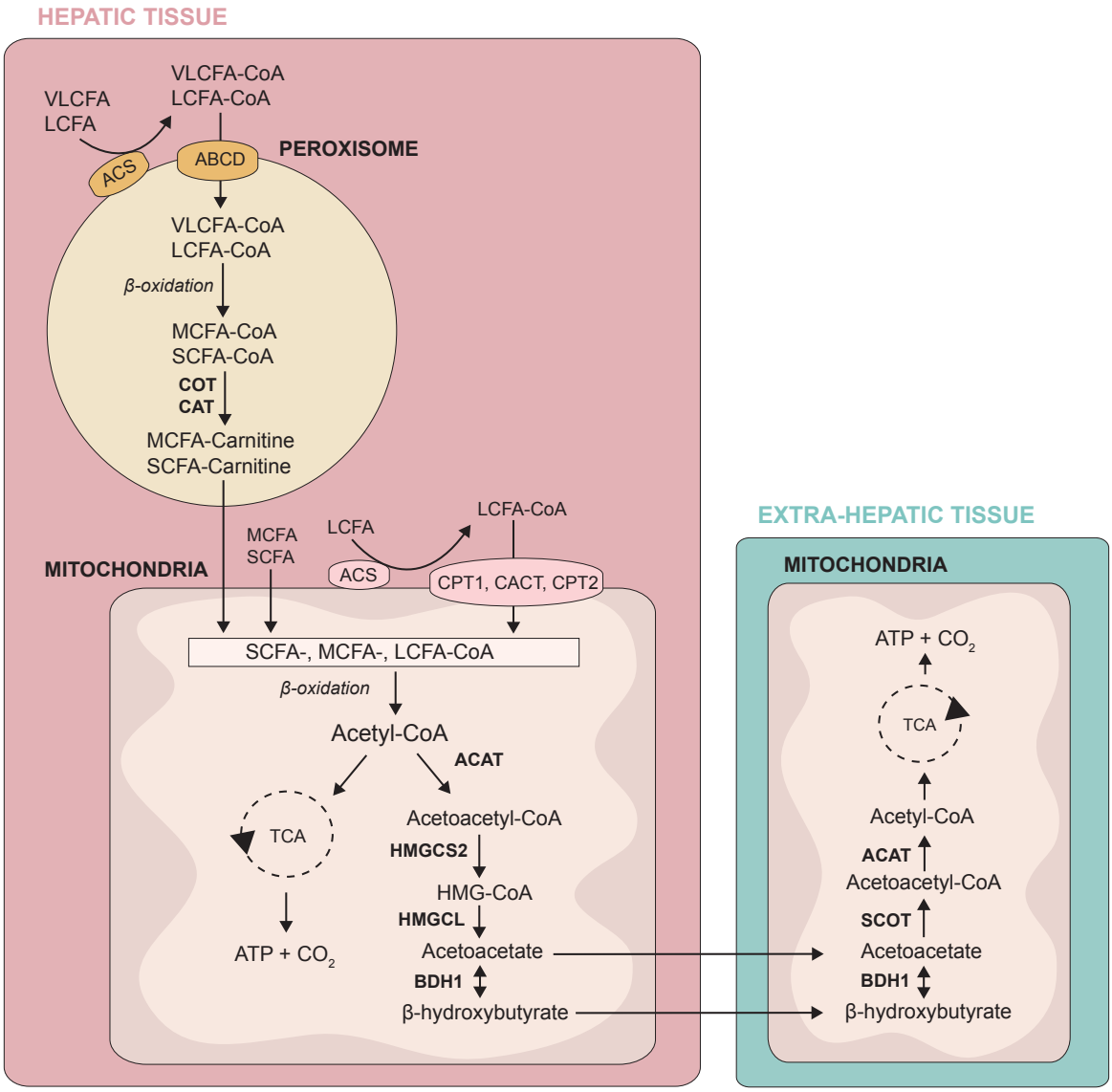

FIGURE 1 | Pathways of peroxisomal and mitochondrial fatty acid β-oxidation and ketogenesis in hepatic tissue and ketolysis in extra-hepatic tissue.

1.2.2. Neonatal ketogenesis

Prenatal to postnatal transition. Although the primitive liver is formed at embryological day 8.5 (E8.5) in mice and at 4 weeks gestational age in humans, its functional metabolic capacity is not fully evolved until after birth[43]. As such, during the prenatal period, the fetus is entirely dependent on the placental nutrient transfer from maternal circulation, which mainly comprises amino acids and carbohydrates in the form of glucose and lactate, as well as a small amount of fats. Due to their limited ability to permeate the placenta as well as their inadequate oxidation in fetal tissues, fatty acids minimally contribute to energy production during the prenatal period. Glycogenesis, however, is active in the fetal liver, and just prior to birth results in the accumulation of large amounts of glycogen stores from 3.4 mg/g of liver tissue at 8 weeks gestational age to 50 mg/g of liver tissue by term. Upon birth, the abrupt cessation of the maternal nutrient supply followed by a brief starvation period prior to feeding, as well as the simultaneous increase and decrease of glucagon and insulin levels, respectively, promotes rapid utilization of hepatic glycogen stores, causing a drop to 10% of their initial levels within the first 12-hours post-birth [44,45].

Following the depletion of glycogen stores, breast milk constitutes as the only exogenous source of energy for the newborn, beginning as early as 1-2 hours post-birth and up until weaning[46]. Glucose supplied by breast milk and endogenous hepatic glucose production stabilize blood glucose concentrations. While blood ketone levels, which are initially low up to 8-hours post-birth due to limited hepatic ketogenic capacity, rapidly increase within 12-hours post-birth to levels (12-22 μmol kg/min) comparable to adults after several days of fasting[44]. The nutrient composition of breast milk is considered to be essential for the activation of hepatic ketogenesis and varies between species. In comparison to humans (~53% fat, 41% carbohydrates, 6%

protein), rodents have a greater fat and lower carbohydrate content of breast milk (~69% fat, 6% carbohydrates, 25% protein)[46]. Specifically, the fat content of breast milk mainly comprises polyunsaturated LCFA in humans and MCFA in rodents (mice, rats), both of which are transported to liver mitochondria and serve as substrates of FAO and downstream ketogenesis. Regardless, in all species, the fat content of breast milk accounts for >50% of energy intake[39]. This transition from the low-fat, high-carbohydrate prenatal environment to the high-fat, low-carbohydrate postnatal environment promotes increased ketone body production and utilization in neonates, providing 25% of their basal energy needs[44,45]. In particular, due to the greater brain: body mass of the newborn, a significant portion of ketone bodies are utilized by the brain. In rodents, the permeability of the blood-brain barrier to β-OHB is increased at birth and suckling to accommodate greater ketone utilization and is returned to adult levels post-weaning[39].

Suckling to weaning transition. As the newborn's metabolic capacity matures, they begin to gradually replace their milk intake with solid food, thereby transitioning from a high-fat, low carbohydrate diet to a low-fat, high-carbohydrate diet. This weaning period normally occurs between 2-4 weeks after birth in rodents, with traces of chow found in the stomachs of mice as early as postnatal day 12 (p12)[43], and between 6 months to 2 years after birth in humans[47]. Moreover, in rodents, this transition in nutrient environment is particularly pronounced, as the fat content from breast milk to rodent chow significantly drops from >60% to <15%, and the carbohydrate content increases from <10% to >40%. As a result, post-weaning, fat-derived metabolic pathways of FAO and ketogenesis are reduced[48-50], while carbohydrate-derived metabolic pathways of lipogenesis and glycogenesis are increased in the liver, concomitant with a decrease and increase in glucagon and insulin levels, respectively[46,51].

These ketogenic adaptations are mediated by the expression and activity of Hmgcs2, the fate-committing enzyme of ketogenesis. In rodents, methylation of *Hmgcs2* at its 5' regulatory sequence, has been associated with its transcriptional suppression in fetal livers[52], while hypomethylation has been associated with its transcriptional activation at birth[53,54]. Consistently, Hmgcs2 activity is modulated by succinylation, with desuccinylation and activation of Hmgcs2 occurring at suckling and increased succinylation and inhibition of Hmgcs2 occurring post-weaning[55].

1.2.3. HMG-CoA Synthase II (HMGCS2)

Structure and function. Hmgcs2 is a mitochondrial-specific enzyme that catalyzes the first irreversible reaction of ketogenesis. Although Hmgcs2 expression and its ketogenic function is mainly restricted to the liver, previous studies have implicated a role for Hmgcs2 in renal ketogenesis[56,57], intestinal stem cell differentiation and homeostasis[58-60] and gonadal development[61]. Hmgcs2 is initially expressed as an immature protein in the cytosol and contains a mitochondrial targeting peptide sequence that is cleaved in the mitochondrial matrix. While structural analyses of Hmgcs2 are limited, it is known that Hmgcs2 exists as a homodimer, which is important for its enzymatic activity in ketogenesis[62,63].

Hmgcs1 and Hmgcs2 Isomers. There are two functionally distinct HMG-CoA synthases located in different compartments of the cell; mitochondrial Hmgcs2 is critical for ketogenesis, whereas cytosolic Hmgcs1 contributes to sterol biosynthesis. Both enzymes catalyze the same reaction; the conversion of AcAc-CoA and acetyl-CoA to HMG-CoA and CoA. In the cytosol, the HMG-CoA produced is converted to HMG-CoA reductase by mevalonate, which feeds into the isoprenoid pathway for the synthesis of cholesterol and other important biomolecules. HMG-CoA produced in the mitochondria is converted to AcAc by HMGCL, which feeds into the

ketogenesis pathway to produce additional ketone bodies, acetone and β-OHB. Mitochondrial Hmgcs2 is stimulated by fasting, whereas cytosolic Hmgcs1 is repressed by fasting. The two genes also contain different promoter sequences that represent important control sites for their independent pathways. *Hmgcs2* promoter contains a peroxisome proliferator regulatory element (PPRE) that allows transcriptional regulation by peroxisomal proliferator-activated receptor (PPARα/γ), whereas *Hmgcs1* promoter contains sterol regulatory elements (SRE) that allows transcriptional regulation by sterol regulatory-element binding protein (SREBP1/2)[64].

Transcriptional and post-translational regulation of Hmgcs2. Fatty acids have been shown to induce the transcription of *Hmgcs2* through activation of and interaction with peroxisome proliferator-activated receptor alpha (PPARα). PPARα, predominantly expressed in the liver, regulates the transcription of genes involved in FAO and ketogenesis. Specifically, PPARα can activate *Hmgcs2* gene expression by interacting with retinoid X receptor alpha (RXRα) and binding to PPRE sites in its promoter region[65]. Hmgcs2 can also directly interact with PPARα/RXRα, translocate to the nucleus and act as a co-factor for transactivation[33]. Palmitoylation of Hmgcs2, involving the covalent addition of free fatty acids through protein acylation at cysteine residues, has been shown to mediate this interaction with PPARα[66]. Thus, palmitoylated Hmgcs2 may amplify its own expression to meet increased ketogenic demands, such as under excess fatty acid exposure (i.e., T2D, obesity). Besides PPARα/RXRα, transcription factors SP1 and CREB can also bind to the promoter region of *Hmgcs2* to activate its transcription, while transcription factors HNF4 and ARP1 can compete with PPARα/RXRα to inhibit the transcription of *Hmgcs2*. The COUP transcription factor can either activate or repress the transcription of *Hmgcs2*, based on its binding site and tissue expression[42,64]. Additionally,

Hmgcs2 expression can be induced through the fibroblast growth factor 21 (FGF21)/PPARα axis[67,68].

Hmgcs2 is also regulated through post-translational modifications of lysine residue succinylation and acetylation by NAD^+-dependent deacylase sirtuin 5 (SIRT5)[69,70] and deacetylase sirtuin 3 (SIRT3)[71,72], respectively. While increased succinyl-CoA and succinylation inhibit Hmgcs2 activity, reduced acetylation activates Hmgcs2. Additionally, serine phosphorylation of Hmgcs2 has been shown to increase its enzymatic activity in ketogenesis[73]. Moreover, the transcription factor forkhead box A2 (FOXA2) is an activator of lipid metabolism and ketogenesis and regulates the activity of Hmgcs2 through insulin and glucagon signalling. Insulin inhibits Hmgcs2 through Akt-mediated phosphorylation and deactivation of Foxa2, while glucagon stimulates Hmgcs2 through p300-mediated acetylation and activation of Foxa2[74,75]. Overall, these regulatory mechanisms targeting Hmgcs2 gene expression and protein activity, are important in the control of hepatic ketogenesis during developmental stages (neonatal period, aging), nutrient changes (i.e., dietary interventions), and disease states (i.e., T2D, obesity, fatty liver)[32,76,77].

1.2.4. Mitochondrial HMGCS2 deficiency

Mitochondrial HMGCS2 (mHS) deficiency, a rare inborn disorder of ketone body metabolism, results in hepatic ketogenic failure during periods of prolonged fasting (>12-19 h) or sickness[78]. Since the first case of mHS reported in 1997, an approximate 43 patients of 31 families have been thus diagnosed and a total of 37 different mutations in *HMGCS2* have been reported[79], with the majority being missense mutations in exon 2, the longest exon of *HMGCS2* (445 bp)[80]. mHS is inherited in an autosomal recessive manner[81] with patients having compound heterozygous mutations that result in the loss of function of Hmgcs2[80].

Hypoketotic hypoglycemia and fatty liver development are common clinical presentations of mHS patients[62]. Other clinical manifestations of the disorder include metabolic acidosis, hepatomegaly, encephalopathy, seizures, and respiratory infection and distress (i.e., Kussmaul breathing, pneumonia)[79,81,82]. The frequency and severity of these symptoms decrease with age, with the average age of onset being 0-6 years[81,83] and most patients presenting with symptoms prior to the age of 3 years[79]. Whereas the acute management of symptoms involves correction of hypoglycemia and metabolic acidosis via glucose and bicarbonate infusions, respectively, chronic treatment involves the implementation of L-carnitine supplementation, avoidance of prolonged fasting periods, and infection prevention[84,85]. Although no concrete biomarkers have yet been established, elevated ratios of plasma FFA: TKB (total ketone body) and acetyl carnitine (C2): carnitine (C0), as well as increased urinary concentrations of 4-hydroxy-6-methyl-2-pyranone (4HMP) and secondary products of FAO (i.e., dicarboxylic acids), are often strong indicators of mHS[62,79,83]. It has been suggested that the accumulation of fatty acid intermediates in the urine profile of mHS patients, may result from the inhibition of mitochondrial β-oxidation and the compensatory activation of alternative FAO pathways, such as peroxisomal β-oxidation and microsomal ω-oxidation, as a result of impaired ketogenesis[83]. Overall, if managed early and adequately, patients with mHS generally have a good prognosis. Together, the clinical presentation of mHS deficiency arises from the inability to produce energy-carrying ketone bodies for extra-hepatic tissues and the consequential metabolic stress from the build-up of acetyl-CoA or AcAc-CoA.

1.2.5. Extra-hepatic ketolysis

Ketone bodies produced in the liver from ketogenesis can either be (1) terminally oxidized in the mitochondria of extra-hepatic tissues, (2) directed to sterol synthesis or lipogenesis pathways, or

(3) excreted in the urine[32]. Ketone bodies are removed from the liver and taken up by the heart, brain and skeletal muscle, which comprise the three main extra-hepatic consumers of ketone bodies. In the mitochondria of these extra-hepatic tissues, the oxidation of β-OHB to AcAc is catalyzed by BDH1. Succinyl-CoA:3-oxacid CoA transferase (SCOT, or OXCT1), a key fate-committing mitochondrial enzyme of ketolysis, is ubiquitously expressed in all tissues except for the liver and converts AcAc to AcAc-CoA. AcAc-CoA is subsequently converted to acetyl-CoA, which can then either enter the Tricarboxylic acid (TCA) cycle for ATP generation or be used for sterol biosynthesis and DNL (**Fig. 1**)[31,32].

1.2.6. Additional regulatory roles of ketone bodies

Besides their fat-metabolizing and energy-generating capacity, ketone bodies provide other health benefits, including protection from oxidative stress and inflammation that are achieved through their epigenetic and signalling functions, mainly mediated by β-OHB[32]. Although, AcAc and β-OHB exist in a 1:1 ratio with total ketone body levels rarely exceeding 0.3 mM under normal feeding conditions, upon ketogenic conditions β-OHB concentrations can increase almost 4-fold in comparison to AcAc, reaching approximately 6.0 mM with an extended fast. At concentrations >1 mM, βHB can act as a class I histone deacetylase (HDAC) inhibitor to regulate gene transcription, particularly activating the transcription factor forkhead box O3 (FOXO3) involved in cell survival and oxidative stress response[86] and suppressing gluconeogenic gene expression[87]. β-OHB in conjunction with CoA (β-OHB-CoA) can also mediate histone lysine β-hydroxybutyrylation (kbhb), a recently discovered post-translation modification. In particular, the more common histone 3 lysine 9 β-hydroxybutyrylation (H3K9bhb) epigenetic mark has been found in fasted livers and is involved in the upregulation of genes associated with redox homeostasis, nucleotide metabolism, PPAR signalling, and circadian rhythm[88-90]. In addition to

its epigenetic role, β-OHB through Hcar2 (hydroxycarboxylic acid receptor 2) signalling, can elicit an M2 phenotype of intrahepatic macrophages, thereby mediating anti-inflammatory and hepatoprotective effects[91]. Overall, due to their multi-dimensional roles and benefits, increased ketone body supplementation through ketogenic diets[92-94] and ketone ester formulations[95] have gained popularity for stimulating weight loss[96,97] and improving metabolic disorder (i.e., T2D, obesity, NAFLD).

RATIONALE, HYPOTHESIS & AIM

Since current ineffective diagnostic measures and lack of direct pharmacological interventions make it difficult to prevent and reverse NAFLD, the discovery of new biomarkers and therapeutic options for NAFLD are key areas of investigation. Recent studies have shown an association between dysregulated ketogenesis and NAFLD pathogenesis. Aberrant ketogenesis has been observed to be correlated with the degree of steatosis in NAFLD patients[98-100] and an inborn error of ketogenesis (mHS deficiency) is commonly associated with the development of the fatty liver. In addition, ketogenic insufficiency through antisense oligonucleotide (ASO)-mediated *Hmgcs2* knockdown in adult mice results in hepatic inflammation and injury, characteristic of advanced NAFLD[101,102]. Despite the important findings from these studies, several areas remain to be investigated, including (1) what is the causative genetic factor underlying impaired ketogenesis in NAFLD, (2) what is the necessity relationship between ketogenesis and a fat-enriched dietary environment during fatty liver development, and (3) whether the degree of ketogenic activity is associated with susceptibility to NAFLD development and progression. Importantly, it is not yet known (4) whether increased ketogenesis is sufficient to reverse NAFLD. Thus, to address these questions, ***I hypothesize that impaired ketogenesis will result in the progression of NAFLD and that activated ketogenesis will result in the improvement of NAFLD.*** To test this, I propose the following primary aim:

Primary Aim: To investigate the requirement of Hmgcs2-mediated ketogenesis in NAFLD development and treatment.

MATERIALS & METHODS

2.1. Mice

2.1.1. Housing & Care

All animal experiments were performed in accordance with protocols (#2950 and #2962) approved by the Animal Care Committee in the Animal Care and Veterinary Service (ACVS) at the University of Ottawa and conformed to the standards of the Canadian Council on Animal Care. Experiments were performed in male mice. C57BL/6J mice were utilized for high-fat diet (HFD)-induced NAFLD models. All mice were housed in standard vented cages in temperature- and humidity-controlled rooms with 12-hour light-dark cycles (21-22 ^{o}C, 30-60% humidity for normal housing), and free access to water and a low-fat, high-carbohydrate chow diet in which 22% of calories were from fat, 55% from carbohydrates and 23% from protein (2019 Teklad Global Diet; Envigo). For HFD studies, 8-week-old mice were placed on a high-fat, low-carbohydrate diet in which 45% of calories were from fat, 35% from carbohydrates and 20% from protein (D12451; Research Diets).

2.1.2. Early weaning

The early weaning protocol was adapted from previous studies[103,104]. The day of birth was termed as postnatal day 0 (p0). Post-birth and during the suckling period, the mother and pups were undisturbed, except briefly on a weekly basis to change cages. At p14, pups were prematurely weaned and provided with a low-fat, high-carbohydrate chow diet (2019 Teklad Global Diet; Envigo) in the form of soaked cubes placed on the cage floor for easy access. Mice were maintained up until 1-week post-weaning or p21. Control suckling mice were kept with the mother until p21.

2.1.3. Generation of *Hmgcs2* knockout mouse

Mice lacking *Hmgcs2* gene, C57BL/6N-*Hmgcs2*$^{em1(IMPC)Tcp}$ (*Hmgcs2* knockout) were generated at The Centre for Phenogenomics (TCP; Toronto, Canada) essentially as described in Gertsenstein & Nutter[105]. Briefly, C57BL/6NCrl zygotes were electroporated with Cas9 ribonucleoprotein complexes with single guide RNAs having spacer sequences of CTAATATTACGCTTGAAAGT targeting the 5' side and GTGCCTGACTGTAGATGAGA targeting the 3' side of a critical region. This resulted in a 1000-bp deletion, Chr3:98290599 to 98291598_insT (GRCm38). All procedures involving animals were performed in compliance with the Animals for Research Act of Ontario and the Guidelines of the Canadian Council on Animal Care. The local Animal Care Committee reviewed and approved all procedures conducted on animals at TCP.

Founders were identified by endpoint PCR using PCR primers flanking the deletion target, Fwd: 5'-AATTCAGAATTCAAAGCTACCTGGG-3' and Rev: 5'-CTCAGAGGCTCCAGGAGATTAAT-3'. The wild-type allele would produce a 2,208-bp amplicon and the deletion fragment a 1,209-bp amplicon. Founders were backcrossed to wild-type C57BL/6NCrl mice and N1 progeny identified using the same PCR. Sanger sequencing of deletion amplicons from N1 mice was used to identify the definitive deletion sequence. Mice were maintained at TCP by crossing *Hmgcs2*$^{em1(IMPC)Tcp}$ heterozygotes with C57BL/6NCrl wild-type mice. N2 backcrosses were shipped to the University of Ottawa to establish a breeding colony. This strain is available from the Canadian Mouse Mutant Repository at TCP.

2.1.4. Mouse genotyping

DNA extraction. DNA for genotyping was extracted from ~2 mm ear notch samples. Briefly, 300 µL of 0.5N NaOH was added to each sample and placed in heat block at 95^{o}C for 45 minutes. 100 µL of 0.5 M Tris-HCl buffer (pH 8.0) was then added to each sample for neutralization and

incubated for 1 hour at room temperature. After centrifugation at 12,000 rpm for 1 minute, the supernatant was used for PCR reaction.

PCR analysis. PCR was conducted using 2× Dream Taq™ Hot Start Green PCR Master Mix (Thermo Scientific™), a common forward primer (FP) and two reverse primers (RP1, RP2) spanning exon 2 of *Hmgcs2*, and 2 μL of isolated DNA in thermocycler (Mastercyler® ep gradient; Eppendorf). PCR products were analyzed on a 1.5% agarose gel electrophoresis using SYBR Safe DNA gel stain (Invitrogen) and visualized using blue light illuminator. Expected band sizes for wild-type (WT) and knockout (KO) were 327 and 203 base-pairs (bp), respectively (**Fig. 2A-B**). Primer sequences are indicated in **Table 1**.

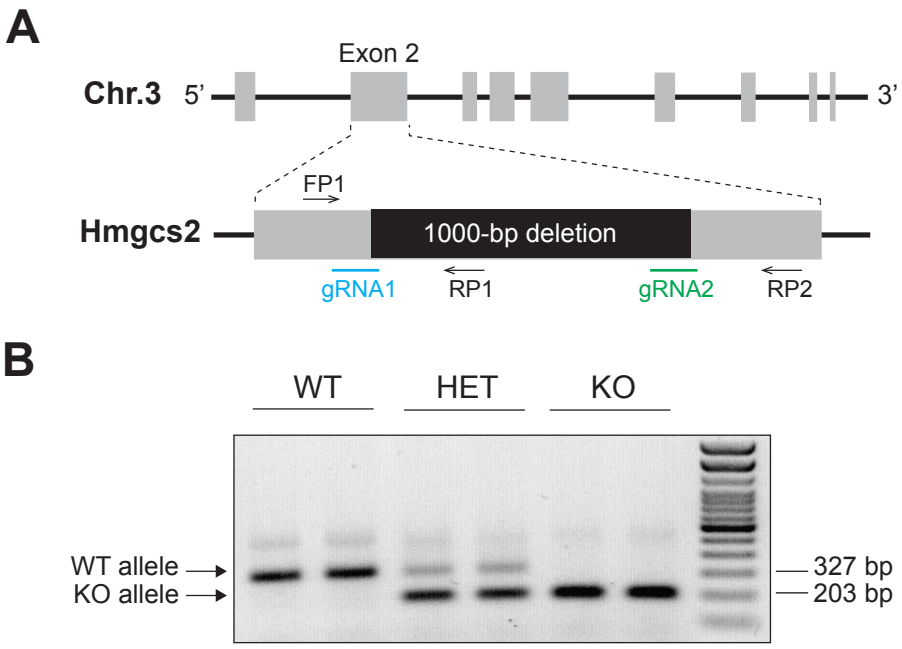

FIGURE 2 | CRISPR/Cas9-mediated generation and genotypic validation of *Hmgcs2* knockout mouse model. (**A**) CRISPR-Cas9 mediated 1000-bp deletion within exon 2 of *Hmgcs2* on chromosome 3, utilizing a pair of guide RNAs (gRNA1, gRNA2). (**B**) Gel electrophoresis showing wild-type (WT; 327 base-pair) and knockout (KO; 203 base-pair) alleles generated through a polymerase chain reaction using a common forward primer (FP1) and two reverse primers (RP1, RP2) spanning the deletion region.

TABLE 1. Genotyping primer sequences for *Hmgcs2*

Primer	Sequence
Common forward primer (FP)	CCTCCTAGACATGCATGCCC
Wild-type reverse primer (RP1)	ACCCAACCAATAATGTGGCA
Knockout reverse primer (RP2)	AGTTGCTCTTGCCAGTGGTT

2.1.5. Adenovirus overexpression

Adenovirus vectors encoding *GFP* (Ad-*GFP*; #1060 Vector BioLabs) and human *HMGCS2* (Ad-h-*HMGCS2*; ADV-211285 Vector BioLabs) were produced and titrated by Vector BioLabs. *HMGCS2* overexpression mouse model was achieved by a single intravenous injection of Ad-h-*HMGCS2* (1.0×10^9 PFU) through tail vein. Ad-GFP was used for control group. *HMGCS2* overexpression in the liver was confirmed by qPCR primers specific for human *HMGCS2* in contrast to endogenous mouse *Hmgcs2*.

2.2. Metabolic phenotyping

Body composition. Body fat and lean masses of the mouse were measured using the EchoMRI-3-in-1 machine (Echo Medical Systems, Houston, TX, USA).

Blood glucose and ketone. A glucometer (Contour® Next One; Ascensia Diabetes Care Inc.) and ketone meter (Freestyle Optium Neo and β-ketone Test Strips; Abbott Diabetes Care Ltd.) were used for measuring blood glucose and ketone levels, respectively.

Glucose and insulin tolerance test (GTT, ITT). Glucose (1 mg/g of body weight) and insulin (0.65 mU/g of body weight, Humalog®; Eli Lilly Canada Inc) were intraperitoneally administered to mice after an overnight (15-hour) and 6-hour fasting with *ad libitum* access to water, for GTT and ITT, respectively. Blood samples were obtained from the tail vein at the indicated intervals and glucose levels were measured using a glucometer.

Plasma B-OHB analysis. Plasma was collected after centrifugating whole blood samples at 3000 rpm for 10 mins and then used to measure β-OHB levels using a Ketone Body Assay kit (MAK134, Sigma-Aldrich).

2.3. Histological analysis of liver tissue

2.3.1. Tissue processing

Harvested liver tissue samples were fixed in 4% paraformaldehyde, washed with phospho-buffered saline (PBS) and dehydrated in 70% EtOH. Samples were then processed in the Epredia^{TM} STP 120 Spin Tissue Processor (Fischer Scientific) using the following program: 70% alcohol for 2 hours, 80% alcohol for 1 hour, 95% alcohol for 1 hour, 100% alcohol for 3 hours, Toluene for 3 hours and paraffin for 3 hours. Paraffin-embedded blocks were made using the HistoStar^{TM} Embedding Workstation and were sectioned using a microtome (Leica RM2235).

2.3.2. H&E and PSR staining

5 μm thick tissue sections were deparaffinized and rehydrated. For Hematoxylin and eosin (H&E) staining, slides were incubated in hematoxylin solution (EprediaTM Modified Harris Hematoxylin #72711; Fisher Scientific) for 3 minutes, followed by 10 seconds in acid alcohol, 1 minute in PBS, and 8 minutes in Eosin, with distilled water washing steps in between. For Picrosirius red (PSR) staining, slides were incubated in PSR solution for 1 hour at room temperature (RT), followed by two 10-second changes in 0.5% acetic acid solution. Stained sections were then dehydrated and mounted with permount media (30% glycerol in PBS). Imaging was performed using the Aperio VERSA 8 Scanner (Leica Biosystems).

2.3.3. Immunohistochemistry.

5 μm thick tissue sections were deparaffinized and rehydrated. Slides were washed with PBS (pH 7.4) on a shaker for 5 mins. Antigen retrieval was performed using citric acid (pH 6.0) in a microwave for 2.5 minutes. Slides were washed with PBS for 5 mins. Tissue sections, circled with liquid blocker pen, were incubated in 10% normal horse serum blocking for 15 minutes at

RT, followed by an overnight incubation with anti-Perilipin 2 (Plin2) antibody (1:150, NB110-40877; Novus Biologicals) at 4ºC. The next morning, after two 5-minute washes in PBS, tissue sections were incubated with the biotinylated horse anti-rabbit IgG secondary antibody (1:100, BA-1100; Vector Laboratories) for 15 minutes at RT. After a 5-minute wash with PBS, slides were incubated in 3% hydrogen peroxide (BDH7540-2; VWR) for 30 mins. Slides were then washed with distilled water, followed by three 5-minute changes in PBS. The VECTASTAIN Elite ABC reagent (PK-6100; Vector Laboratories) was added to tissue sections for 30 minutes at RT and then slides were washed in two 15-minute changes in PBS. DAB solution (D5905-50TAB; Sigma-Aldrich) was added to tissue sections for 15-20 seconds and immediately washed off in two 5-minute changes of distilled water. A counterstain in hematoxylin for 1 min was performed followed by 10 seconds in acid alcohol and 1 minute in PBS. Upon dehydration, slides were mounted with permount media and imaged using the Aperio VERSA 8 Scanner (Leica Biosystems).

2.4. Cell culture

2.4.1. Adenoviral infection

HepG2 hepatoma cells were cultured in EMEM supplemented with lipoprotein-free fetal bovine serum (FBS) at 37ºC with 5% CO_2 and were allowed to reach 70-80% confluency. Cells were then supplied with 1.5 mM water-soluble oleic acid (#01257; Sigma) for 24 hours, followed by adenovirus infection (7.5 MOI) of Ad-GFP (#1060, Vector BioLabs) and Ad-h-*HMGCS2* (ADV-211285, Vector BioLabs). After 24 hours, cells were harvested for downstream molecular and imaging analysis.

2.4.2. Oil Red O staining

HepG2 cells were seeded at 1 x 10^5 cells/well in a 6-well plate. Cells were fixed in 10% formalin in PBS for 30-45 minutes prior to staining. After washing, cells were stained in freshly prepared Oil Red O solution (0.5% in isopropanol, Sigma) for 30-60 minutes. Stained cells were imaged using a light microscope. For lipid quantification, the dye was extracted from the cells by isopropanol with 4% NP-40 and absorbance was determined at 490 nm.

2.5. RT-qPCR

For liver, 1 mL of TRIzol™ Reagent (Invitrogen) was added per 50-100 mg of tissue sample and tissue homogenization was carried out using a Mini-Beadbeater (BioSpec Products) at 40-60 Hz for intervals of 15-seconds. For cells seeded at a density of 5 x 10^4 cells/well in a 12-well plate, 1 mL of TRIzol™ Reagent (Invitrogen) was added per well and cell lysis was carried out by pipetting cell lysates up and down several times. Chloroform was added to samples in a 1:5 ratio to TRIzol™ Reagent. Samples were centrifuged at 12,000 g for 15 minutes at 4°C to allow for phase separation. After the clear aqueous phase was collected and mixed with 70% ethanol, total RNA was purified using the PureLink™ RNA Mini Kit (Invitrogen). Complementary DNA (cDNA) was synthesized from 1-2 µg of RNA using the High-Capacity cDNA Reverse Transcription Kit and RNaseOUT™ (Invitrogen). Synthesized cDNA was diluted to a final concentration of 5 ng/µL for quantitative PCR (qPCR). Gene expression assay was conducted using Power SYBR Green Master Mix (Thermofisher) on Quant studio 5 (Applied Biosystems) and relative cycle threshold (CT) values were normalized by housekeeping TATA-Box Binding Protein (*Tbp*) gene. Primer sequences are indicated in **Table 2**.

TABLE 2. qPCR primer sequences for gene expression analysis

Gene	Forward (5' – 3')	Reverse (5' – 3')
Mouse		
Acat1	GTCTGGCTAGTATTTGCAACG	TTCAGCCGGTCACATGG
Hmgcl	GGACTTCATCTGTCAAGCC	TCATTGTATACACCCAATTCCC
Hmgcs2	GGTGTCCCGTCTAATGGAGA	ACACCCAGGATTCACAGAGG
Bdh1	GAATTCAGCCTGCCGGTTTG	TGCATCCCGCTGTCAGGTAA
Pparg	CACCAGTGTGAATTACAGCAAATC	AGCTGATTCCGAAGTTGGTG
Fsp27	CTGGAGGAAGATGGCACAAT	GGGCCACATCGATCTTCTTA
Plin2	GACCTTGTGTCCTCCGCTTAT	CAACCGCAATTTGTGGCTC
Srebp1c	CGCTACCGGTCTTCTATCAATG	TTGCTTTTGTGTGCACTTCG
Acc1	ATTGACCCAGACTGGCTTGAA	GTGTGAAGGCTGCTTTGTGAAC
Fasn	CCCTTGATGAAGAGGGATCA	ACTCCACAGGTGGGAACAAG
Ppara	CCGCAATGGACCATGTAAC	CAGCTCTAGCATGGCCTTTT
Cpt1a	GAGACTTCCAACGCATGACA	ATGGGTTGGGGTGATGTAGA
Mcad	GCTCGTGAGCACATTGAAAA	CATTGTCCAAAAGCCAAACC
Human		
HMGCS2	GGTGCCTTCTCTTATGGCTC	GACACACACTTTCGGGAGG
FSP27	GGGATACAGTGTTCATGGTCCT	TCAATCTTCTTGGCAGGCTTATG
PLIN2	TTGCAGTTGCCAATACCTATGC	CCAGTCACAGTAGTCGTCACA
SREBP1C	ACAGTGACTTCCCTGGCCTAT	GCATGGACGGGTACATCTTCAA
ACC1	GCTCCTTGTCACCTGCTTCT	CAAGGCCAAGCCATCCTGTA
FASN	AGCGGCTCTGAGACCTCGGA	GCAGGCTGTGTCCAGTGCGA

2.6. Western Blot

Tissue dissociation. 1 mL of RIPA lysis and extraction buffer (#89900; Thermo Scientific™) containing protease inhibitor (#78442; Thermo Scientific™) was added per 100 mg of liver tissue, and samples were homogenized using a Mini-Beadbeater (BioSpec Products) at 40-60 Hz for intervals of 15-seconds. Tissue lysates were placed on ice for 30 minutes and then centrifuged at 10,000 g for 30 minutes at 4°C for collection of the supernatant.

Cell dissociation. 200 µL of RIPA lysis and extraction buffer (#89900; Thermo Scientific™) was added to each well in a 6-well dish containing approximately 780, 000 cells/well. Cells were collected using a cell scraper and placed on ice for 30 minutes. Cell lysates were then centrifuged at maximum speed for 20 minutes and the supernatant was collected.

Protein quantification was performed using the Pierce Rapid Gold BCA Protein Assay Kit (A53225; Thermo Scientific™). 10 µg of *in vivo* protein samples and 75 µg of *in vitro* protein samples were prepared by the addition of 4× Laemmli sample buffer (#1610747; Bio-Rad) containing 0.1M DTT, and heated for 10 minutes at 100 °C. Samples were then loaded onto 10% Tris-Glycine gels and gel electrophoresis was performed at 160 volts for 1 hour, using the BioRad stain free system. Following this, transfer was completed at 100 volts for 1 hour (BioRad PowerPac). 0.45 µm PVDF membranes (Thermo Scientific™) were blocked with EveryBlot blocking buffer (#12010020; Bio-Rad) and blotted with primary and secondary antibodies at indicated dilutions (**Table 3**). Blots were developed using Clarity™ Western ECL Substrate (#170-5060; Bio-Rad) and Bio-Rad Imager. Quantification and analysis were completed by Image Lab 6.1 Software (Bio-Rad).

TABLE 3. List of antibodies used for Western Blot

Antibody	Species	Dilution	Source	Catalog #
Primary				
Hmgcs2	Mouse	1:1000 (*in vivo*) 1: 500 (*in vitro*)	Santa Cruz Biotechnology	sc-393256
β-actin	Rabbit	1: 2500 (*in vivo*) 1: 5000 (*in vitro*)	Cell Signalling Technology	5125S
β-tubulin	Rabbit	1: 500	Abcam	ab6046
Secondary				
Anti-mouse		1: 5000 (*in vivo*) 1: 1000 (*in vitro*)	Cell Signalling Technology	7076
Anti-rabbit		1: 5000	Cell Signalling Technology	7074

2.7. Untargeted liver metabolome profiling

Liver metabolites were quantified by liquid chromatography mass spectrometry (LC-MS). Sample temperature was maintained on ice or dry ice where possible, and all solvents were MS grade and pre-equilibrated to -20°C.

2.7.1. Metabolite extraction

Mice were kept under constant 2.5% isoflurane anesthesia for the duration of tissue harvesting. Harvested liver tissue samples were washed in ice-cold 0.9% filtered (0.2 μM) saline, weighed, and immediately snap-frozen in liquid nitrogen. Frozen liver samples of approximately 25-35 mg of wet tissue weight were transferred to pre-chilled 2 mL screw cap microtubes containing 2.8 mm ceramic beads (Omni International, PN: 19-646-3). 1140 μL of cold 50% MeOH / 50% LC/MS water solution was added to the tubes and vortexed 10 seconds. 660 μL of acetonitrile was then added to samples and tubes were vortexed for another 10 seconds. Tissue homogenization was carried out using a Mini-Beadbeater (BioSpec Products) at 40-60 Hz for intervals of 15-seconds. 1800 μL dichloromethane and 900 μL LC/MS grade water were then added for liquid-liquid extraction. Samples were vortexed, incubated on ice for 10 minutes and then centrifuged for 10 minutes at 4000 rpm at 1°C. The resulting upper phase, consisting of polar metabolites, was separated into two fractions (for +ESI and –ESI injections), dried with a refrigerated (-4°C) centrivap concentrator (Labconco) and stored at -80°C before LC-MS analyses.

2.7.2. LC-MS metabolite quantification

Samples to be injected in +ESI were resuspended with 75% acetonitrile, cleared by centrifugation and run on an Agilent 6545B Q-TOF mass spectrometer equipped with a 1290 Infinity II ultra-

high performance LC (Agilent Technologies). Continuous internal mass calibration was executed using signals from purine (12,000 full width at half maximum (FWHM) resolution) and hexakis (1H, 1H, 3H-tetrafluoropropoxy) phosphazine (24,000 FWHM resolution). All study samples were randomized before analysis and run using both high and low pH hydrophilic interaction chromatography (HILIC-Z) in positive ionization mode. HILIC separation was obtained using the Poroshell 120 HILIC-Z column (2.1 100 mm, 2.7 mm; Agilent) and corresponding guard column. The chromatographic conditions and mass spectrometry acquisition parameters are described elsewhere[106]. Metabolite identification was confirmed by exact mass, retention time and subsequent MS/MS fragmentation of metabolite standards and quality control samples. These identifications correspond to Metabolomics Standards Initiative identification level 1[107]. A targeted list of metabolites was quantified (relative quantification) by external standard calibration curves with Mass Hunter Quant (Agilent).

Samples to be analysed in –ESI were resuspended in water and run on an Agilent 6470A tandem quadruple mass spectrometer equipped with a 1290 Infinity II ultra-high performance LC (Agilent Technologies) utilizing the Metabolomics Dynamic MRM Database and Method (Agilent), which uses an ion-pairing reverse phase chromatography[108]. This method was further optimized for phosphate-containing metabolites with the addition of 5 µM InfinityLab deactivator (Agilent) to mobile phases A and B, which requires decreasing the backflush acetonitrile to 90%. Multiple reaction monitoring (MRM) transitions were optimized using authentic standards and quality control samples. Metabolites were quantified by integrating the area under the curve (AUC) of each compound using external standard calibration curves with Mass Hunter Quant (Agilent). No corrections for ion suppression or enhancement were performed, as such, uncorrected metabolite concentrations are presented. Metabolite

concentrations were normalized by wet tissue weight, log transformed (base 10) and pareto-scaled prior to multivariate statistical analysis using MetaboAnalyst 5.0[109,110].

2.8. Statistical Analysis

All data were presented as mean ± SEM. Statistical analyses were performed with GraphPad Prism 9.0 software (GraphPad Software). Unpaired two-tailed Student's *t*-test or one-way or two-way analysis of variance (ANOVA) for more than two groups were used as appropriate. *P* values less than 0.05 were considered statistically significant.

RESULTS

3.1. HFD-induced NAFLD mice present with impaired ketogenesis and Hmgcs2 expression

In addition to the altered metabolic pathways in NAFLD pathogenesis (i.e., lipid uptake, secretion, oxidation, synthesis)[111,112], recent studies have demonstrated that NAFLD patients exhibit dysregulated ketogenesis, which is negatively correlated with the severity of the disease (i.e., hepatosteatosis)[98]. To gain molecular insight into NAFLD-related impaired ketogenesis in a preclinical model, we compared healthy mice fed a normal chow diet with NAFLD mice fed a HFD (45% kcal fat) for 32 weeks. H&E staining and Plin2 immunostaining of liver sections confirmed HFD-induced severe hepatosteatosis, as NAFLD mice showed hypertrophied hepatocytes with significant accumulation of lipids, particularly microvesicular steatosis, associated with advanced NAFLD and characterized by the build-up of numerous small lipid droplets surrounding centrally located nuclei within hepatocytes[113] (**Fig. 3A**). In addition, unlike healthy mice showing significant reductions ($P< 0.05$) in plasma glucose levels upon fasting, NAFLD mice comparatively maintained greater levels of plasma glucose at 6-hour and 24-hour post-fasting (**Fig. 3B**), suggesting NAFLD-associated dysregulated glucose metabolism. Importantly, concurrent measurements of plasma ketone bodies (β-OHB) revealed that, in contrast to healthy mice showing fasting-induced ketogenesis with plasma ketone levels up to 1.3 ± 0.06 mmol/L at 24-hour fasting, NAFLD mice failed to increase plasma ketone levels beyond 0.8 ± 0.03 mmol/L (**Fig. 3C**). This result suggests a suppressed ketogenic response in NAFLD mice, which corroborates recent findings in NAFLD patients[98-100].

Next, to understand the molecular contribution underlying the altered ketogenic response of NAFLD mice, the hepatic expression of ketogenic pathway genes, such as *Acat1*, *Hmgcs2*, *Hmgcl* and *Bdh1*, was examined (**Fig. 4A**). Among these, only *Hmgcs2*, known to be the rate-

limiting enzyme of ketogenesis[32], was significantly increased with 24-hour fasting in healthy mice (2.1-fold, $P<0.001$) and to a comparatively lesser extent ($P = 0.006$) in NAFLD mice (1.6-fold, $P = 0.007$) (**Fig. 4B**). Furthermore, quantitative analysis of Western blot consistently showed increases in hepatic Hmgcs2 protein expression (2.3-fold, $P = 0.015$) after 24-hour fasting in healthy mice, while no similar fasting-induced changes were observed in NAFLD mice (**Fig. 4C**). Together, these results suggest that NAFLD mice with metabolic dysfunction have reduced ketogenic function associated with a blunted response of the fate-committing ketogenic enzyme, Hmgcs2.

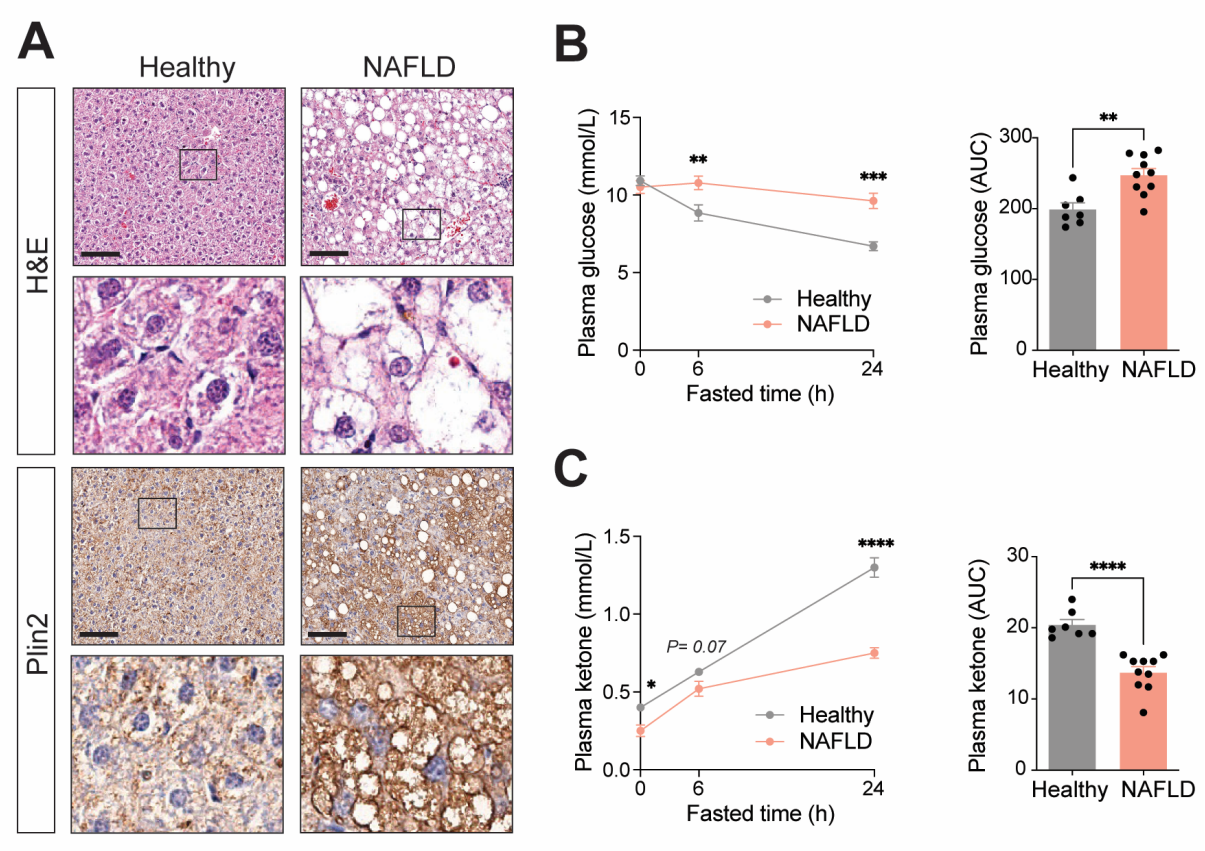

FIGURE 3 | HFD-induced NAFLD mice present with metabolic dysfunction and impaired fasting-induced ketogenesis. (**A**) Haematoxylin & Eosin (H&E) and lipid droplet associated Perilipin 2 (Plin2) immunohistochemical staining of liver sections from healthy mice fed chow diet and NAFLD mice fed 45% kcal high-fat diet (HFD) for 32 weeks. Scale bar = 100 μm. Boxes indicate regions of higher magnification. Plasma levels of (**B**) ketone bodies and (**C**) glucose at baseline and 6- and 24-hour post-fasting and their respective area under the curves (AUC). Data represented as mean ± SEM. Statistical analysis performed by student's *t*-test and two-way ANOVA. **P* ≤ 0.05; ***P* ≤ 0.01; ****P* ≤ 0.001; *****P* ≤ 0.0001.

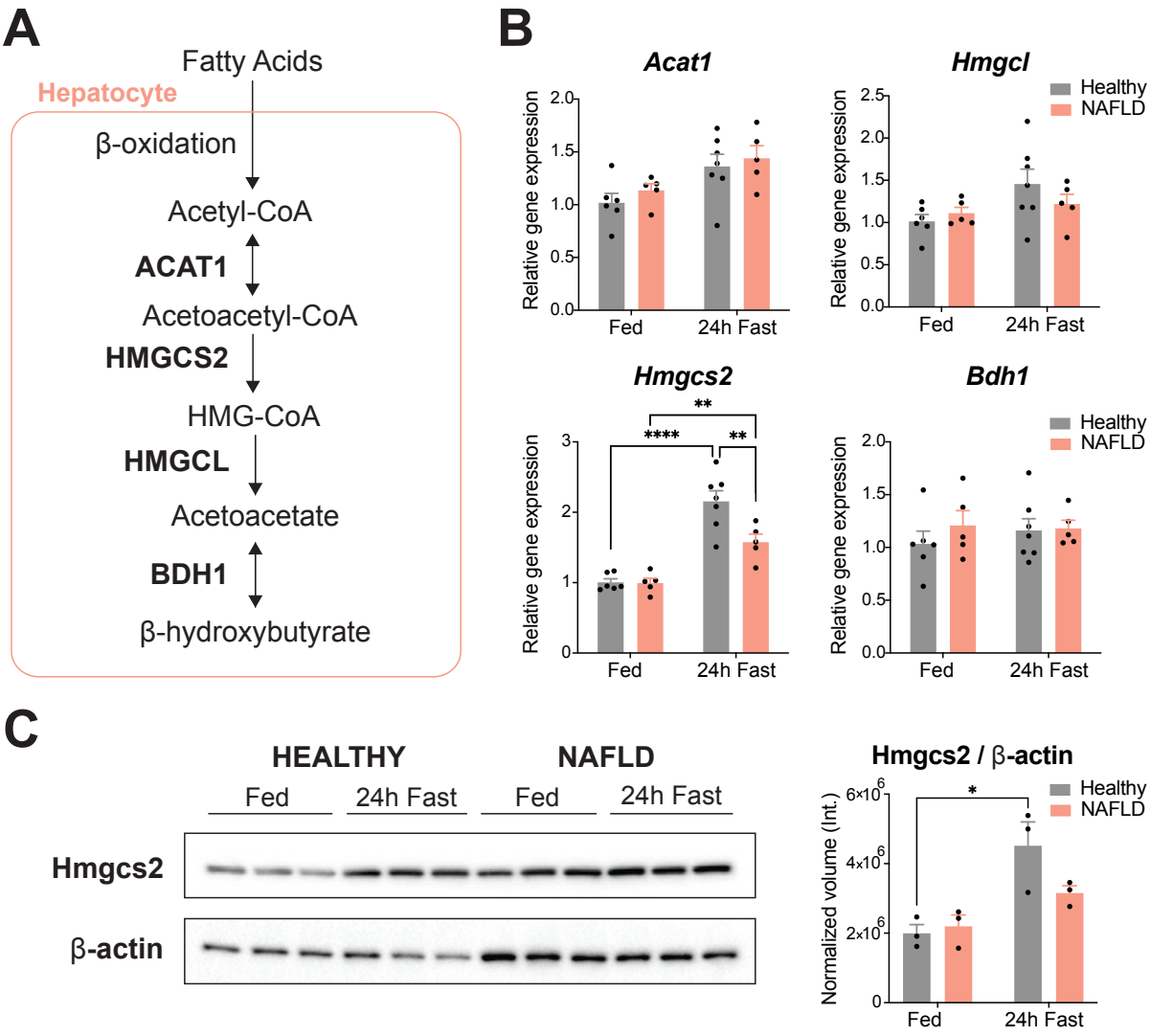

FIGURE 4 | HFD-induced NAFLD mice exhibit abnormal Hmgcs2 expression in the liver. (**A**) Schematic of hepatic ketogenic pathway with key metabolites and enzymes. (**B**) mRNA expression analysis of ketogenic enzymes in the liver, including *Acat1*, *Hmgcl*, *Hmgcs2*, and *Bdh1*, in fed and 24-hour fast. (**C**) Hmgcs2 protein expression and quantification in healthy and NAFLD mouse livers in fed and 24-hour fast. Data represented as mean ± SEM. Statistical analysis performed by two-way ANOVA. *$P \leq 0.05$; **$P \leq 0.01$; ****$P \leq 0.0001$.

3.2. Genetic deletion of *Hmgcs2* promotes spontaneous fatty liver development in postnatal mice

To determine a causal relationship between impaired ketogenesis and NAFLD development *in vivo*, we examined an *Hmgcs2* gene knockout (*Hmgcs2*-KO) mouse model, generated using CRISPR/Cas9-mediated gene targeting (**Fig. 2A-B**). Hmgcs2 protein expression measured in the liver confirmed successful knockout of *Hmgcs2* gene in mice (**Fig. 5A**). A higher lethargy and mortality of *Hmgcs2*-KO mice between p14 and p21 from preliminary assessments (*data not shown*) demonstrated ketone bodies as critical energy substrates during postnatal development, due to the transition from a carbohydrate- to a fat-enriched dietary environment from the pre- to postnatal period[39,43,44,46,114]. Thus, we examined WT, *Hmgcs2* heterozygous (*Hmgcs2*-HET) and *Hmgcs2*-KO mice at three different developmental stages of p0, p4 and p14 (**Fig. 5B**). Gene expression analysis showed that *Hmgcs2* mRNA levels in the liver of WT mice were significantly elevated at p4 and p14, compared to p0 (**Fig. 5C**). Consistently, WT mice exhibited a dramatic increase in plasma ketone body levels from p0 to p14, representing an increased metabolic demand for hepatic ketogenesis during postnatal development (**Fig. 5D**). These elevations in plasma ketone levels, however, were not observed in *Hmgcs2*-KO mice with consistently low *Hmgcs2* mRNA expression, thereby further confirming a phenotypic knockout of ketogenesis. Interestingly, *Hmgcs2*-HET mice had significantly ($P = 0.04$) greater plasma ketone levels in comparison to WT mice at p14, despite lower *Hmgcs2* mRNA levels, possibly indicating a compensatory increase in ketogenesis as a result of reduced *Hmgcs2* gene dosage. Ketogenic deficiency resulted in a mild but significant reduction in growth at p14, as observed by lower body weight of *Hmgcs2*-KO mice (**Fig. 5E**), which appeared to be largely due to a decrease in lean mass (**Fig. 5F**), compared to WT mice. Fat mass, however, was slightly greater in *Hmgcs2*-KO mice compared to both WT ($P = 0.09$) and *Hmgcs2*-HET ($P < 0.0001$) mice.

Notably, the livers of *Hmgcs2*-KO mice were significantly heavier relative to WT and *Hmgcs2*-HET mice at p4 and p14 (**Fig. 6A**). P14 *Hmgcs2*-KO livers were pale, large, and fattier in comparison to the dark healthy livers of WT mice (**Fig. 6B-C**). H&E and Plin2 stainings of liver sections at p14 further confirmed the accumulation of small lipid droplets, microvesicular steatosis, in the hepatocytes of *Hmgcs2*-KO mice (**Fig. 6D**). Consistent with the staining, Plin2 mRNA expression, which noticeably increased from p0 to p14 in *Hmgcs2*-KO mice, was significantly higher in comparison to WT and *Hmgcs2*-HET mice at p14 (**Fig. 6E**). Other lipid accumulation gene markers, including *Pparg* and *Fsp27*, were also markedly elevated in livers of *Hmgcs2*-KO mice compared to WT and *Hmgcs2*-HET mice, supporting the extensive fatty liver phenotype in the *Hmgcs2* deficient mice (**Fig. 7A**). In addition, *Hmgcs2*-KO mouse livers showed decreased expression of lipid synthesis gene markers, such as *Srebp1c*, *Acc1*, and *Fasn* (**Fig. 7B**) and increased expression of lipid oxidation gene markers, including *Ppara*, *Cpt1a*, and *Mcad* (**Fig. 7C**), possibly suggesting a compensatory suppression and activation of these pathways, respectively, in order to offload the large amounts of lipid accumulation in the liver. Convincingly, this metabolic phenotype in postnatal *Hmgcs2*-KO mice was consistently observed in a very recent study utilizing a different mouse model of *Hmgcs2* deficiency[115]. Therefore, these results collectively suggest a causal role of impaired ketogenesis, specifically Hmgcs2 deficiency, in the development of fatty liver disease in postnatal mice, analogous to the rare inborn mHS deficiency disorder, in which patients frequently present with fatty liver[62,80,81,116].

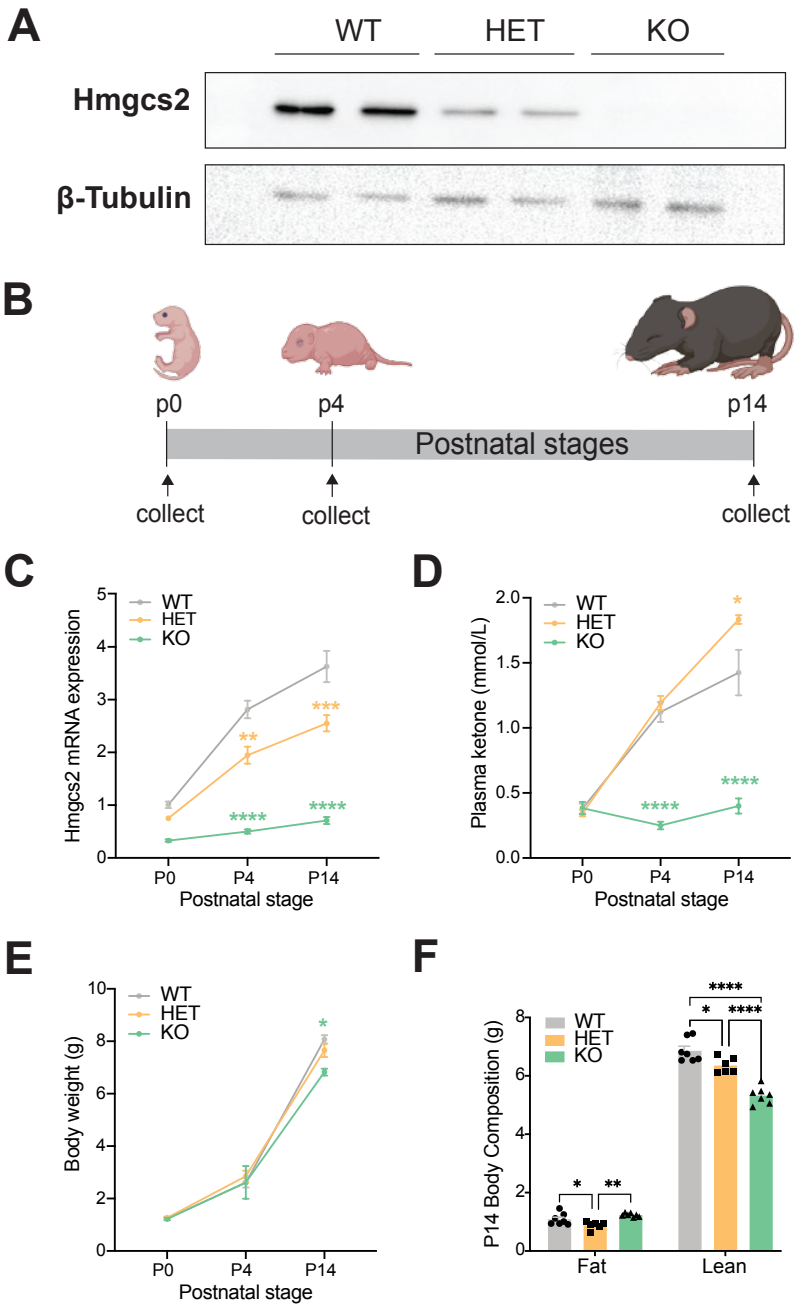

FIGURE 5 | Ketogenic deficiency through *Hmgcs2* knockout results in the reduction of body weight and fat mass in postnatal mice. (**A**) Liver Hmgcs2 protein expression in wild-type (WT), *Hmgcs2*-heterozygous (HET) and knockout (KO) mice. (**B**) Schematic representing the postnatal stages of p0, p4, and p14 at which the mice were examined. (**C**) *Hmgcs2* gene expression in the liver, **(D)** plasma ketone bodies, (**E**) and body weights during postnatal development. (**F**) Body composition analysis showing fat and lean masses in WT, HET and KO mice at p14. Data represented as mean ± SEM. Statistical analysis performed by one and two-way ANOVA. *$P \leq 0.05$; **$P \leq 0.01$; ***$P \leq 0.001$; ****$P \leq 0.0001$. (Created with Biorender.com).

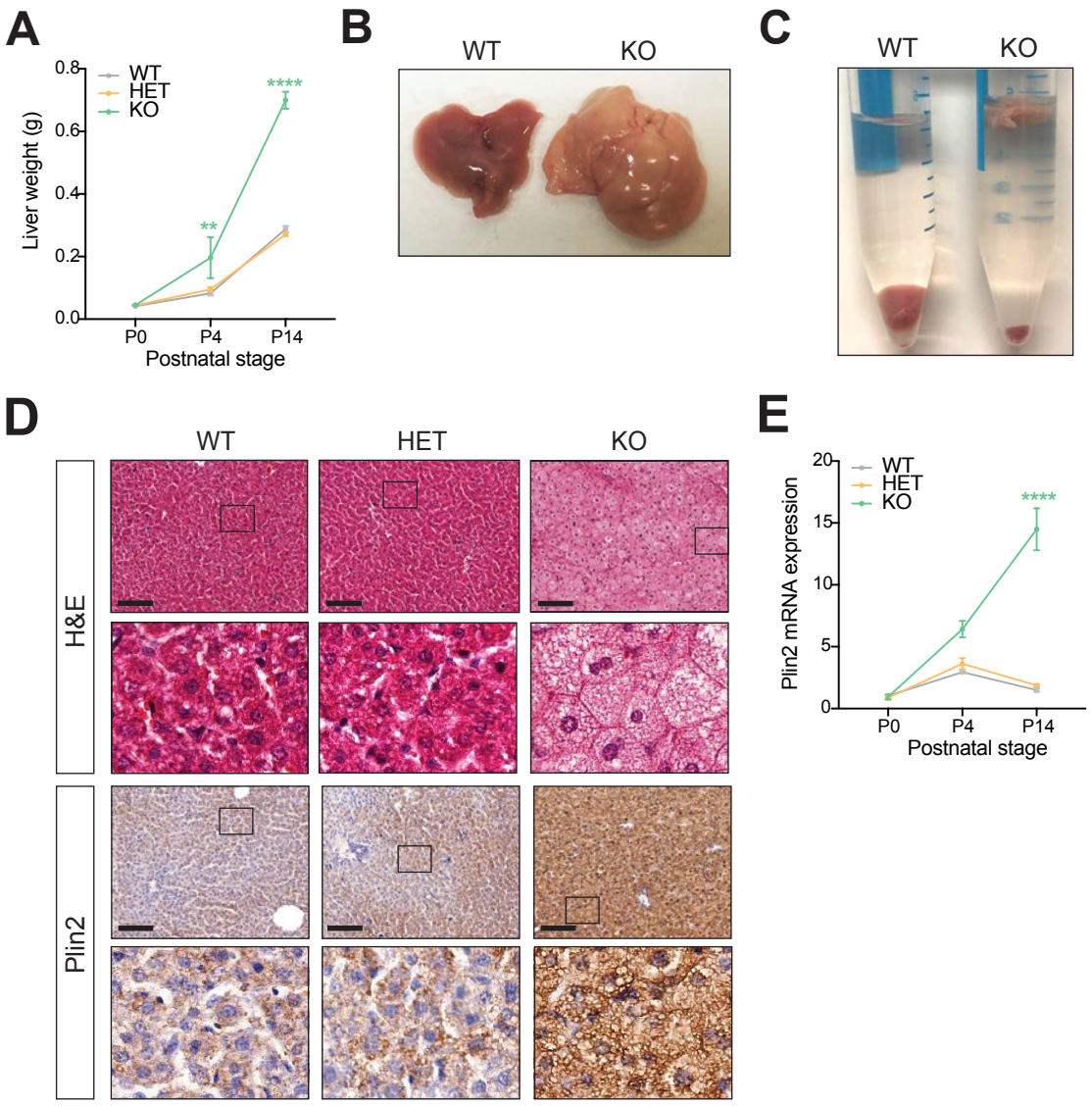

FIGURE 6 | Ketogenic deficiency through *Hmgcs2* knockout results in fatty liver development in postnatal mice. (**A**) Liver weight during postnatal developmental stages of WT, *Hmgcs2*- HET and KO mice. Representative liver image of p14 WT and KO mice (**B**) upon collection and (**C**) fixed in tube containing 4% PFA. (**D**) H&E and anti-Plin2 IHC stainings of p14 WT, HET and KO mouse liver sections. Scale bar = 100μm. Boxes indicate regions of higher magnification. (**E**) Liver RT-qPCR of *Plin2* in postnatal mice. Data represented as mean ± SEM. Statistical analysis performed by two-way ANOVA. $^{**}P \leq 0.01$; $^{****}P \leq 0.0001$.

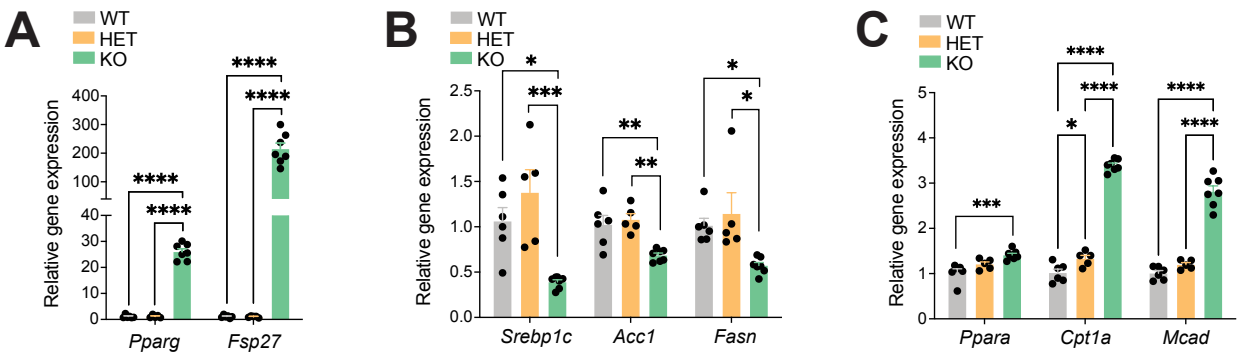

FIGURE 7 | Ketogenic deficiency through *Hmgcs2* knockout results in differential expression of genes involved in lipid metabolism in livers of p14 mice. Liver RT-qPCR of (**A**) lipid accumulation markers *Pparg*, *Fsp27*, (**B**) lipid synthesis mediators *Srebp1c*, *Acc1*, *Fasn* and (**C**) lipid oxidation mediators *Ppara*, *Cpt1a*, *Mcad* in p14 WT, *Hmgcs2*- HET and -KO mice. Data represented as mean ± SEM. Statistical analysis performed by one-way ANOVA. **P* ≤ 0.05; ***P* ≤ 0.01; ****P* ≤ 0.001; *****P* ≤ 0.0001.

3.3. A fat-enriched nutritional environment is a prerequisite for fatty liver development in ketogenic deficiency

The increased production and utilization of ketone bodies in the postnatal period has been attributed to a surplus of dietary fat provided in the form of breast milk during suckling[39,43,44,46,114]. To determine the contribution of this fat-enriched dietary environment in the development of the fatty liver phenotype of postnatal ketogenic deficient mice, we subjected WT and *Hmgcs2*-KO mice to early weaning (**Fig. 8A**), in order to achieve a transition from the high-fat, low-carbohydrate breast milk (~29% fat, 2% carbohydrate) to the low-fat, high carbohydrate chow diet (9% fat, 44.9% carbohydrate)[43,46,103,104]. Early-wean mice were separated from the mother at p14, a week prior to normal weaning, and were provided with a normal chow diet in the form of soaked cubes, whereas control suckling mice were kept with the mother and continued to have breast milk. The livers of both early-wean and suckling mice were examined at p21. Consistent with the earlier postnatal stages of p0, p4 and p14, hepatic *Hmgcs2* mRNA expression remained significantly low in p21 suckling and early-wean *Hmgcs2*-KO mice (**Fig. 8B**). Notably, the difference in plasma ketone levels between p21 WT and *Hmgcs2*-KO mice seen at suckling was reduced by early weaning, as it mildly decreased plasma ketone levels in WT mice (**Fig. 8C**). This suggests a reduced metabolic demand for ketogenesis at early weaning as a result of a change in dietary environment. *Hmgcs2*-KO early-wean mice had slightly lower body weights relative to WT mice (**Fig. 8D**), which was consistent with their lean mass, while no difference in fat mass was observed (**Fig. 8E-F**).

Importantly, early weaning significantly ($P = 0.043$) reduced the liver weights in *Hmgcs2*-KO mice, thereby making the liver weight difference between WT and *Hmgcs2*-KO mice seen at suckling indistinguishable (**Fig. 9A**). Indeed, upon collection at p21, *Hmgcs2*-KO early-wean mice showed healthier livers in comparison to the enlarged and fatty livers of *Hmgcs2*-KO

suckling mice (**Fig. 9B**), suggesting reductions in liver fat content. H&E and Plin2 stainings of p21 liver sections confirmed that, in contrast to the severe microvesicular steatosis in *Hmgcs2*-KO mice at suckling, a marked reduction in lipid accumulation was observed in the livers of *Hmgcs2*-KO early-wean mice, where their phenotype was comparable to WT mice (**Fig. 9C**). Specifically, early weaning removed lipid droplets almost entirely at the center of the liver in *Hmgcs2*-KO mice, while some lipid accumulation remained at the periphery of the liver, mainly in the form of macrovesicular steatosis (i.e., large lipid droplets displacing nuclei within hepatocytes) (**Fig. 10)**. Additionally, while *Hmgcs2*-KO mice at suckling had greater expression of hepatic lipid accumulation gene markers (*Pparg*, *Fsp27*, *Plin2*) in comparison to WT suckling mice, early weaning significantly lowered this marker gene expression in *Hmgcs2*-KO mouse livers, further supporting an improvement in the fatty liver phenotype (**Fig. 11**). Together, these results suggest that a fat-enriched dietary environment is required for ketogenic deficiency-induced fatty liver disease.

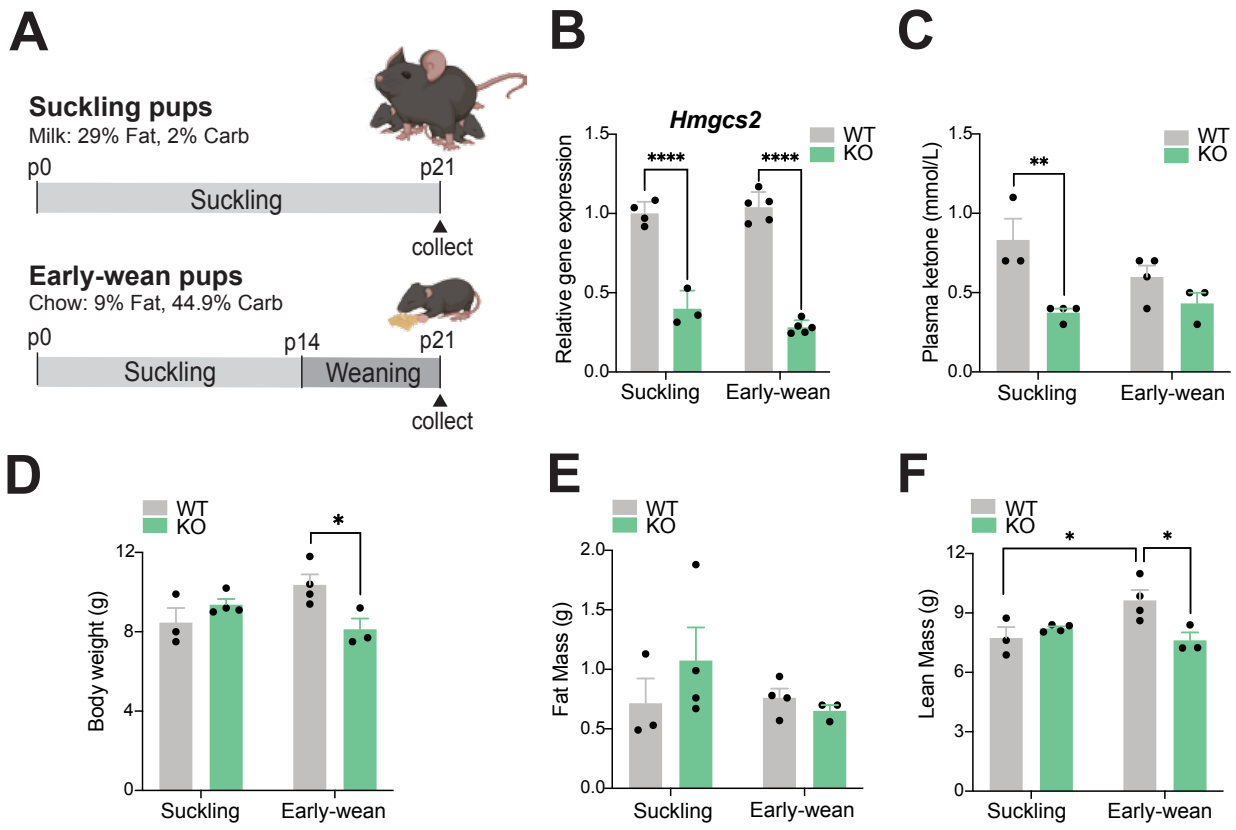

FIGURE 8 | The removal of a fat-enriched dietary environment reduces ketogenic demand of postnatal wild-type mice. (**A**) Schematic representing the early weaning of postnatal WT and *Hmgcs2*-KO mice. Early-wean mice were separated from their mother at p14 and transitioned from a high-fat breast milk (29% fat, 2% carbohydrate) to a normal chow diet (9% fat, 44.9% carbohydrate). Suckling control mice remained on breast milk feeding until collection at p21. (**B**) *Hmgcs2* gene expression in the liver, (**C**) plasma ketone bodies, (**D**) body weights, (**E**) fat masses, (**F**) and lean masses of suckling and early-wean WT and *Hmgcs2*-KO mice at p21. Data represented as mean ± SEM. Statistical analysis performed by the two-way ANOVA. **P* ≤ 0.05; ***P* ≤ 0.01; *****P* ≤ 0.0001. (Created with Biorender.com).

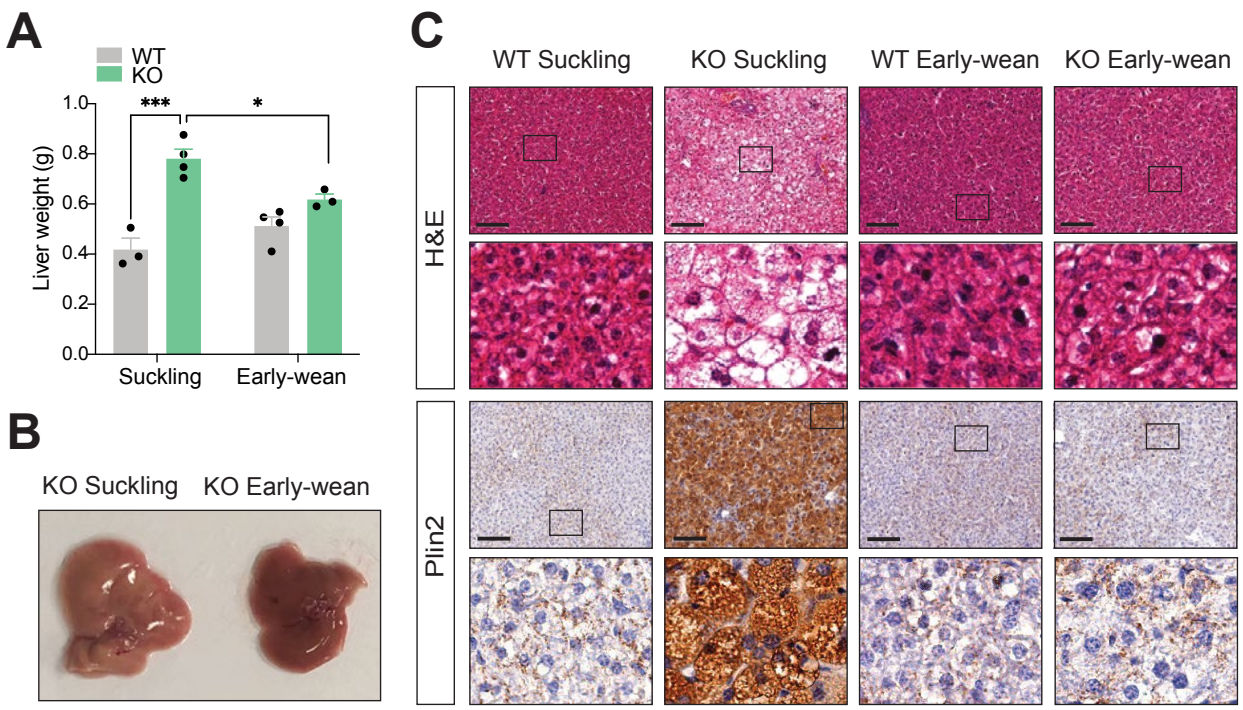

FIGURE 9 | The removal of a fat-enriched dietary environment prevents fatty liver development in postnatal ketogenic deficient mice. (**A**) Liver weights of suckling and early-wean WT and *Hmgcs2*-KO mice at p21. (**B**) Representative liver image of *Hmgcs2*-KO suckling and early-wean mice at p21. (**C**) H&E and anti-Plin2 IHC stainings of liver sections. Scale bar = 100 μm. Boxes indicate regions of higher magnification. Data represented as mean ± SEM. Statistical analysis performed by the two-way ANOVA. $*P \leq 0.05$; $***P \leq 0.001$.

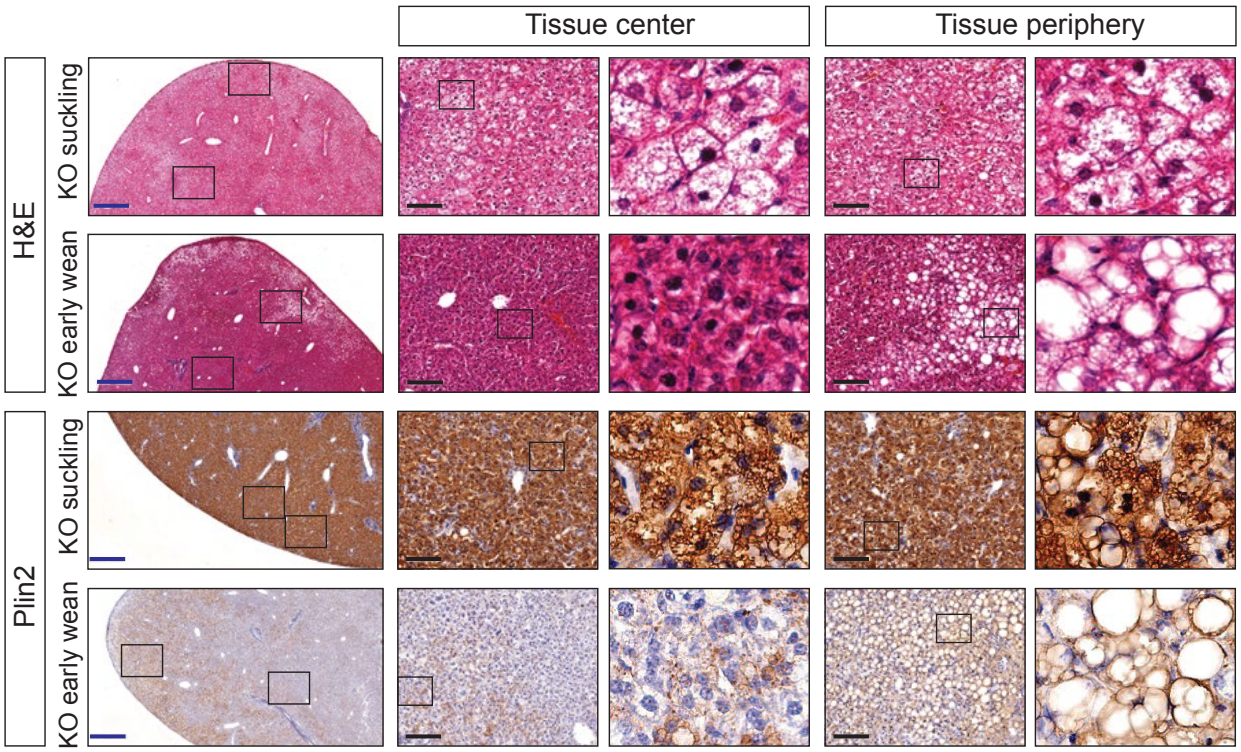

FIGURE 10 | The removal of a fat-enriched dietary environment promotes a shift from microvesicular to macrovesicular hepatosteatosis in postnatal ketogenic deficient mice. H&E and Plin2 IHC stainings of liver sections of p21 *Hmgcs2*-KO mice at suckling and early weaning, with magnifications at tissue center and periphery. Blue scale bar = 500μm. Black scale bar = 100μm. Boxes indicate regions of higher magnification.

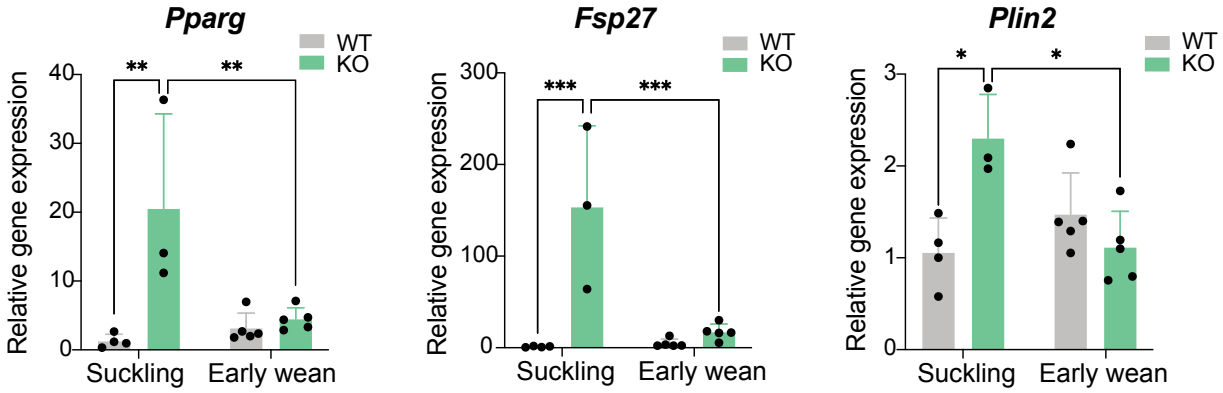

FIGURE 11 | The removal of a fat-enriched dietary environment suppresses lipid accumulation marker gene expression in livers of postnatal ketogenic deficient mice. Hepatic gene expression analysis of lipid accumulation markers *Pparg*, *Fsp27*, and *Plin2* of suckling and early-wean WT and *Hmgcs2*-KO mice at p21. Data represented as mean ± SEM. Statistical analysis performed by the two-way ANOVA. **P* ≤ 0.05; ***P* ≤ 0.01; ****P* ≤ 0.001.

3.4. Reduced ketogenesis in adult mice increases susceptibility to NAFLD development

As the severity of NAFLD is negatively correlated with ketogenic function[98], we next questioned whether the degree of ketogenic function affects the progression of NAFLD. Interestingly, while plasma ketone levels during postnatal development were indistinguishable between WT and *Hmgcs2*-HET mice, 8-week-old *Hmgcs2*-HET mice had significantly lower fasting-induced plasma ketone levels compared to WT mice (**Fig. 12A**), suggesting that reduced *Hmgcs2* gene dosage decreased ketogenic function in adult mice, while no differences in fed and fasted glucose levels were observed (**Fig. 12B**). As this finding provides a means to test the effect of reduced ketogenesis on NAFLD development, we subjected 8-week-old *Hmgcs2*-HET mice and littermate WT mice to 45% HFD for 8 weeks (**Fig. 12C**). Interestingly, upon HFD feeding, *Hmgcs2*-HET mice gained more body weight compared to WT mice (**Fig. 12D**), mainly attributed to increases in fat mass (**Fig. 12E**) as well as a slight increase in lean mass (**Fig. 12F**). A difference in fasting-induced ketogenesis between WT and *Hmgcs2*-HET mice was maintained after HFD feeding (**Fig. 12G**), comparable to the values observed at 8-weeks-old. On the other hand, fasting-induced decrease in plasma glucose was not observed in both WT and *Hmgcs2*-HET mice at post-HFD (**Fig. 12H**), suggesting a HFD-induced dysregulation of the fasting glucose response[117]. Post-HFD *Hmgcs2*-HET mice also had greater plasma glucose levels relative to WT mice in the fed state ($P = 0.056$), which was not observed at pre-HFD, indicating the development of HFD-induced NAFLD-related hyperglycemia in *Hmgcs2*-HET mice. To further investigate glucose homeostasis in these mice, an intraperitoneal GTT and ITT were performed post-HFD (**Fig. 13A-B**). Plasma glucose levels in GTT, specifically at the 60- and 120-minute timepoint post-glucose administration, and area-under-the-curve (AUC) were significantly greater in *Hmgcs2*-HET mice compared to WT mice. Interestingly, no difference in insulin sensitivity was noted between WT and *Hmgcs2*-HET mice, as shown by plasma glucose levels or

AUC with ITT. Importantly, the livers of *Hmgcs2*-HET mice were comparatively heavier than WT mice ($P = 0.087$), while no differences in inguinal and perigonadal white tissue (IWAT, PWAT) weight was observed (**Fig. 14A**). H&E and Plin2-stainings of liver sections confirmed greater hepatosteatosis, specifically microvesicular steatosis, in *Hmgcs2*-HET mice (**Fig. 14B**). Together, these findings demonstrate that the degree of ketogenic function, specifically gene dosage of *Hmgcs2*, contributes to NAFLD pathogenesis in adult mice.

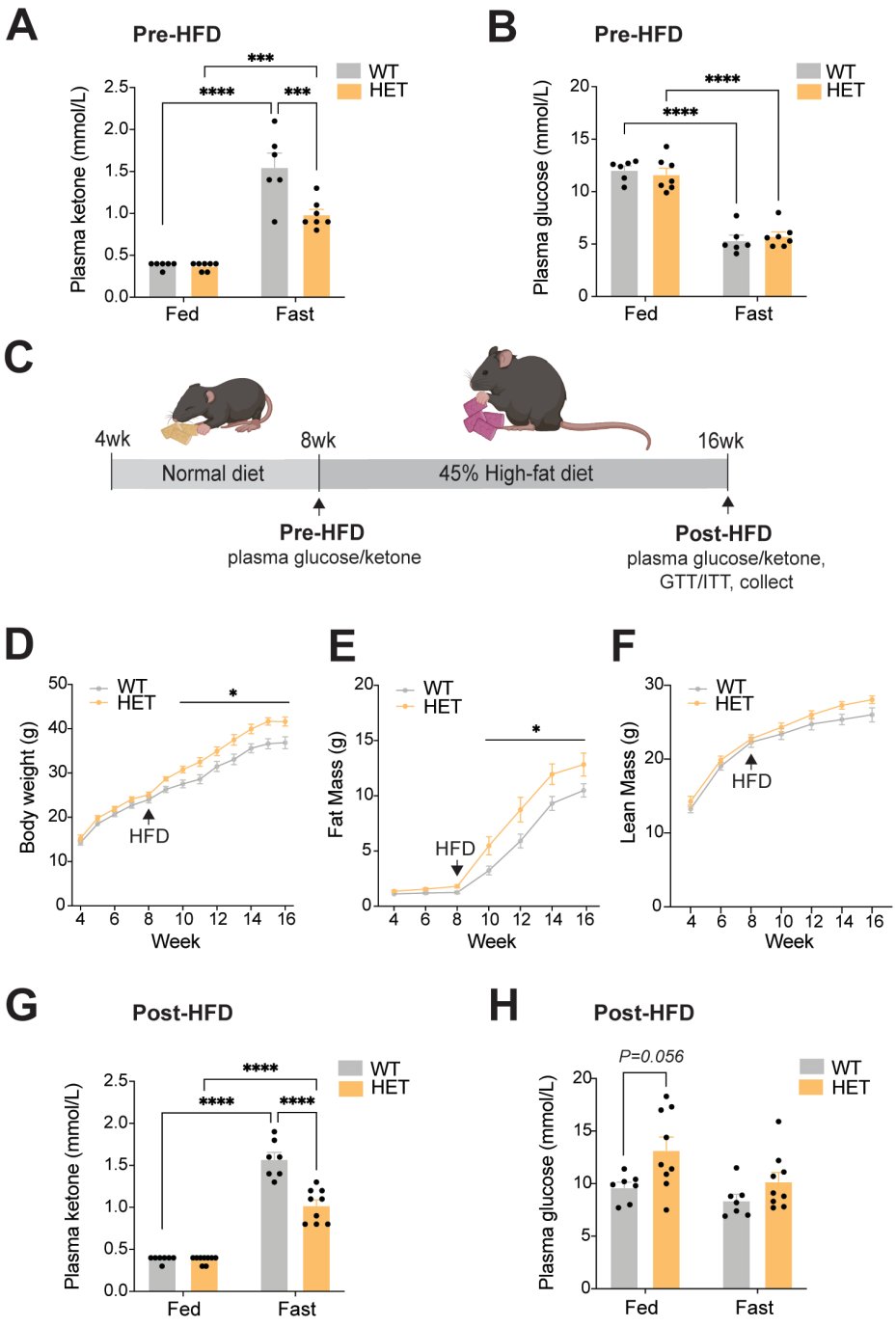

FIGURE 12 | Ketogenic insufficiency increases the susceptibility of HFD-induced metabolic dysfunction. Plasma levels of (**A**) ketone bodies and (**B**) glucose in 8-week-old WT and *Hmgcs2*-HET mice (pre-HFD). (**C**) Schematic for assessment of NAFLD development in WT and *Hmgcs2*-HET mice placed on 8-weeks of HFD. (**D**) Weekly measurements of body weights. Biweekly measurements of (**E**) fat and (**F**) lean masses. Plasma levels of (**G**) ketone bodies and (**H**) glucose in post-HFD WT and *Hmgcs2*-HET mice. Data represented as mean ± SEM. Statistical analysis performed by two-way ANOVA. *$P \leq 0.05$; ***$P \leq 0.001$; ****$P \leq 0.0001$. (Created with Biorender.com).

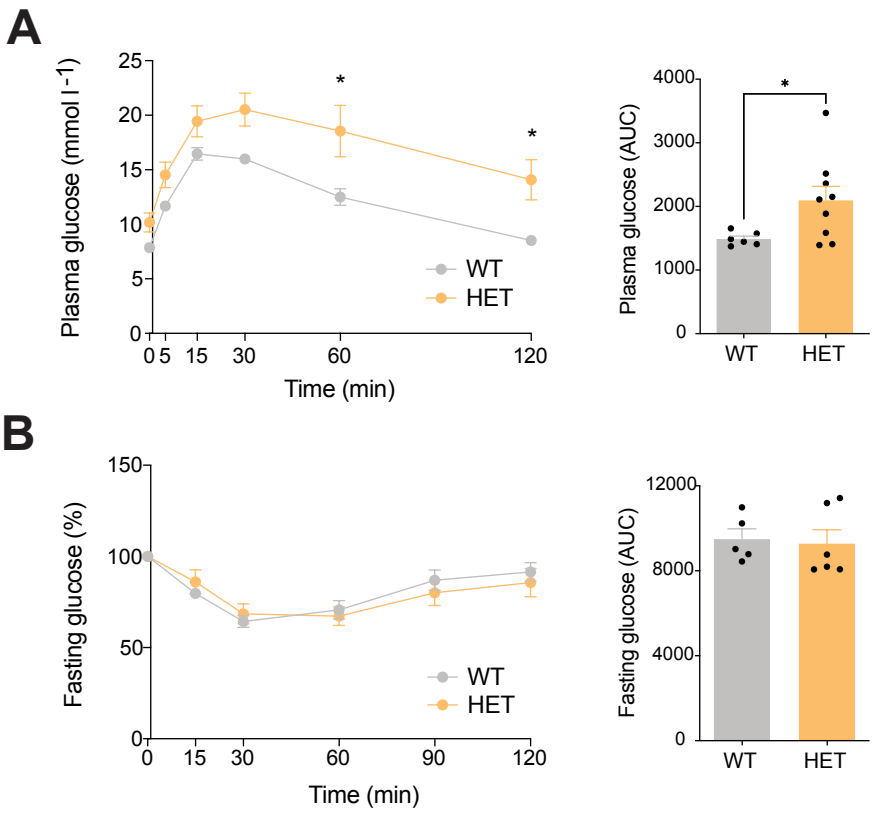

FIGURE 13 | Ketogenic insufficiency results in impaired HFD-induced glucose tolerance. Intraperitoneal (**A**) glucose tolerance test (GTT) and (**B**) insulin tolerance test (ITT) and their respective AUCs of post-HFD WT and *Hmgcs2*-HET mice. Data represented as mean ± SEM. Statistical analysis performed by student's *t*-test and two-way ANOVA. *$P \leq 0.05$.

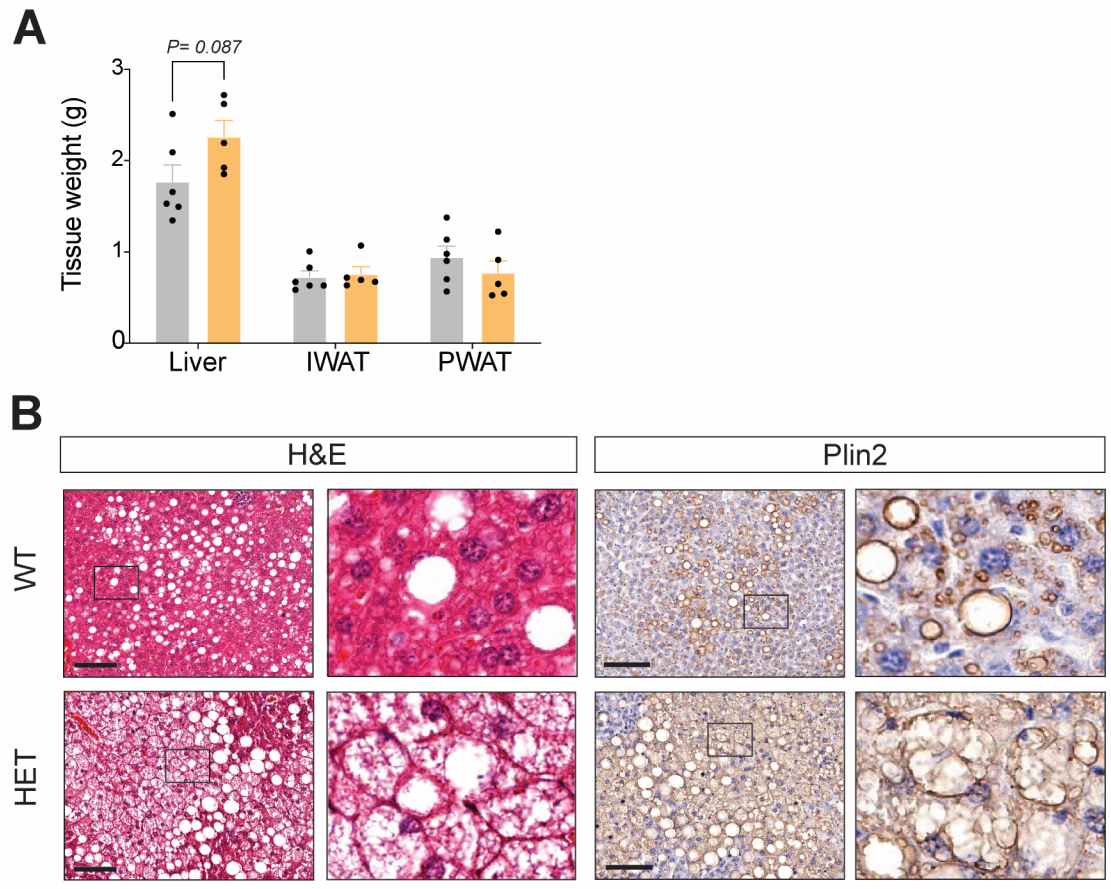

FIGURE 14 | Ketogenic insufficiency increases the susceptibility of HFD-induced hepatosteatosis. (**A**) Tissue weights of liver, inguinal and perigonadal white adipose (IWAT, PWAT) of WT and *Hmgcs2*-HET mice. (**B**) Representative H&E and anti-Plin2 IHC staining of liver sections. Scale bar = 100 μm. Boxes indicate regions of higher magnification. Data represented as mean ± SEM. Statistical analysis performed by student's *t*-test.

3.5. Increased ketogenesis through *HMGCS2* overexpression improves HFD-induced NAFLD in mice

Next, we tested whether increased ketogenesis by modulating Hmgcs2 expression is sufficient to treat NAFLD in mice. A previous study has demonstrated in an *in vitro* model that *HMGCS2* overexpression (OE) in HepG2 hepatocytes can sufficiently activate ketogenesis and increase fatty acid oxidation[118]. Thus, to drive ketogenesis *in vivo*, we intravenously injected 34-weeks of HFD-induced NAFLD mice with adenovirus overexpressing human *HMGCS2* (Ad-*HMGCS2*) (**Fig. 15A**), which has a 95% protein sequence homology to mouse Hmgcs2. A *GFP*-expressing adenovirus (Ad-*GFP*) was used for control mice. Human *HMGCS2* mRNA expression was increased in Ad-*HMGCS2* mouse livers compared to Ad-*GFP* mouse livers ($P < 0.0001$) (**Fig. 15B**), while mouse *Hmgcs2* mRNA expression was reduced ($P = 0.0003$) (**Fig. 15C**), suggesting a plausible compensatory suppression of endogenous *Hmgcs2* as a result of human *HMGCS2*-OE. Plasma β-OHB ketone levels were also significantly increased in Ad-*HMGCS2* mice (**Fig. 15D**), confirming successful phenotypic activation of ketogenesis.

HMGCS2-OE led to gradual reductions in body weight at 2- and 3-weeks post-virus injection compared to control (**Fig. 16A**), which was mainly attributed to decreases in fat mass, not lean mass (**Fig. 16B-C**). Intraperitoneal GTT and ITT performed both pre- and post-virus injection revealed that glucose handling and insulin sensitivity were significantly improved in Ad-*HMGCS2* mice, compared to Ad-*GFP* mice (**Fig. 16D-E**). Notably, at collection, livers of Ad-*HMGCS2* mice were dark and healthy in contrast to the pale and fatty livers of Ad-*GFP* control mice (**Fig. 17A**), although no difference in liver weight was observed (**Fig. 17B**). Histological analyses with H&E and Plin2 stainings also showed an improvement in hepatosteatosis in Ad-*HMGCS2* mice, specifically marked reductions in the advanced

microvesicular steatosis seen in Ad-*GFP* mice (**Fig. 17C**). On the other hand, PSR staining showed no difference in hepatic fibrosis between Ad-*GFP* and Ad-*HMGCS2* mice. Supporting a reduction in liver fat content, gene expression analysis showed significantly lower marker gene expression of lipid accumulation (*Pparg*, *Fsp27*, *Plin2*) and lipid synthesis (*Srebp1c*, *Acc1*, *Fasn*) in Ad-*HMGCS2* mice (**Fig. 17D-E**). Together, these results suggest that increased ketogenesis by *HMGCS2*-OE effectively improved hepatosteatosis and its associated glucose abnormalities in mice.

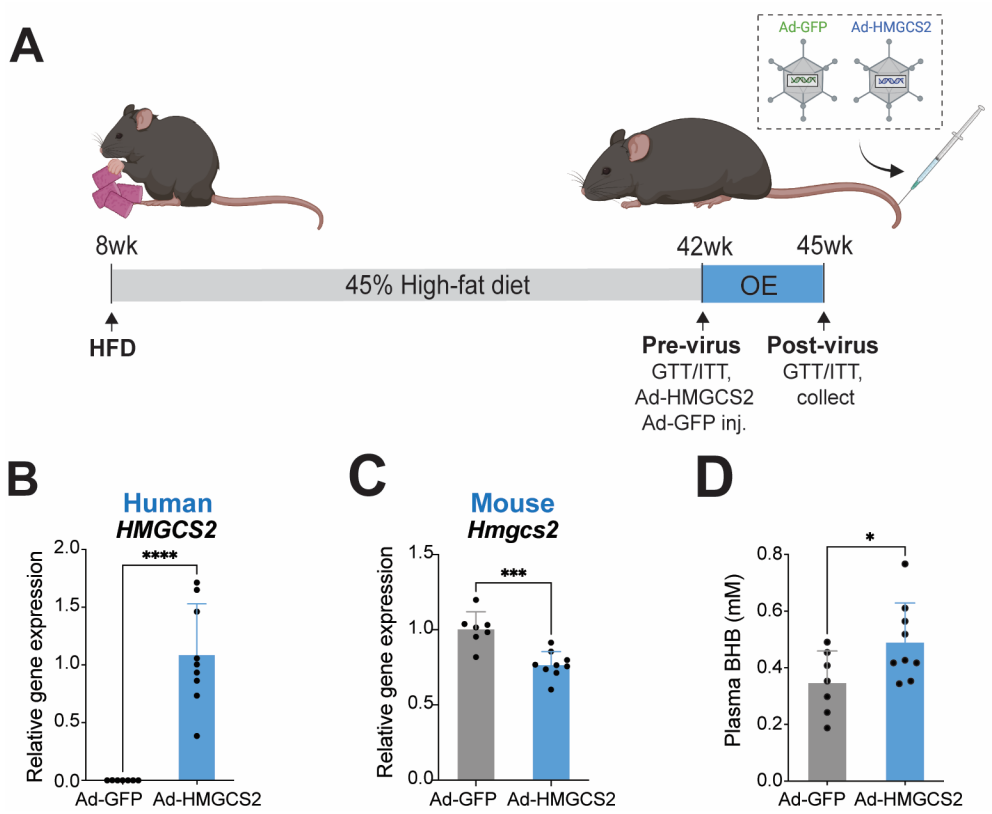

FIGURE 15 | Adenovirus-mediated *HMGCS2* overexpression *in vivo* results in ketogenesis activation. (**A**) Schematic of NAFLD mice fed with HFD for 34-weeks that were intravenously administered with adenovirus overexpressing *GFP* (Ad-*GFP*) or *HMGCS2* (Ad-*HMGCS2*) and maintained for 3 weeks prior to collection. Liver mRNA expression of (**B**) human *HMGCS2* and (**C**) mouse *Hmgcs2*. (**D**) Plasma levels of β-hydroxybutyrate (BHB). Data represented as mean ± SEM. Statistical analysis performed by student's *t*-test. **P* ≤ 0.05; ****P* ≤ 0.001; *****P* ≤ 0.0001. (Created with Biorender.com).

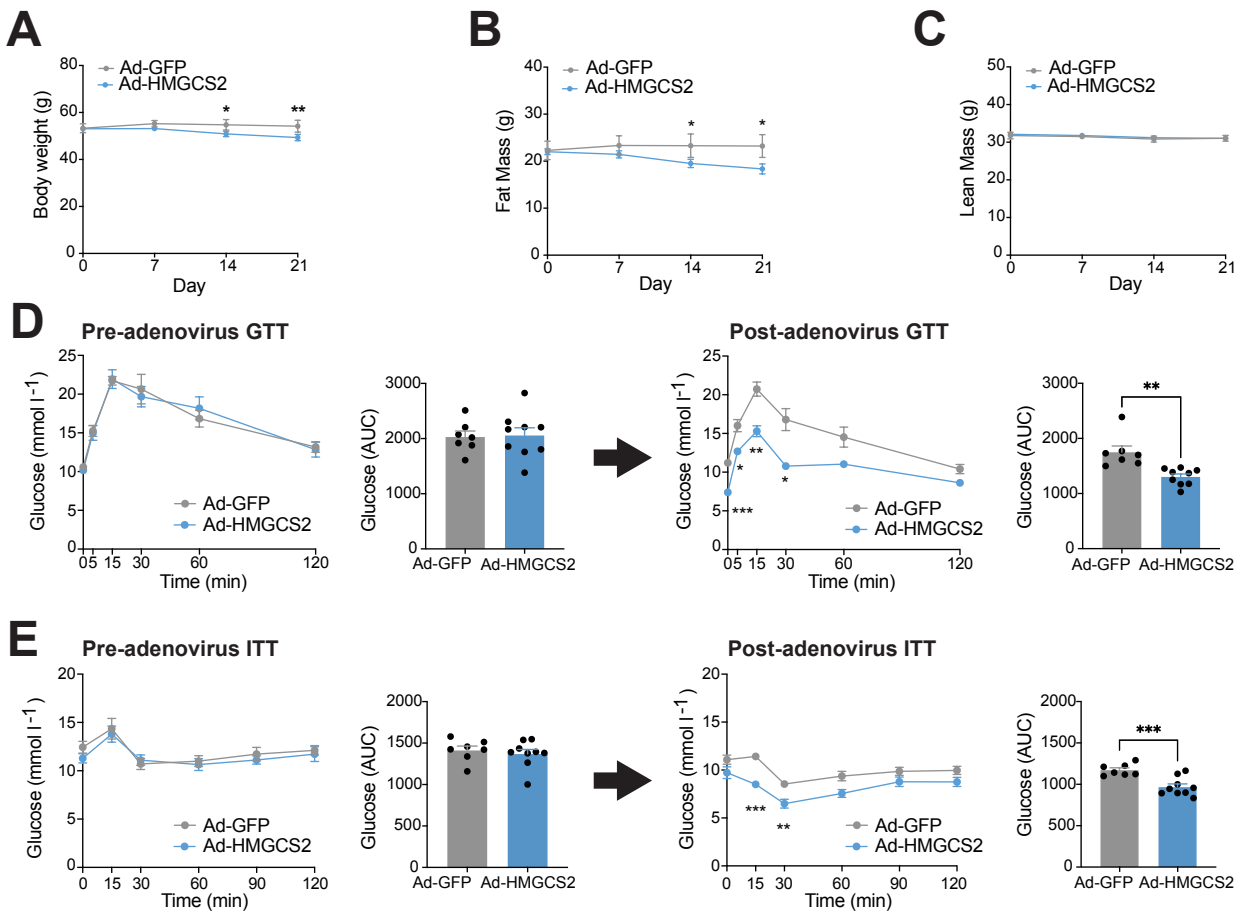

FIGURE 16 | Ketogenesis activation through *HMGCS2* overexpression results in gross metabolic improvements in HFD-induced NAFLD mice. Weekly measurements of (**A**) body weight, (**B**) fat mass and (**C**) lean mass for 3 weeks post-virus administration of Ad-*GFP* and Ad-*HMGCS2* mice. Pre- and post-virus (**D**) GTT and (**E**) ITT and their respective AUCs. Data represented as mean ± SEM. Statistical analysis performed by student's *t*-test and two-way ANOVA. **P* ≤ 0.05; ***P* ≤ 0.01, ****P* ≤ 0.001.

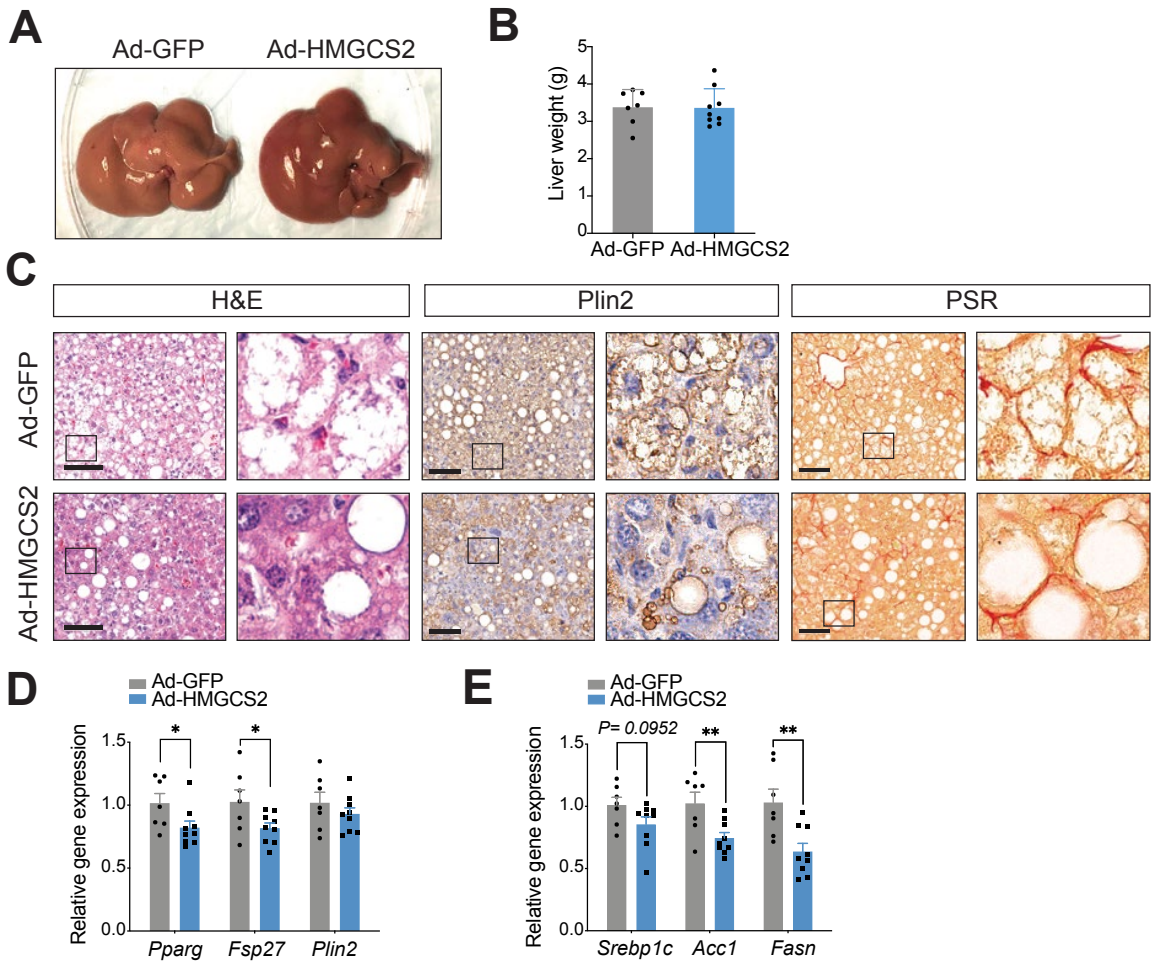

FIGURE 17 | Ketogenesis activation through *HMGCS2* overexpression results in the improvement of hepatosteatosis in HFD-induced NAFLD mice. (**A**) Representative liver image and (**B**) liver wight at 3-weeks post-virus administration of Ad-*GFP* and Ad-*HMGCS2* mice. (**C**) H&E, anti-Plin2 IHC, and Picrosirius red (PSR) stainings of liver sections. Scale bar = 100 μm. Boxes indicate regions of higher magnification. Gene expression analysis of (**D**) lipid accumulation markers (*Pparg*, *Fsp27*, *Plin2*) and (**E**) lipid synthesis mediators (*Srebp1c*, *Acc1*, *Fasn*). Data represented as mean ± SEM. Statistical analysis performed by student's *t*-test. **P* ≤ 0.05; ***P* ≤ 0.01.

3.6. *HMGCS2* overexpression *in vitro* improves NAFLD-related lipid accumulation in hepatocytes

Since the liver contains heterogenous cell populations, including hepatocytes, Kupffer cells and hepatic stellate cells[119], we next examined the hepatocyte-specific anti-steatosis effect of *HMGCS2*-OE by testing it against an *in vitro* model of hepatic lipid accumulation. Oleic acid, known to induce lipid accumulation in HepG2 cells[120,121], was administered at 0-hours, followed by Ad-*GFP* or Ad-*HMGCS2* transfection at 24-hours and cell collection and assessment at 48-hours (**Fig. 18A**). Elevated HMGCS2 mRNA ($P < 0.0001$) and protein ($P = 0.0002$) expression confirmed successful overexpression (**Fig. 18B-C**). Visualization of neutral lipids, such as triglycerides, with Oil-red O staining of HepG2 cells and its quantification, showed that the significant lipid accumulation seen in Ad-*GFP*-treated control cells ($P = 0.0001$) was markedly reduced with *HMGCS2*-OE ($P = 0.0002$) (**Fig. 18D-E**), thus validating the comparable reduction of hepatic lipid accumulation seen *in vivo*. Also, consistent with *in vivo* study, reduced mRNA levels of lipid synthesis (*SREBP1C*) and accumulation (*PLIN2*) marker genes were observed in *HMGCS2*-OE cells (**Fig. 18F**). Collectively, these findings further support the direct anti-steatosis role of *HMGCS2*-OE in hepatocytes.

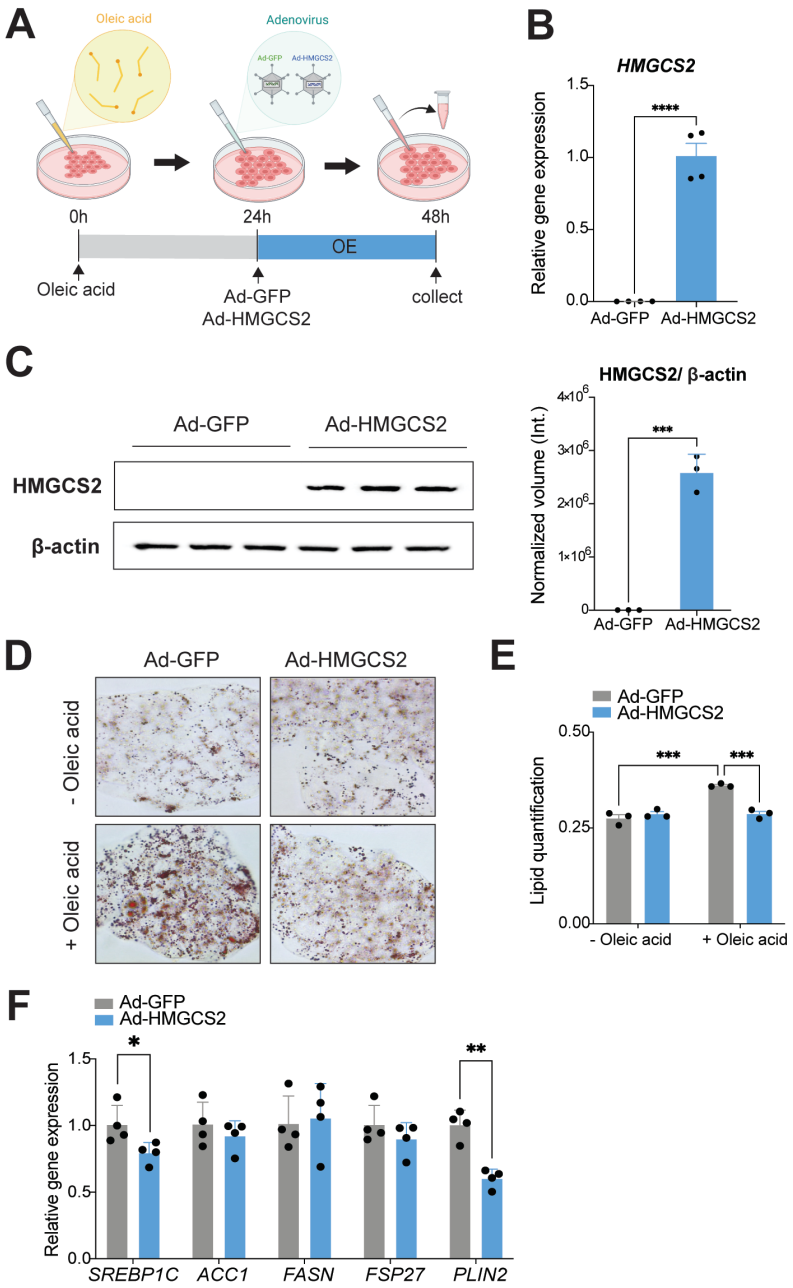

FIGURE 18 | *HMGCS2* overexpression *in vitro* ameliorates lipid accumulation in HepG2 cells. (**A**) Schematic representing timeline of *in vitro* experiment, starting with oleic acid treatment at 0-hours, adenovirus mediated overexpression of *GFP* (Ad-*GFP*) or *HMGCS2* (Ad-*HMGCS2*) at 24-hours and cell collection at 48-hours. (**B**) RT-qPCR and (**C**) western blot quantification of HMGCS2 levels in HepG2 cells. (**D**) Oil-red-O staining and (**E**) its quantification of Ad-*GFP* and Ad-*HMGCS2* treated HepG2 cells in the absence (-) and presence (+) of oleic acid. (**F**) RT-qPCR of lipid synthesis (*SREBP1C*, *ACC1*, *FASN*) and accumulation (*FSP27*, *PLIN2*) genes in Ad-*GFP* and Ad-*HMGCS2* treated HepG2 cells. Data represented as mean ± SEM. Statistical analysis performed by student's *t*-test and two-way ANOVA. *$P \leq 0.05$; **$P \leq 0.01$, ***$P \leq 0.001$; ****$P \leq 0.0001$. (Created with Biorender.com).

3.7. Increased ketogenesis through *HMGCS2* overexpression regulates central metabolic pathways in the liver

To gain mechanistic insights into the metabolic improvements by *HMGCS2*-OE, we conducted a metabolomics analysis in our mouse model. Specifically, to capture early metabolic changes by *HMGCS2*-OE, rather than the final metabolic outcomes, liver tissue was harvested from HFD-induced NAFLD mice (32-weeks on 45% kcal fat diet) just 4-days after Ad-*HMGCS2* virus injection (**Fig. 19A**). Notably, acute *HMGCS2*-OE significantly decreased the transcript levels of lipid accumulation and synthesis genes, such as *Plin2*, *Srebp1c* and *Fasn*, in the liver, suggesting active modulation in lipid metabolism (**Fig. 19B-C**). A total of 119 metabolites were identified through an untargeted LC-MS-based metabolomics protocol combining triple quadrupole (QQQ) and quadrupole time-of-flight (QTOF) mass spectrometers. Partial Least Squares – Discriminant Analysis (PLS-DA), a supervised method of pattern recognition, was applied, which showed a clear distinction of the Ad-*HMGCS2*-treated group from the Ad-*GFP* control group, along both the primary (31.4%) and secondary (11.1%) components (**Fig. 20A**). Differential expression analysis for individual metabolites identified a total of 37 significantly ($P < 0.05$) differential metabolites between the two groups, as shown in the heatmap (**Fig. 20B**). Of these, 28 metabolites were upregulated, while 9 were downregulated in Ad-*HMGCS2* compared to Ad-*GFP* mouse livers. To gain the functional insight on these metabolites, a quantitative pathway enrichment analysis using a KEGG metabolic pathway database was performed, generating the top 25 enriched metabolite sets (**Fig. 20C**). Specifically, we found a significant enrichment of *HMGCS2*-induced metabolites in central hepatic pathways, mostly upstream of ketogenesis, including glycolysis, pentose phosphate pathway (PPP), purine/pyrimidine metabolism, fatty acid degradation and the TCA cycle. Metabolites within these pathways were further specified through individual box plots in a pathway-metabolite summary schematic (**Fig. 21**). The

concentrations of metabolites and energy substrates feeding into these pathways, such as UDP-glucose/galactose and hexoses in glycolysis, $NADP^+$ in PPP, ADP ribose and GMP in purine metabolism, glutamine in purine and pyrimidine metabolism[122], and NAD^+ in TCA cycle, were decreased, while all other metabolic intermediates produced from these pathways were increased with *HMGCS2*-OE, suggesting an improved metabolic flux of these pathways. Notably, the concentration of Coenzyme A (CoA), associated with increased ketogenesis, was significantly greater in Ad-*HMGCS2* mouse livers compared to Ad-*GFP*. In support of this increased ketogenesis, Ad-*HMGCS2* mouse livers showed greater levels of the amino acids phenylalanine and tyrosine, feeding into ketogenic pathways, while reduced levels of glutamine, serine, and threonine, with the exception of aspartate, feeding into gluconeogenic pathways (**Table 4**). Additionally, metabolites involved in amino acid synthesis, specifically 2-aminoadipic acid in lysine biosynthesis and N-acetylglutamic acid in arginine biosynthesis, were increased with *HMGCS2*-OE. Together, these results suggest that the activation of ketogenesis through *HMGCS2*-OE can drive metabolic flux through upstream pathways, which may provide a mechanism of hepatic fat reduction.

To further understand the relevance of the altered metabolites in the context of ketogenesis, key metabolites involved in glycolysis and TCA cycle in our *HMGCS2*-OE model were compared with those measured in the two previously demonstrated *Hmgcs2* deficient mouse models, including ASO-targeted *Hmgcs2* knockdown[101,102] and CRISPR/Cas9-mediated *Hmgcs2* knockout[115] (**Table 5**). Importantly, CoA, pantothenic acid, succinate, and malate were increased by *HMGCS2*-OE, while being decreased with *Hmgcs2* suppression (*Hmgcs2* knockdown or knockout). NAD^+ and $NADP^+$ concentrations, however, were reduced in both overexpression and suppression models. While this may indicate abnormal metabolic activity in *Hmgcs2*-KO mice[115,123], their depletion with *HMGCS2*-OE could be due to increased metabolic flux of the

TCA cycle and PPP, which utilize two molecules of NAD^+ and $NADP^+$, respectively. Together, ketogenesis-dependent metabolomic and metabolic outcomes seen in previous loss-of-function and our gain-of-function models collectively support the role of ketogenesis in hepatic metabolic regulation underlying the development and improvement of NAFLD, respectively.

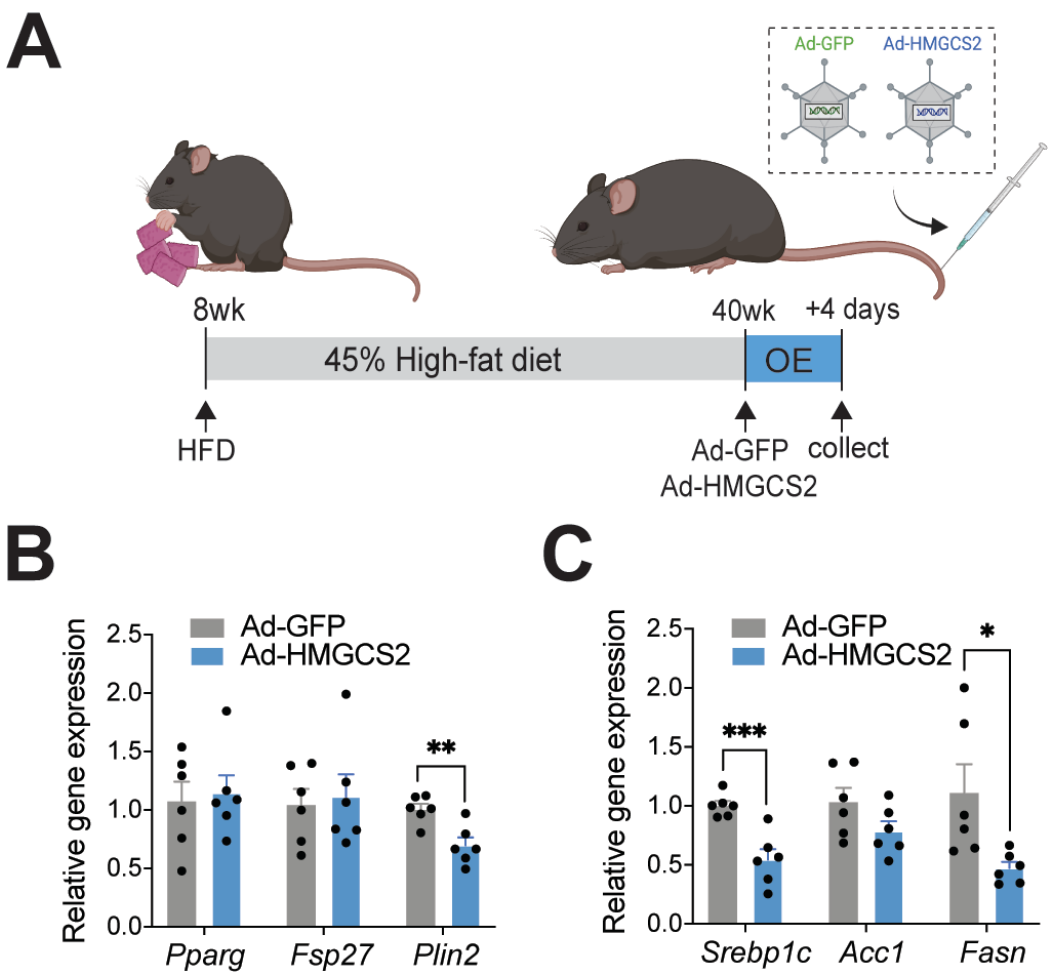

FIGURE 19 | Acute *HMGCS2* overexpression *in vivo* results in the reduction of lipid marker gene expression in livers of HFD-induced NAFLD mice. (**A**) Schematic of 32-weeks HFD-fed mice administered with adenovirus overexpressing *GFP* (Ad-*GFP*) or *HMGCS2* (Ad-*HMGCS2*) and maintained for 4 days prior to liver collection. (**B**) Liver RT-qPCR of lipid accumulation markers *Pparg*, *Fsp27*, *Plin2* and (**C**) lipid synthesis mediators *Srebp1c*, *Acc1*, *Fasn*. Data represented as mean ± SEM. Statistical analysis performed by two-way ANOVA. **P* ≤ 0.05; ***P* ≤ 0.01; ****P* ≤ 0.001. (Created with Biorender.com).

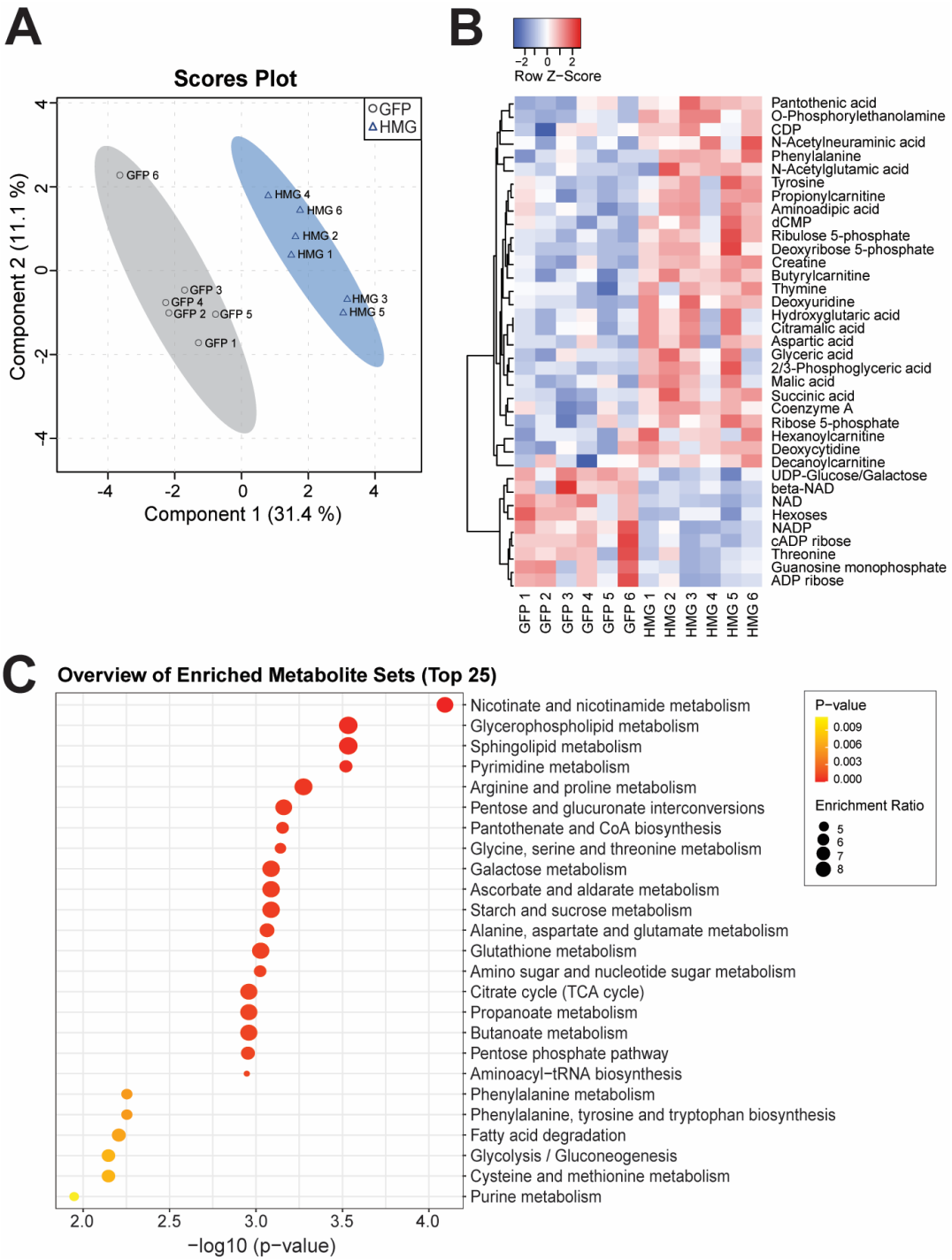

FIGURE 20 | Acute *HMGCS2* overexpression *in vivo* results in the differential expression of liver metabolites captured through an LC-MS/MS untargeted metabolomics approach. (**A**) Partial Least Squares-Discriminant Analysis (PLS-DA) score plot showing a separation of Ad-*GFP* and Ad-*HMGCS2* groups. (**B**) Heatmap showing differential expression of 37 significant ($P < 0.05$) metabolites between Ad-*GFP* and Ad-*HMGCS2* mice. (**C**) Quantitative pathway enrichment analysis showing the top 25 enriched metabolite sets generated through the KEGG metabolic pathway database.

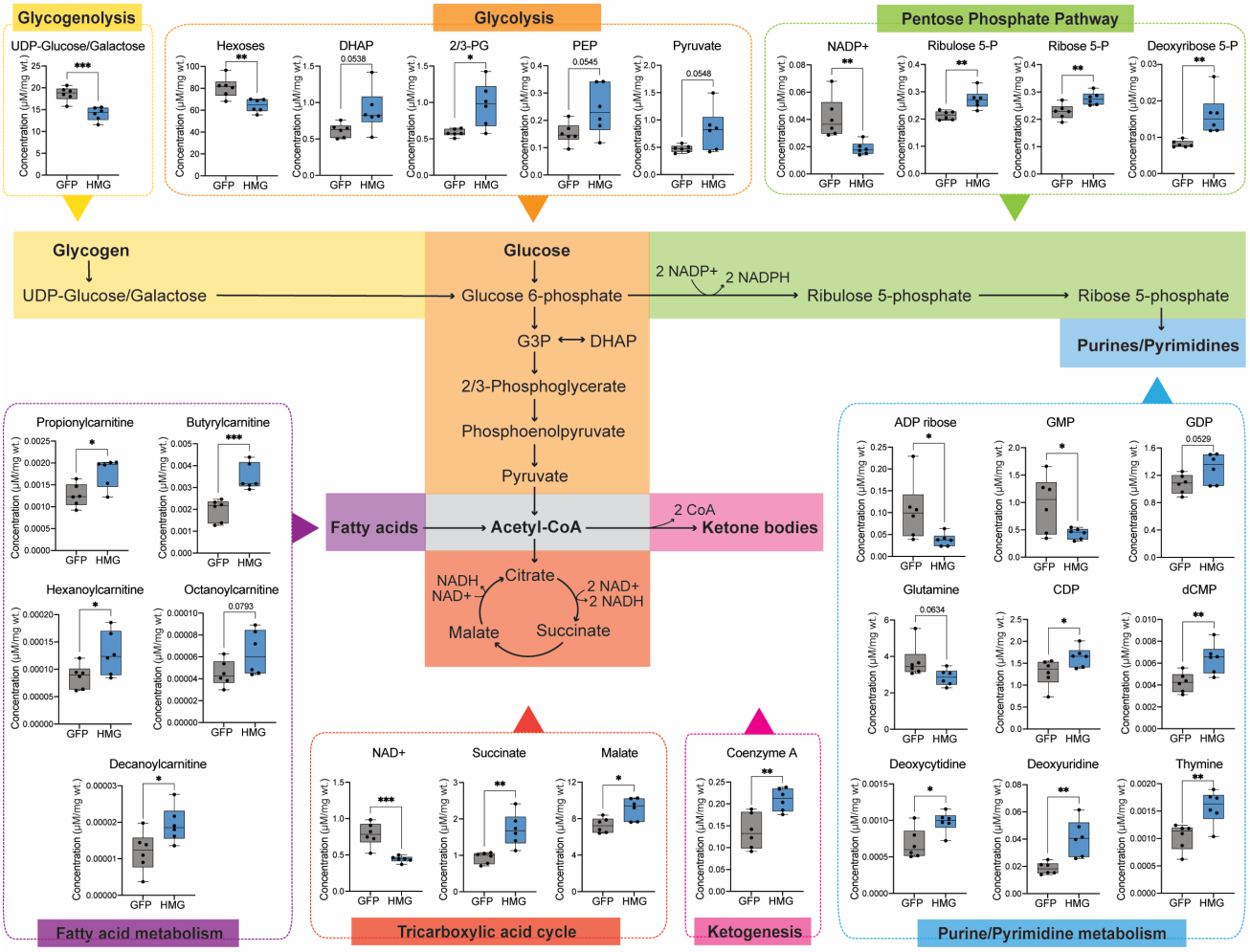

FIGURE 21 | An integrative pathway-metabolite schematic depicting key metabolomic changes seen in livers of acute *HMGCS2* overexpression mice. Individual box plots of metabolites associated with key hepatic pathways (glycogenesis, glycolysis, pentose phosphate pathway, purine/pyrimidine metabolism, fatty acid metabolism, tricarboxylic acid cycle, and ketogenesis) in Ad-*GFP* and Ad-*HMGCS2* mice. Data represented as mean ± SEM. Statistical analysis performed by student's *t*-test. **P* ≤ 0.05; ***P* ≤ 0.01, ****P* ≤ 0.001.

TABLE 4 | Changes in hepatic amino acid (AA) metabolite levels with *HMGCS2* overexpression

Metabolite	Classification	Direction of Change	P-value
2-aminoadipic acid	AA synthesis	↑	0.035
N-acetylglutamic acid	AA synthesis	↑	0.034
Phenylalanine	Ketogenic (or gluconeogenic)	↑	0.005
Tyrosine	Ketogenic (or gluconeogenic)	↑	0.023
Aspartate	Gluconeogenic	↑	0.030
Glutamine	Gluconeogenic	↓	0.063
Serine	Gluconeogenic	↓	0.067
Threonine	Gluconeogenic (or ketogenic)	↓	0.041

TABLE 5 | Key metabolite changes in mouse models of Hmgcs2 overexpression and suppression

Metabolite	*HMGCS2* OE	*Hmgcs2* ASO[1, 2]	*Hmgcs2* KO[3]
Acetyl-CoA	NC	↑	↑
Coenzyme A	↑	↓	NM
Pantothenic acid	↑	↓	NM
Succinate	↑	↓	↓
Malate	↑	NM	↓
NAD+	↓	NC	↓
NADP+	↓	NM	↓

**OE = overexpression; ASO = antisense oligonucleotide; KO = knockout*
**NC = no change; NM = not measured*
1 Cotter et al., JCI, 2014; 2 d'Avignon et al., JCI, 2018; 3 Arima et al., Nature Metabolism, 2021

3.8. SUMMARY OF RESULTS

In the present study, mouse models of ketogenic insufficiency and activation through regulating the rate-limiting enzyme Hmgcs2, were utilized to examine the importance of hepatic ketogenesis as a lipid removal pathway in NAFLD pathogenesis and treatment, respectively. Postnatal *Hmgcs2*-KO mice showed rapid development of fatty liver in the presence of a fat-enriched dietary environment and adult *Hmgcs2*-HET mice presented with increased susceptibility to NAFLD-related metabolic dysfunction upon a HFD. Moreover, we showed that increased ketogenesis through *HMGCS2*-OE resulted in improvements in hepatosteatosis and overall metabolism in NAFLD mice.

DISCUSSION

4.1. Ketogenesis is dysregulated in the presence of HFD-induced metabolic dysfunction

The liver is a key metabolic organ involved in the maintenance of systemic energy homeostasis. As a nutrient sensor, the liver efficiently modulates metabolic pathways according to its dietary macronutrient environment[124,125]. In particular, the liver, under hormonal regulation, undergoes metabolic adaptations from the fed to the fasted state, transitioning from a high to low dietary carbohydrate content, respectively. In the fed state, insulin promotes the storage of glucose and fatty acids through pathways of glycogenesis and lipogenesis. In contrast, in the fasted state, glucagon stimulates the mobilization of energy substrate stores through glycogenolysis and lipolysis, while activating pathways of FAO and ketogenesis for alternative energy production[126,127].

In NAFLD, a disruption of this energy homeostasis occurs. Specifically, perturbations in lipid metabolism, involving excess fatty acid supply and impaired removal, contribute to the buildup of excessive hepatic fat associated with NAFLD[111,112]. Ketogenesis can be activated in response to increased exogenous or endogenous fat in the liver, which can offload significant portions of hepatic fat through the conversion of oxidized fatty acids into energy-carrying ketone bodies for extra-hepatic tissues[98,128-131]. However, chronic lipid exposure, such as prolonged HFD feeding, can lead to ketogenic dysfunction, a plausible mechanism of NAFLD pathogenesis[98,132]. Herein, we demonstrate that NAFLD mice on 32-weeks of HFD present with significant reductions in fasting-induced plasma ketone levels and hepatic Hmgcs2 expression, indicating insufficient activation of the ketogenic pathway. Specifically, among all other enzymes in the ketogenic pathway, *Hmgcs2* mRNA and protein levels were significantly increased with fasting, which was dysregulated with HFD-induced NAFLD. Together, these findings support the master regulatory role of Hmgcs2 in hepatic ketogenesis[101].

The findings of our study and others, however, show a discrepancy in the ketogenic response of HFD-fed mice because unlike our study and another[132], ketone body level and hepatic *Hmgcs2* mRNA expression were elevated in mice fed 16-weeks of HFD[132-134]. This difference can be mainly attributed to the durations of HFD exposure (32 weeks vs. 16 weeks) and the development of insulin resistance. Compared to moderate insulin resistance seen in mice fed 16-weeks of HFD[132-134], 32-weeks of HFD feeding results in severe insulin resistance in mice[132]. As insulin suppresses Hmgcs2 expression in hepatocytes[135,136], it is reasonable to postulate that in the presence of hepatic insulin resistance, higher insulin levels inhibit ketogenesis. This possibility is supported by a recent study, demonstrating that NAFLD patients with insulin resistance show impaired ketogenesis, which correlates with their degree of intrahepatic lipid accumulation[98]. Diminished ketogenesis has also been previously reported in patients with NASH[137], as well as in obese and diabetic patients[138-140]. Specifically, in one study, obese patients with fatty liver showed reduced total ketone body levels in comparison to obese patients without fatty liver[100]. These findings suggest that insulin resistance may be a contributor to ketogenic dysfunction in NAFLD, yet HMGCS2 expression has not been causally linked to reduced ketogenesis in NAFLD patients. In the present study, our loss- and gain-of-function experiments strongly suggest Hmgcs2 as a vital factor in NAFLD development and treatment.

4.2. Postnatal fatty liver development is prevented by ketogenesis in a fat-enriched dietary environment

Here we provided evidence to support a causal role of ketogenic deficiency in NAFLD, as loss of *Hmgcs2* resulted in the severe and rapid development of fatty liver in postnatal mice. Notably, this postnatal fatty liver phenotype was consistently shown in a recent study using a different *Hmgcs2*-KO mouse model[115], further emphasizing *Hmgcs2* as a critical rate-limiting genetic

factor of ketogenesis and hepatic lipid metabolism. This dramatic phenotype is primarily contributed by the vital role of hepatic ketogenesis during the postnatal period. From approximately a few hours to 2-weeks post-birth, breast milk constitutes as the only source of exogenous energy for rodents. This high-fat to low-carbohydrate dietary ratio of breast milk (fat: ~29% and carbohydrate: ~2%)[141] activates hepatic ketogenesis in neonates[39,44,46], and is demonstrated by a rise in plasma ketone and hepatic *Hmgcs2* mRNA levels in WT postnatal mice from p0 to p14 seen in our study and from embryonic day 18.5 (E18.5) to postnatal day 7 (p7) as shown in another study[115]. However, in the absence of functional ketogenesis, this postnatal fat-enriched dietary environment leads to the pathogenic accumulation of fat in the liver via insufficient disposal of excess fat-derived acetyl-CoA through the TCA cycle, as demonstrated by our study and another recent study using a different *Hmgcs2*-KO mouse model[115].

We achieved a nearly complete rescue of the severe lipid accumulation in ketogenesis-deficient *Hmgcs2*-KO mouse livers by altering the nutritional environment, suggesting an interrelation between ketogenesis and a fat-enriched dietary environment in the development of the fatty liver. In comparison to the ketogenic composition of breast milk, the rodent chow diet is low in fat (~9%) and high in carbohydrates (~44.9%). As such, early weaning at p14, one week prior to the normal weaning at ~p21[43], resulted in a substantial decrease in hepatic fat in *Hmgcs2*-KO mice, confirmed by liver weight and histological and molecular markers of lipid accumulation. In particular, a reduction in Plin2 staining, which emphasizes small lipid droplets[142], depicted a shift from diffuse microvesicular steatosis to focal macrovesicular steatosis at liver tissue periphery in early wean *Hmgcs2*-KO mice, associated with better clinical outcomes of fatty liver[9]. Although not tested, it is likely that the intrahepatic fat composition (i.e., triglyceride, cholesterol content) also changes with the dietary macronutrient environment of suckling *Hmgcs2*-KO mice.

Our finding described herein of ketogenesis-deficient postnatal *Hmgcs2*-KO mice provide a successful preclinical model of the human condition of mHS deficiency, an inborn error of ketone body metabolism. These genetic errors of ketone metabolism are a subgroup within FAO disorders, and involve deficiencies in enzymes of ketogenesis (i.e., HMGCS2, HMGCL) and ketolysis (i.e., ACAT1, OXCT1/SCOT, MCT1/SLC16A1). Although patients often are asymptomatic, they can rapidly develop severe, life-threatening conditions upon periods of fasting or sickness, generally within their first year of life[78,143,144]. Specifically, hypoketotic hypoglycemia and fatty liver are common clinical presentations of mHS and mitochondrial HMGCL (mHL) deficiency[81,85]. Treatment and management of these conditions often involve reducing the utilization of FAO and ketogenesis pathways associated with these enzyme deficiencies. For acute treatment, an intravenous glucose infusion is commonly administered to patients, which results in the rapid secretion of insulin that subsequently suppresses adipose lipolysis-mediated fatty acid delivery to the liver for FAO and ketogenesis. For chronic management, patients are often advised to avoid fasting for long periods and reduce their high-fat dietary content[143,145]. Patients with mHL deficiency have also been advised to supplement with carbohydrate-rich diets with moderate protein restriction, specifically leucine, which feeds into the alternative branched-chain amino acid ketogenic pathway and involves HMGCL activity[143,145,146]. Additionally, in one previous study, a patient with carnitine acylcarnitine transferase (CACT) deficiency, a long-chain FAO disorder, was treated with low-fat skim milk, replacing the high-fat breast milk, and showed normal growth and development following one year of treatment without additional metabolic episodes[147]. To our knowledge, a similar reduction in milk fat content has not yet been clinically implemented for inborn errors of ketogenesis, including mHS and mHL deficiency. Thus, our early-weaning study in postnatal ketogenic deficient mice suggests that a modified form of this treatment may be helpful in treating mHS

and mHL patients, especially those presenting with fatty liver. As breast milk contains important nutrients for the development of the newborn[148], complete removal of the breast milk diet may not be feasible, instead defatted breast milk[149] or occasionally supplementing with low-fat milk formulations and high-carbohydrate dietary alternatives to reduce the overall intake of the high-fat breast milk, can be tested. Moreover, supplementation with ketone ester formulations, which have previously shown benefits in patients with FAO disorders (i.e., MAD, CACT, CPT2 deficiencies)[150-152] and inborn errors of ketogenesis (i.e., mHL deficiency)[152], as well as a reduction in the mother's diet to that of low-fat during pregnancy and lactation, would be interesting avenues to explore in the treatment and prevention of fatty liver in our postnatal ketogenic deficient mice. Overall, these findings highlight the importance of the ketogenic pathway and the macronutrient dietary environment as crucial contributors to the development of fatty liver in postnatal mice.

4.3. The degree of ketogenic activity impacts adult fatty liver development

The implication of ketogenesis in the development and progression of fatty liver disease is further supported by our study using *Hmgcs2*-HET mice that exhibited reduced ketogenic function. Along with their underlying ketogenic insufficiency, exogenous HFD intake and the increased age of the adult mice, in comparison to postnatal mice, may all be compounding factors in the development of metabolic dysfunction, as the prevalence and severity of NAFLD and other metabolic conditions (i.e., T2D), increase in adulthood[153,154]. For example, while WT and *Hmgcs2*-HET mice were indistinguishable at the postnatal stage, upon HFD, adult *Hmgcs2*-HET mice showed worse metabolic dysfunction associated with NAFLD, including hyperglycemia and hepatosteatosis. This indicates that one functional *Hmgcs2* allele is ketogenic insufficient in a fat-enriched dietary environment, being prone to the development of NAFLD. Similarly, adult

Hmgcs2-ASO mice with ketogenic insufficiency develop a more severe form of the NAFLD-like phenotype with increased hepatic inflammation and fibrosis, seen only upon HFD and not on a chow diet[101]. Thus, the findings of our study indicate that reduced ketogenesis may predispose to fatty liver development and metabolic complications in adulthood. As such, the measurement of fasting ketone levels, currently not a standard diagnostic method of screening metabolic disorders, could be critical in identifying patients who are susceptible to fatty liver disease development and associated liver diseases, including hepatocellular carcinoma (HCC). In fact, since lower HMGCS2 expression in HCC is associated with higher mortality and metastasis[155-157], detecting underlying disorders of ketone body metabolism could prevent metabolic and clinical consequences later in life. Moreover, as NAFLD pathogenesis has been associated with genes encoding mediators of lipid metabolism (i.e., *PNPLA3*, *TM6SF2*)[1,2], it would be interesting to examine a genetic link associated with ketogenic mediators (i.e., *HMGCS2* and *HMGCL*).

4.4. Ketogenic activation provides a potential therapeutic approach to treat fatty liver disease

Our findings, in support of previous studies in both postnatal[115] and adult[101,102] mice, strongly suggest ketogenic deficiency to be a key contributor in NAFLD pathogenesis. As such, the opposite, ketogenic activation, supported by our *HMGCS2* overexpression study, may be a possible therapeutic strategy in the alleviation of NAFLD as an effective lipid disposal pathway. Overexpression of the human homolog of *HMGCS2* in mice, resulting in a modest increase in plasma ketone levels (<1 mM), leads to significant reductions in plasma glucose and hepatic fat, indicating overall improvements in the fatty liver and metabolic conditions caused by long-term HFD feeding. A decrease in lipid accumulation in *HMGCS2*-overexpressed HepG2 cells further confirmed a hepatocyte-specific ketogenic role in lipid metabolism. Moreover, our findings

suggest a possible mechanism underlying the protective effects of dietary interventions against NAFLD and other metabolic conditions (e.g. hyperglycaemia and dyslipidemia), as a ketogenic diet[23] and IF[24-26] are known to activate ketogenesis. Although, no direct pharmacotherapeutic against NAFLD has been developed, current drugs, such as metformin[158] and GLP-1 agonists[159], being clinically used for the treatment of other metabolic diseases have shown benefits in alleviating different aspects of NAFLD pathology[13]. Among these, increased ketogenesis has been suggested as a mechanism of SGLT2 inhibitors mediating health benefits[22]. Therefore, it would be informative to test whether the metabolic benefits of dietary interventions and SGLT2 inhibitors against NAFLD are mediated via Hmgcs2 activation.

Although HMGCS2's expression and activity have not yet been assessed in NAFLD patients, multiple studies point towards a correlation between HMGCS2 expression and the advanced pathological presentation, clinical stage, and worse overall survival of HCC patients[155,156]. HMGCS2 expression was downregulated in tumor tissues and showed an antimetastatic potential in HCC[157]. Additionally, in mice, knockdown of *HMGCS2* expression promoted HCC through increased cell proliferation and migration (i.e., metastasis)[155], while a ketogenic diet increased *HMGCS2* expression and inhibited HCC tumor growth[160]. Due to this anti-tumor activity, HMGCS2 may be a potential prognostic marker of HCC. Collectively, these studies support the clinical development and use of ketogenesis-activating therapies against NAFLD and associated metabolic diseases.

4.5. Metabolomic changes underlying the improvement of fatty liver by ketogenic activation

Our *in vivo* metabolomics analysis of liver metabolites suggests a potential mechanism of anti-NAFLD effects of *HMGCS2*-OE, as it reveals pathways associated with oxidative (i.e., TCA), sugar (i.e., glucose), amino acid, lipid, and nucleotide (i.e., PPP, purine, pyrimidine) metabolism

to be particularly enriched. Notably, several key metabolites involved in oxidative metabolism showed a reverse trend with previous *Hmgcs2* suppression models[101,102,115], thereby strengthening our findings in *HMGCS2*-OE mice. In particular, CoA, regenerated through ketogenesis, and pantothenic acid, a precursor of CoA synthesis, were increased in the livers of *HMGCS2*-OE mice, while being reduced in *Hmgcs2*-ASO mice[101], indicating abnormal lipid metabolism and TCA cycle in ketogenic insufficiency. Decreased CoA concentrations upon HFD have previously been shown[161], and impaired CoA synthesis, involving precursors such as pantothenic acid, is associated with hepatosteatosis[162]. Thus, the increase of CoA strongly supports Hmgcs2-mediated activation of ketogenesis and improvement in hepatic oxidative metabolism.

4.5.1. Oxidative metabolism.

Succinate and malate, commonly linked to the TCA cycle, were found to be increased in *HMGCS2*-OE mice, while being reduced in *Hmgcs2* suppression mouse models. In ketogenic insufficiency, a compensatory and dysfunctional increase in TCA flux was suggested for the maintenance of mitochondrial energetics and was associated with an accumulation of intrahepatic mitochondrial acetyl-CoA[102]. Similarly, increased TCA flux in HFD mice[132] and NAFLD/NASH patients[163,164] is associated with mitochondrial dysfunction, oxidative stress, and inflammation. Thus, increased concentrations of malate and succinate in the setting of ketogenic activation may suggest a reduced contribution of TCA flux in *HMGCS2*-OE mice. However, it is possible that these metabolite concentrations may be replenished through alternative pathways. Succinate, for example, may be recycled through ketolysis by the enzymatic activity of SCOT, which converts AcAc to AcAc-CoA for terminal ketone oxidation. Although SCOT is not expressed in hepatocytes, an intrahepatic ketone shuttle has been suggested as a mechanism of allowing for hepatocyte-produced AcAc to be transported and oxidized in neighbouring Kupffer cells of the

liver[165]. This may also explain the reduction in NAD^+ levels, utilized in ketolysis in *HMGCS2*-OE livers. Thus, in the setting of increased ketogenesis, hepatic Kupffer cells may subsequently increase rates of ketolysis, thereby consuming NAD^+ and regenerating succinate. Alternatively, hepatic succinate accumulation may result from a compensatory inhibition of the succinate dehydrogenase (SDH) complex of the respiratory chain, which may occur in the setting of increased mitochondrial substrate flux (i.e., fatty acids), through chronic HFD exposure[166,167] and, in our case, ketogenic activation. Thus, increased succinate levels in *HMGCS2*-OE may suggest an adaptive reduction in SDH activity to prevent ROS accumulation and mitochondrial dysfunction. On the other hand, increased levels of malate can be recycled through the malate-aspartate shuttle[168] as well as through malate-pyruvate cycling[169]. This possibility is supported by concurrent increases in hepatic aspartate and pyruvate levels in *HMGCS2*-OE livers. Further investigation through flux studies is required to understand the involvement of these anaplerotic and cataplerotic pathways in ketogenic activation and NAFLD improvement.

4.5.2. Glucose metabolism.

In accordance with phenotypic reductions in plasma glucose levels, the low hexoses and high glycolytic intermediate concentrations suggest reduced gluconeogenesis and activated glycolysis in *HMGCS2*-OE mice. Previously, a mechanism of increased mitochondrial import and decarboxylation of pyruvate has been proposed in relation to ketogenesis[170,171], suggesting that the accumulation of pyruvate in *HMGCS2*-OE mice may likely be fluxed towards oxidative pathways, rather than gluconeogenesis and lipogenesis. The contrary has been presented in ketogenic insufficient mice, in which increased concentrations of mitochondrial acetyl-CoA contribute to the inhibition of the pyruvate dehydrogenase (PDH) complex involved in decarboxylation of pyruvate[101]. Additionally, *HMGCS2*-OE mice showed reduced hepatic

concentrations of UDP-glucose, a substrate of glycogenesis. As ketogenic insufficient mice show increased hepatic glycogen stores[102], it is possible that upon activation of ketogenesis, these glycogen stores are mobilized through glycogenolysis[39], thereby providing additional glucose substrate for glycolysis.

4.5.3. Amino acid metabolism

Activated ketogenesis and reduced gluconeogenesis in *HMGCS2*-OE mice may also be supported by increased concentrations of ketogenic amino acids (i.e., phenylalanine, tyrosine) and decreased levels of gluconeogenic amino acids (i.e., glutamine, serine, threonine), respectively. However, as phenylalanine and tyrosine can feed into the production of both acetyl-CoA and acetoacetyl-CoA for ketogenesis as well as fumarate for gluconeogenesis through TCA anaplerosis[172,173], their contribution to either is unclear with the current data and would require further *in vivo* metabolomic flux studies in *HMGCS2*-OE mice. Moreover, hepatic levels of 2-aminoadipic acid and N-acetylglutamic acid, involved in amino acid synthesis, were consistently greater in *HMGCS2*-OE mice. Since elevated amino acid catabolism has been associated with the development of NASH[174], it is possible that Hmgcs2-mediated ketogenesis may increase amino acid synthesis for the alleviation of NAFLD pathogenesis, as amino acids serve as critical biomolecules in protein synthesis and detoxification in the liver[175].

4.5.4. Fatty acid metabolism

It was notable that *HMGCS2*-OE mice showed increased concentration of short- (C3, C4, C6) and medium-chain (C8, C10) acylcarnitines in the liver. Acylcarnitines constitute as the by-products of substrate catabolism, mainly resulting from FAO. LCFA require carnitine transport proteins, whereas SCFA and MCFA can readily enter the mitochondria. Thus, the buildup of

these short- and medium-chain acylcarnitines is unlikely related to increased inner mitochondrial fatty acid delivery. Another critical subcellular compartment for β-oxidation is the peroxisome. Peroxisomal β-oxidation breaks down VLCFA (>C16) and LCFA (>C12) into MCFA (C8-C12) and SCFA (<C8). These fatty acids are subsequently trans-esterified into short- and medium-chain acylcarnitines by peroxisomal carnitine proteins, which are transported to the mitochondria, where they undergo complete β-oxidation, producing acetyl-CoA (**Fig. 1**)[34-37]. Although mitochondrial β-oxidation constitutes as the major pathway of fatty acid breakdown, it is possible that in the setting of increased mitochondrial Hmgcs2-mediated ketogenesis, peroxisomal β-oxidation may be concurrently activated to alleviate mitochondrial stress[40]. Indeed, impairments in peroxisomal β-oxidation of VLCFA are associated with NAFLD pathogenesis in mice[176]. Additionally, it can be proposed that as the rate of fatty acid catabolism may surpass energy requirements under the conditions of enhanced ketogenesis, greater acylcarnitines and free CoA levels were produced by accumulating acyl-CoA intermediates which may be re-esterified into acylcarnitines through the carnitine shuttle system to maintain mitochondrial function[177]. Our findings are in contrast to previous studies, in which rodents chronically fed a HFD have shown reduced hepatic acylcarnitine levels, particularly of short- and medium-chain, indicating a dysregulation in FAO[177,178]. Altogether, the increased hepatic content of short- and medium-chain acylcarnitines suggest compensatory mechanisms of preventing mitochondrial dysfunction in the livers of *HMGCS2*-OE mice, although a closer evaluation of both mitochondrial and peroxisomal activities is required to make this conclusion.

4.5.5. Nucleotide metabolism

We detected higher concentrations of intermediate metabolites of the PPP and its branching purine and pyrimidine nucleotide synthesis pathways in the *HMGCS2*-OE liver. This is a novel finding as there are very few studies to our knowledge that show a direct association of these pathways to liver disease. In one study, however, inhibition of dihydroorotate dehydrogenase (DHODH) involved in pyrimidine biosynthesis and overexpression of uridine phosphorylase 1 (Upase1) involved in pyrimidine catabolism, promoted microvesicular steatosis, while uridine supplementation suppressed microvesicular steatosis in both mouse models[179], suggesting an indirect protective and therapeutic role of the pyrimidine pathway in the fatty liver. Additionally, another study has reported that a reduction of the intermediates of purine and pyrimidine metabolism is observed in the diabetic pancreas and correlated with their insulin depletion[180]. Thus, increases in purine and pyrimidine synthesis in *HMGCS2*-OE may contribute to metabolic improvements in NAFLD, although further mechanistic interpretation of this will be required.

Overall, the activation of the ketone body synthesis pathway largely reprograms hepatic intermediary metabolism for improvements in NAFLD, suggesting an integrative role of ketogenesis in FAO, TCA, glycolysis/glycogenolysis, PPP and purine/pyrimidine metabolism. As many of these metabolic pathways are multidirectional and interrelated, future metabolomic flux and gene expression analysis studies in *HMGCS2*-OE models will be pertinent in enhancing our understanding of these metabolic pathways, their intermediates, and mediators, in ketogenic activation and NAFLD.

CONCLUSION

The findings of our study demonstrate that ***Hmgcs2-mediated ketogenesis is a key contributor to NAFLD pathogenesis and treatment.*** Specifically, we show (1) that impaired ketogenesis in HFD-induced NAFLD mice is mediated by reduced hepatic expression of Hmgcs2; (2) that Hmgcs2-associated ketogenic deficiency and a fat-enriched dietary environment are both required for postnatal fatty liver development; (3) that insufficient level of ketogenic function or *Hmgcs2* gene dosage promote adult-onset NAFLD upon HFD; (4) and that *HMGCS2* overexpression-mediated ketogenesis activation improves HFD-induced NAFLD and metabolic dysfunction. A limitation of this study, however, is the lack of hepatocyte-specific *in vivo* models for both *Hmgcs2*-KO and *HMGCS2*-OE, as ketogenesis can occur in extra-hepatic tissues, such as the kidney and intestine. We are currently exploring these to enhance the interpretation of our study. Overall, our findings suggest impaired ketogenesis and dysregulated hepatic Hmgcs2 expression as possible markers of NAFLD progression and susceptibility, while proposing ketogenic activation as a possible therapeutic target in the clinical intervention of NAFLD.

REFERENCES

1 Benedict, M. & Zhang, X. Non-alcoholic fatty liver disease: An expanded review. *World J Hepatol* **9**, 715-732, doi:10.4254/wjh.v9.i16.715 (2017).

2 Yu, J., Marsh, S., Hu, J., Feng, W. & Wu, C. The Pathogenesis of Nonalcoholic Fatty Liver Disease: Interplay between Diet, Gut Microbiota, and Genetic Background. *Gastroenterol Res Pract* **2016**, 2862173, doi:10.1155/2016/2862173 (2016).

3 Arshad, T., Golabi, P., Henry, L. & Younossi, Z. M. Epidemiology of Non-alcoholic Fatty Liver Disease in North America. *Curr Pharm Des* **26**, 993-997, doi:10.2174/1381612826666200303114934 (2020).

4 Huang, D. Q., El-Serag, H. B. & Loomba, R. Global epidemiology of NAFLD-related HCC: trends, predictions, risk factors and prevention. *Nat Rev Gastroenterol Hepatol* **18**, 223-238, doi:10.1038/s41575-020-00381-6 (2021).

5 Non-alcoholic Fatty Liver Disease Study, G. *et al.* Epidemiological modifiers of non-alcoholic fatty liver disease: Focus on high-risk groups. *Dig Liver Dis* **47**, 997-1006, doi:10.1016/j.dld.2015.08.004 (2015).

6 Kotronen, A. *et al.* Liver fat is increased in type 2 diabetic patients and underestimated by serum alanine aminotransferase compared with equally obese nondiabetic subjects. *Diabetes Care* **31**, 165-169, doi:10.2337/dc07-1463 (2008).

7 Targher, G. *et al.* Prevalence of nonalcoholic fatty liver disease and its association with cardiovascular disease among type 2 diabetic patients. *Diabetes Care* **30**, 1212-1218, doi:10.2337/dc06-2247 (2007).

8 Younossi, Z. M. *et al.* Nonalcoholic fatty liver disease in lean individuals in the United States. *Medicine (Baltimore)* **91**, 319-327, doi:10.1097/MD.0b013e3182779d49 (2012).

9 Tandra, S. *et al.* Presence and significance of microvesicular steatosis in nonalcoholic fatty liver disease. *J Hepatol* **55**, 654-659, doi:10.1016/j.jhep.2010.11.021 (2011).

10 Chrysavgis, L., Ztriva, E., Protopapas, A., Tziomalos, K. & Cholongitas, E. Nonalcoholic fatty liver disease in lean subjects: Prognosis, outcomes and management. *World J Gastroenterol* **26**, 6514-6528, doi:10.3748/wjg.v26.i42.6514 (2020).

11 Liu, Z. *et al.* The effect of the TM6SF2 E167K variant on liver steatosis and fibrosis in patients with chronic hepatitis C: a meta-analysis. *Sci Rep* **7**, 9273, doi:10.1038/s41598-017-09548-9 (2017).

12 Pafili, K. & Roden, M. Nonalcoholic fatty liver disease (NAFLD) from pathogenesis to treatment concepts in humans. *Mol Metab* **50**, 101122, doi:10.1016/j.molmet.2020.101122 (2021).

13 Gottlieb, A., Mosthael, W., Sowa, J. P. & Canbay, A. Nonalcoholic-Fatty-Liver-Disease and Nonalcoholic Steatohepatitis: Successful Development of Pharmacological Treatment Will Depend on Translational Research. *Digestion* **100**, 79-85, doi:10.1159/000493259 (2019).

14 Dyson, J. K., Anstee, Q. M. & McPherson, S. Non-alcoholic fatty liver disease: a practical approach to diagnosis and staging. *Frontline Gastroenterol* **5**, 211-218, doi:10.1136/flgastro-2013-100403 (2014).

15 Sumida, Y., Nakajima, A. & Itoh, Y. Limitations of liver biopsy and non-invasive diagnostic tests for the diagnosis of nonalcoholic fatty liver disease/nonalcoholic steatohepatitis. *World J Gastroenterol* **20**, 475-485, doi:10.3748/wjg.v20.i2.475 (2014).

16 Cleveland, E., Bandy, A. & VanWagner, L. B. Diagnostic challenges of nonalcoholic fatty liver disease/nonalcoholic steatohepatitis. *Clin Liver Dis (Hoboken)* **11**, 98-104, doi:10.1002/cld.716 (2018).
17 Alexander, M. *et al.* Real-world data reveal a diagnostic gap in non-alcoholic fatty liver disease. *BMC Med* **16**, 130, doi:10.1186/s12916-018-1103-x (2018).
18 Komiya, C. *et al.* Ipragliflozin Improves Hepatic Steatosis in Obese Mice and Liver Dysfunction in Type 2 Diabetic Patients Irrespective of Body Weight Reduction. *PLoS One* **11**, e0151511, doi:10.1371/journal.pone.0151511 (2016).
19 Scheen, A. J. Beneficial effects of SGLT2 inhibitors on fatty liver in type 2 diabetes: A common comorbidity associated with severe complications. *Diabetes Metab* **45**, 213-223, doi:10.1016/j.diabet.2019.01.008 (2019).
20 Polidori, D. *et al.* Intra- and inter-subject variability for increases in serum ketone bodies in patients with type 2 diabetes treated with the sodium glucose co-transporter 2 inhibitor canagliflozin. *Diabetes Obes Metab* **20**, 1321-1326, doi:10.1111/dom.13224 (2018).
21 Prattichizzo, F., De Nigris, V., Micheloni, S., La Sala, L. & Ceriello, A. Increases in circulating levels of ketone bodies and cardiovascular protection with SGLT2 inhibitors: Is low-grade inflammation the neglected component? *Diabetes Obes Metab* **20**, 2515-2522, doi:10.1111/dom.13488 (2018).
22 Capozzi, M. E. *et al.* The Limited Role of Glucagon for Ketogenesis During Fasting or in Response to SGLT2 Inhibition. *Diabetes* **69**, 882-892, doi:10.2337/db19-1216 (2020).
23 Luukkonen, P. K. *et al.* Effect of a ketogenic diet on hepatic steatosis and hepatic mitochondrial metabolism in nonalcoholic fatty liver disease. *Proc Natl Acad Sci U S A* **117**, 7347-7354, doi:10.1073/pnas.1922344117 (2020).
24 Cai, H. *et al.* Effects of alternate-day fasting on body weight and dyslipidaemia in patients with non-alcoholic fatty liver disease: a randomised controlled trial. *BMC Gastroenterol* **19**, 219, doi:10.1186/s12876-019-1132-8 (2019).
25 Kim, K. H. *et al.* Intermittent fasting promotes adipose thermogenesis and metabolic homeostasis via VEGF-mediated alternative activation of macrophage. *Cell Res* **27**, 1309-1326, doi:10.1038/cr.2017.126 (2017).
26 Kim, Y. H. *et al.* Thermogenesis-independent metabolic benefits conferred by isocaloric intermittent fasting in ob/ob mice. *Sci Rep* **9**, 2479, doi:10.1038/s41598-019-39380-2 (2019).
27 Johari, M. I. *et al.* A Randomised Controlled Trial on the Effectiveness and Adherence of Modified Alternate-day Calorie Restriction in Improving Activity of Non-Alcoholic Fatty Liver Disease. *Sci Rep* **9**, 11232, doi:10.1038/s41598-019-47763-8 (2019).
28 Horrillo, D. *et al.* Development of liver fibrosis during aging: effects of caloric restriction. *J Biol Regul Homeost Agents* **27**, 377-388 (2013).
29 Marinho, T. S., Ornellas, F., Barbosa-da-Silva, S., Mandarim-de-Lacerda, C. A. & Aguila, M. B. Beneficial effects of intermittent fasting on steatosis and inflammation of the liver in mice fed a high-fat or a high-fructose diet. *Nutrition* **65**, 103-112, doi:10.1016/j.nut.2019.02.020 (2019).
30 Cotter, D. G. Ketone Body Metabolism Preserves Hepatic Function during Adaptation to Birth and in Overnutrition. . *Arts & Sciences Electronic Theses and Dissertations* **444** (2015).
31 Puchalska, P. & Crawford, P. A. Metabolic and Signaling Roles of Ketone Bodies in Health and Disease. *Annu Rev Nutr* **41**, 49-77, doi:10.1146/annurev-nutr-111120-111518 (2021).

32 Puchalska, P. & Crawford, P. A. Multi-dimensional Roles of Ketone Bodies in Fuel Metabolism, Signaling, and Therapeutics. *Cell Metab* **25**, 262-284, doi:10.1016/j.cmet.2016.12.022 (2017).
33 Meertens, L. M., Miyata, K. S., Cechetto, J. D., Rachubinski, R. A. & Capone, J. P. A mitochondrial ketogenic enzyme regulates its gene expression by association with the nuclear hormone receptor PPARalpha. *EMBO J* **17**, 6972-6978, doi:10.1093/emboj/17.23.6972 (1998).
34 Violante, S. *et al.* Peroxisomes contribute to the acylcarnitine production when the carnitine shuttle is deficient. *Biochim Biophys Acta* **1831**, 1467-1474, doi:10.1016/j.bbalip.2013.06.007 (2013).
35 Schrader, M., Costello, J., Godinho, L. F. & Islinger, M. Peroxisome-mitochondria interplay and disease. *J Inherit Metab Dis* **38**, 681-702, doi:10.1007/s10545-015-9819-7 (2015).
36 Reuter, S. E. & Evans, A. M. Carnitine and acylcarnitines: pharmacokinetic, pharmacological and clinical aspects. *Clin Pharmacokinet* **51**, 553-572, doi:10.2165/11633940-000000000-0000010.1007/BF03261931 (2012).
37 Reddy, J. K. & Hashimoto, T. Peroxisomal beta-oxidation and peroxisome proliferator-activated receptor alpha: an adaptive metabolic system. *Annu Rev Nutr* **21**, 193-230, doi:10.1146/annurev.nutr.21.1.193 (2001).
38 Houten, S. M., Wanders, R. J. A. & Ranea-Robles, P. Metabolic interactions between peroxisomes and mitochondria with a special focus on acylcarnitine metabolism. *Biochim Biophys Acta Mol Basis Dis* **1866**, 165720, doi:10.1016/j.bbadis.2020.165720 (2020).
39 Girard, J., Ferre, P., Pegorier, J. P. & Duee, P. H. Adaptations of glucose and fatty acid metabolism during perinatal period and suckling-weaning transition. *Physiol Rev* **72**, 507-562, doi:10.1152/physrev.1992.72.2.507 (1992).
40 Fransen, M., Lismont, C. & Walton, P. The Peroxisome-Mitochondria Connection: How and Why? *Int J Mol Sci* **18**, doi:10.3390/ijms18061126 (2017).
41 Laffel, L. Ketone bodies: a review of physiology, pathophysiology and application of monitoring to diabetes. *Diabetes Metab Res Rev* **15**, 412-426, doi:10.1002/(sici)1520-7560(199911/12)15:6<412::aid-dmrr72>3.0.co;2-8 (1999).
42 Grabacka, M., Pierzchalska, M., Dean, M. & Reiss, K. Regulation of Ketone Body Metabolism and the Role of PPARalpha. *Int J Mol Sci* **17**, doi:10.3390/ijms17122093 (2016).
43 Nakagaki, B. N. *et al.* Immune and metabolic shifts during neonatal development reprogram liver identity and function. *J Hepatol* **69**, 1294-1307, doi:10.1016/j.jhep.2018.08.018 (2018).
44 Ward Platt, M. & Deshpande, S. Metabolic adaptation at birth. *Semin Fetal Neonatal Med* **10**, 341-350, doi:10.1016/j.siny.2005.04.001 (2005).
45 Grijalva, J. & Vakili, K. Neonatal liver physiology. *Semin Pediatr Surg* **22**, 185-189, doi:10.1053/j.sempedsurg.2013.10.006 (2013).
46 Ferre, P., Decaux, J. F., Issad, T. & Girard, J. Changes in energy metabolism during the suckling and weaning period in the newborn. *Reprod Nutr Dev* **26**, 619-631, doi:10.1051/rnd:19860413 (1986).
47 Weaning from the breast. *Paediatr Child Health* **9**, 249-263, doi:10.1093/pch/9.4.249 (2004).

48 Thumelin, S., Forestier, M., Girard, J. & Pegorier, J. P. Developmental changes in mitochondrial 3-hydroxy-3-methylglutaryl-CoA synthase gene expression in rat liver, intestine and kidney. *Biochem J* **292 (Pt 2)**, 493-496, doi:10.1042/bj2920493 (1993).
49 Serra, D., Asins, G. & Hegardt, F. G. Ketogenic mitochondrial 3-hydroxy 3-methylglutaryl-CoA synthase gene expression in intestine and liver of suckling rats. *Arch Biochem Biophys* **301**, 445-448, doi:10.1006/abbi.1993.1169 (1993).
50 Benito, M., Whitelaw, E. & Williamson, D. H. Regulation of ketogenesis during the suckling-weanling transition in the rat. Studies with isolated hepatocytes. *Biochem J* **180**, 137-144, doi:10.1042/bj1800137 (1979).
51 Girard, J. *et al.* Fatty acid oxidation and ketogenesis during development. *Reprod Nutr Dev* **25**, 303-319, doi:10.1051/rnd:19850221 (1985).
52 Hall, I. H. *et al.* Anti-inflammatory activity of amine-carboxyboranes in rodents. *Arch Pharm (Weinheim)* **328**, 39-44, doi:10.1002/ardp.19953280108 (1995).
53 Ferre, P., Satabin, P., Decaux, J. F., Escriva, F. & Girard, J. Development and regulation of ketogenesis in hepatocytes isolated from newborn rats. *Biochem J* **214**, 937-942, doi:10.1042/bj2140937 (1983).
54 Arias, G., Matas, R., Asins, G., Hegardt, F. G. & Serra, D. The effect of fasting and insulin treatment on carnitine palmitoyl transferase I and mitochondrial 3-hydroxy-3-methylglutaryl coenzyme A synthase mRNA levels in liver from suckling rats. *Biochem Soc Trans* **23**, 493S, doi:10.1042/bst023493s (1995).
55 Quant, P. A. *et al.* Control of hepatic mitochondrial 3-hydroxy-3-methylglutaryl-CoA synthase during the foetal/neonatal transition, suckling and weaning in the rat. *Eur J Biochem* **195**, 449-454, doi:10.1111/j.1432-1033.1991.tb15724.x (1991).
56 Zhang, D. *et al.* Proteomics analysis reveals diabetic kidney as a ketogenic organ in type 2 diabetes. *Am J Physiol Endocrinol Metab* **300**, E287-295, doi:10.1152/ajpendo.00308.2010 (2011).
57 Torres, J. A. *et al.* Ketosis Ameliorates Renal Cyst Growth in Polycystic Kidney Disease. *Cell Metab* **30**, 1007-1023 e1005, doi:10.1016/j.cmet.2019.09.012 (2019).
58 Wang, Q. *et al.* Ketogenesis contributes to intestinal cell differentiation. *Cell Death Differ* **24**, 458-468, doi:10.1038/cdd.2016.142 (2017).
59 Kim, J. T. *et al.* Regulation of Ketogenic Enzyme HMGCS2 by Wnt/beta-catenin/PPARgamma Pathway in Intestinal Cells. *Cells* **8**, doi:10.3390/cells8091106 (2019).
60 Cheng, C. W. *et al.* Ketone Body Signaling Mediates Intestinal Stem Cell Homeostasis and Adaptation to Diet. *Cell* **178**, 1115-1131 e1115, doi:10.1016/j.cell.2019.07.048 (2019).
61 Bagheri-Fam, S. *et al.* The gene encoding the ketogenic enzyme HMGCS2 displays a unique expression during gonad development in mice. *PLoS One* **15**, e0227411, doi:10.1371/journal.pone.0227411 (2020).
62 Ago, Y. *et al.* Japanese patients with mitochondrial 3-hydroxy-3-methylglutaryl-CoA synthase deficiency: In vitro functional analysis of five novel HMGCS2 mutations. *Exp Ther Med* **20**, 39, doi:10.3892/etm.2020.9166 (2020).
63 Ramos, M. *et al.* New case of mitochondrial HMG-CoA synthase deficiency. Functional analysis of eight mutations. *Eur J Med Genet* **56**, 411-415, doi:10.1016/j.ejmg.2013.05.008 (2013).
64 Hegardt, F. G. Mitochondrial 3-hydroxy-3-methylglutaryl-CoA synthase: a control enzyme in ketogenesis. *Biochem J* **338 (Pt 3)**, 569-582 (1999).

65 Rodriguez, J. C., Gil-Gomez, G., Hegardt, F. G. & Haro, D. Peroxisome proliferator-activated receptor mediates induction of the mitochondrial 3-hydroxy-3-methylglutaryl-CoA synthase gene by fatty acids. *J Biol Chem* **269**, 18767-18772 (1994).
66 Kostiuk, M. A., Keller, B. O. & Berthiaume, L. G. Palmitoylation of ketogenic enzyme HMGCS2 enhances its interaction with PPARalpha and transcription at the Hmgcs2 PPRE. *FASEB J* **24**, 1914-1924, doi:10.1096/fj.09-149765 (2010).
67 Inagaki, T. *et al.* Endocrine regulation of the fasting response by PPARalpha-mediated induction of fibroblast growth factor 21. *Cell Metab* **5**, 415-425, doi:10.1016/j.cmet.2007.05.003 (2007).
68 Badman, M. K. *et al.* Hepatic fibroblast growth factor 21 is regulated by PPARalpha and is a key mediator of hepatic lipid metabolism in ketotic states. *Cell Metab* **5**, 426-437, doi:10.1016/j.cmet.2007.05.002 (2007).
69 Quant, P. A., Tubbs, P. K. & Brand, M. D. Glucagon activates mitochondrial 3-hydroxy-3-methylglutaryl-CoA synthase in vivo by decreasing the extent of succinylation of the enzyme. *Eur J Biochem* **187**, 169-174, doi:10.1111/j.1432-1033.1990.tb15291.x (1990).
70 Rardin, M. J. *et al.* SIRT5 regulates the mitochondrial lysine succinylome and metabolic networks. *Cell Metab* **18**, 920-933, doi:10.1016/j.cmet.2013.11.013 (2013).
71 Shimazu, T. *et al.* SIRT3 deacetylates mitochondrial 3-hydroxy-3-methylglutaryl CoA synthase 2 and regulates ketone body production. *Cell Metab* **12**, 654-661, doi:10.1016/j.cmet.2010.11.003 (2010).
72 Rardin, M. J. *et al.* Label-free quantitative proteomics of the lysine acetylome in mitochondria identifies substrates of SIRT3 in metabolic pathways. *Proc Natl Acad Sci U S A* **110**, 6601-6606, doi:10.1073/pnas.1302961110 (2013).
73 Grimsrud, P. A. *et al.* A quantitative map of the liver mitochondrial phosphoproteome reveals posttranslational control of ketogenesis. *Cell Metab* **16**, 672-683, doi:10.1016/j.cmet.2012.10.004 (2012).
74 Wolfrum, C., Asilmaz, E., Luca, E., Friedman, J. M. & Stoffel, M. Foxa2 regulates lipid metabolism and ketogenesis in the liver during fasting and in diabetes. *Nature* **432**, 1027-1032, doi:10.1038/nature03047 (2004).
75 von Meyenn, F. *et al.* Glucagon-induced acetylation of Foxa2 regulates hepatic lipid metabolism. *Cell Metab* **17**, 436-447, doi:10.1016/j.cmet.2013.01.014 (2013).
76 Asif, S., Morrow, N. M., Mulvihill, E. E. & Kim, K. H. Understanding Dietary Intervention-Mediated Epigenetic Modifications in Metabolic Diseases. *Front Genet* **11**, 590369, doi:10.3389/fgene.2020.590369 (2020).
77 Cotter, D. G., Schugar, R. C. & Crawford, P. A. Ketone body metabolism and cardiovascular disease. *Am J Physiol Heart Circ Physiol* **304**, H1060-1076, doi:10.1152/ajpheart.00646.2012 (2013).
78 Liu, H. *et al.* Severe clinical manifestation of mitochondrial 3-hydroxy-3-methylglutaryl-CoA synthase deficiency associated with two novel mutations: a case report. *BMC Pediatr* **19**, 344, doi:10.1186/s12887-019-1747-5 (2019).
79 Kilic, M. *et al.* Expanding the clinical spectrum of mitochondrial 3-hydroxy-3-methylglutaryl-CoA synthase deficiency with Turkish cases harboring novel HMGCS2 gene mutations and literature review. *Am J Med Genet A* **182**, 1608-1614, doi:10.1002/ajmg.a.61590 (2020).
80 Wang, Q. *et al.* Clinical, biochemical, molecular and therapeutic characteristics of four new patients of mitochondrial 3-hydroxy-3-methylglutaryl-CoA synthase deficiency. *Clin Chim Acta* **509**, 83-90, doi:10.1016/j.cca.2020.04.004 (2020).

81 Lee, T. *et al.* A Japanese case of mitochondrial 3-hydroxy-3-methylglutaryl-CoA synthase deficiency who presented with severe metabolic acidosis and fatty liver without hypoglycemia. *JIMD Rep* **48**, 19-25, doi:10.1002/jmd2.12051 (2019).
82 Rojnueangnit, K. *et al.* Expanding phenotypic and mutational spectra of mitochondrial HMG-CoA synthase deficiency. *Eur J Med Genet* **63**, 104086, doi:10.1016/j.ejmg.2020.104086 (2020).
83 Pitt, J. J. *et al.* Mitochondrial 3-hydroxy-3-methylglutaryl-CoA synthase deficiency: urinary organic acid profiles and expanded spectrum of mutations. *J Inherit Metab Dis* **38**, 459-466, doi:10.1007/s10545-014-9801-9 (2015).
84 Zhang, P. *et al.* Novel HMGCS2 pathogenic variants in a Chinese family with mitochondrial 3-hydroxy-3-methylglutaryl-CoA synthase deficiency. *Pediatr Investig* **3**, 86-90, doi:10.1002/ped4.12130 (2019).
85 Sass, J. O., Fukao, T. & Mitchell, G. A. Inborn Errors of Ketone Body Metabolism and Transport. *Journal of Inborn Errors of Metabolism and Screening* **6**, doi:10.1177/2326409818771101 (2018).
86 Shimazu, T. *et al.* Suppression of oxidative stress by beta-hydroxybutyrate, an endogenous histone deacetylase inhibitor. *Science* **339**, 211-214, doi:10.1126/science.1227166 (2013).
87 Knutson, S. K. *et al.* Liver-specific deletion of histone deacetylase 3 disrupts metabolic transcriptional networks. *EMBO J* **27**, 1017-1028, doi:10.1038/emboj.2008.51 (2008).
88 Xie, Z. *et al.* Metabolic Regulation of Gene Expression by Histone Lysine beta-Hydroxybutyrylation. *Mol Cell* **62**, 194-206, doi:10.1016/j.molcel.2016.03.036 (2016).
89 Zhang, H. *et al.* Ketogenesis-generated beta-hydroxybutyrate is an epigenetic regulator of CD8(+) T-cell memory development. *Nat Cell Biol* **22**, 18-25, doi:10.1038/s41556-019-0440-0 (2020).
90 Veech, R. L. *et al.* Ketone bodies mimic the life span extending properties of caloric restriction. *IUBMB Life* **69**, 305-314, doi:10.1002/iub.1627 (2017).
91 Chen, Y. *et al.* beta-Hydroxybutyrate protects from alcohol-induced liver injury via a Hcar2-cAMP dependent pathway. *J Hepatol* **69**, 687-696, doi:10.1016/j.jhep.2018.04.004 (2018).
92 Mardinoglu, A. *et al.* An Integrated Understanding of the Rapid Metabolic Benefits of a Carbohydrate-Restricted Diet on Hepatic Steatosis in Humans. *Cell Metab* **27**, 559-571 e555, doi:10.1016/j.cmet.2018.01.005 (2018).
93 Tendler, D. *et al.* The effect of a low-carbohydrate, ketogenic diet on nonalcoholic fatty liver disease: a pilot study. *Dig Dis Sci* **52**, 589-593, doi:10.1007/s10620-006-9433-5 (2007).
94 Perez-Guisado, J. & Munoz-Serrano, A. The effect of the Spanish Ketogenic Mediterranean Diet on nonalcoholic fatty liver disease: a pilot study. *J Med Food* **14**, 677-680, doi:10.1089/jmf.2011.0075 (2011).
95 Moore, M. P. *et al.* A dietary ketone ester mitigates histological outcomes of NAFLD and markers of fibrosis in high-fat diet fed mice. *Am J Physiol Gastrointest Liver Physiol* **320**, G564-G572, doi:10.1152/ajpgi.00259.2020 (2021).
96 Paoli, A., Bosco, G., Camporesi, E. M. & Mangar, D. Ketosis, ketogenic diet and food intake control: a complex relationship. *Front Psychol* **6**, 27, doi:10.3389/fpsyg.2015.00027 (2015).
97 Sumithran, P. *et al.* Ketosis and appetite-mediating nutrients and hormones after weight loss. *Eur J Clin Nutr* **67**, 759-764, doi:10.1038/ejcn.2013.90 (2013).

98 Fletcher, J. A. *et al.* Impaired ketogenesis and increased acetyl-CoA oxidation promote hyperglycemia in human fatty liver. *JCI Insight* **5**, doi:10.1172/jci.insight.127737 (2019).
99 Mey, J. T. *et al.* beta-Hydroxybutyrate is reduced in humans with obesity-related NAFLD and displays a dose-dependent effect on skeletal muscle mitochondrial respiration in vitro. *Am J Physiol Endocrinol Metab* **319**, E187-E195, doi:10.1152/ajpendo.00058.2020 (2020).
100 Inokuchi, T., Orita, M., Imamura, K., Takao, T. & Isogai, S. Resistance to ketosis in moderately obese patients: influence of fatty liver. *Intern Med* **31**, 978-983, doi:10.2169/internalmedicine.31.978 (1992).
101 Cotter, D. G. *et al.* Ketogenesis prevents diet-induced fatty liver injury and hyperglycemia. *J Clin Invest* **124**, 5175-5190, doi:10.1172/JCI76388 (2014).
102 d'Avignon, D. A. *et al.* Hepatic ketogenic insufficiency reprograms hepatic glycogen metabolism and the lipidome. *JCI Insight* **3**, doi:10.1172/jci.insight.99762 (2018).
103 Kikusui, T., Takeuchi, Y. & Mori, Y. Early weaning induces anxiety and aggression in adult mice. *Physiol Behav* **81**, 37-42, doi:10.1016/j.physbeh.2003.12.016 (2004).
104 Mogi, K., Ishida, Y., Nagasawa, M. & Kikusui, T. Early weaning impairs fear extinction and decreases brain-derived neurotrophic factor expression in the prefrontal cortex of adult male C57BL/6 mice. *Dev Psychobiol* **58**, 1034-1042, doi:10.1002/dev.21437 (2016).
105 Gertsenstein, M. & Nutter, L. M. J. Production of knockout mouse lines with Cas9. *Methods* **191**, 32-43, doi:10.1016/j.ymeth.2021.01.005 (2021).
106 Menzies, C. *et al.* Distinct Basal Metabolism in Three Mouse Models of Neurodevelopmental Disorders. *eNeuro* **8**, doi:10.1523/ENEURO.0292-20.2021 (2021).
107 Sumner, L. W. *et al.* Proposed minimum reporting standards for chemical analysis Chemical Analysis Working Group (CAWG) Metabolomics Standards Initiative (MSI). *Metabolomics* **3**, 211-221, doi:10.1007/s11306-007-0082-2 (2007).
108 Sartain, M. The Agilent Metabolomics Dynamic MRM Database and Method. *Agilent Technologies, Inc.* (2017).
109 Pang, Z. *et al.* MetaboAnalyst 5.0: narrowing the gap between raw spectra and functional insights. *Nucleic Acids Res* **49**, W388-W396, doi:10.1093/nar/gkab382 (2021).
110 Di Guida, R. *et al.* Non-targeted UHPLC-MS metabolomic data processing methods: a comparative investigation of normalisation, missing value imputation, transformation and scaling. *Metabolomics* **12**, 93, doi:10.1007/s11306-016-1030-9 (2016).
111 Berlanga, A., Guiu-Jurado, E., Porras, J. A. & Auguet, T. Molecular pathways in non-alcoholic fatty liver disease. *Clin Exp Gastroenterol* **7**, 221-239, doi:10.2147/CEG.S62831 (2014).
112 Dowman, J. K., Tomlinson, J. W. & Newsome, P. N. Pathogenesis of non-alcoholic fatty liver disease. *QJM* **103**, 71-83, doi:10.1093/qjmed/hcp158 (2010).
113 Gluchowski, N. L., Becuwe, M., Walther, T. C. & Farese, R. V., Jr. Lipid droplets and liver disease: from basic biology to clinical implications. *Nat Rev Gastroenterol Hepatol* **14**, 343-355, doi:10.1038/nrgastro.2017.32 (2017).
114 Cotter, D. G., d'Avignon, D. A., Wentz, A. E., Weber, M. L. & Crawford, P. A. Obligate role for ketone body oxidation in neonatal metabolic homeostasis. *J Biol Chem* **286**, 6902-6910, doi:10.1074/jbc.M110.192369 (2011).
115 Arima, Y. *et al.* Murine neonatal ketogenesis preserves mitochondrial energetics by preventing protein hyperacetylation. *Nat Metab* **3**, 196-210, doi:10.1038/s42255-021-00342-6 (2021).

116 Puisac, B. *et al.* Human Mitochondrial HMG-CoA Synthase Deficiency: Role of Enzyme Dimerization Surface and Characterization of Three New Patients. *Int J Mol Sci* **19**, doi:10.3390/ijms19041010 (2018).
117 Kowalski, G. M. *et al.* Reversing diet-induced metabolic dysregulation by diet switching leads to altered hepatic de novo lipogenesis and glycerolipid synthesis. *Sci Rep* **6**, 27541, doi:10.1038/srep27541 (2016).
118 Vila-Brau, A., De Sousa-Coelho, A. L., Mayordomo, C., Haro, D. & Marrero, P. F. Human HMGCS2 regulates mitochondrial fatty acid oxidation and FGF21 expression in HepG2 cell line. *J Biol Chem* **286**, 20423-20430, doi:10.1074/jbc.M111.235044 (2011).
119 Ding, C. *et al.* A Cell-type-resolved Liver Proteome. *Mol Cell Proteomics* **15**, 3190-3202, doi:10.1074/mcp.M116.060145 (2016).
120 Hoang, N. A. *et al.* Differential capability of metabolic substrates to promote hepatocellular lipid accumulation. *Eur J Nutr* **58**, 3023-3034, doi:10.1007/s00394-018-1847-2 (2019).
121 Wu, S. *et al.* In vitro inhibition of lipid accumulation induced by oleic acid and in vivo pharmacokinetics of chitosan microspheres (CTMS) and chitosan-capsaicin microspheres (CCMS). *Food Nutr Res* **61**, 1331658, doi:10.1080/16546628.2017.1331658 (2017).
122 Lane, A. N. & Fan, T. W. Regulation of mammalian nucleotide metabolism and biosynthesis. *Nucleic Acids Res* **43**, 2466-2485, doi:10.1093/nar/gkv047 (2015).
123 Okabe, K., Yaku, K., Tobe, K. & Nakagawa, T. Implications of altered NAD metabolism in metabolic disorders. *J Biomed Sci* **26**, 34, doi:10.1186/s12929-019-0527-8 (2019).
124 Parry, S. A. & Hodson, L. Influence of dietary macronutrients on liver fat accumulation and metabolism. *J Investig Med* **65**, 1102-1115, doi:10.1136/jim-2017-000524 (2017).
125 Hydes, T., Alam, U. & Cuthbertson, D. J. The Impact of Macronutrient Intake on Non-alcoholic Fatty Liver Disease (NAFLD): Too Much Fat, Too Much Carbohydrate, or Just Too Many Calories? *Front Nutr* **8**, 640557, doi:10.3389/fnut.2021.640557 (2021).
126 Rui, L. Energy metabolism in the liver. *Compr Physiol* **4**, 177-197, doi:10.1002/cphy.c130024 (2014).
127 Geisler, C. E., Hepler, C., Higgins, M. R. & Renquist, B. J. Hepatic adaptations to maintain metabolic homeostasis in response to fasting and refeeding in mice. *Nutr Metab (Lond)* **13**, 62, doi:10.1186/s12986-016-0122-x (2016).
128 McGarry, J. D. & Foster, D. W. The regulation of ketogenesis from octanoic acid. The role of the tricarboxylic acid cycle and fatty acid synthesis. *J Biol Chem* **246**, 1149-1159 (1971).
129 Ontko, J. A. Metabolism of free fatty acids in isolated liver cells. Factors affecting the partition between esterification and oxidation. *J Biol Chem* **247**, 1788-1800 (1972).
130 Van Harken, D. R., Dixon, C. W. & Heimberg, M. Hepatic lipid metabolism in experimental diabetes. V. The effect of concentration of oleate on metabolism of triglycerides and on ketogenesis. *J Biol Chem* **244**, 2278-2285 (1969).
131 Williamson, J. R., Scholz, R. & Browning, E. T. Control mechanisms of gluconeogenesis and ketogenesis. II. Interactions between fatty acid oxidation and the citric acid cycle in perfused rat liver. *J Biol Chem* **244**, 4617-4627 (1969).
132 Satapati, S. *et al.* Elevated TCA cycle function in the pathology of diet-induced hepatic insulin resistance and fatty liver. *J Lipid Res* **53**, 1080-1092, doi:10.1194/jlr.M023382 (2012).

133 Sunny, N. E. *et al.* Progressive adaptation of hepatic ketogenesis in mice fed a high-fat diet. *Am J Physiol Endocrinol Metab* **298**, E1226-1235, doi:10.1152/ajpendo.00033.2010 (2010).
134 Satapati, S. *et al.* Mitochondrial metabolism mediates oxidative stress and inflammation in fatty liver. *J Clin Invest* **125**, 4447-4462, doi:10.1172/JCI82204 (2015).
135 Rescigno, T., Capasso, A. & Tecce, M. F. Involvement of nutrients and nutritional mediators in mitochondrial 3-hydroxy-3-methylglutaryl-CoA synthase gene expression. *J Cell Physiol* **233**, 3306-3314, doi:10.1002/jcp.26177 (2018).
136 Nadal, A., Marrero, P. F. & Haro, D. Down-regulation of the mitochondrial 3-hydroxy-3-methylglutaryl-CoA synthase gene by insulin: the role of the forkhead transcription factor FKHRL1. *Biochem J* **366**, 289-297, doi:10.1042/BJ20020598 (2002).
137 Mannisto, V. T. *et al.* Ketone body production is differentially altered in steatosis and non-alcoholic steatohepatitis in obese humans. *Liver Int* **35**, 1853-1861, doi:10.1111/liv.12769 (2015).
138 Soeters, M. R. *et al.* Effects of insulin on ketogenesis following fasting in lean and obese men. *Obesity (Silver Spring)* **17**, 1326-1331, doi:10.1038/oby.2008.678 (2009).
139 Bickerton, A. S. *et al.* Adipose tissue fatty acid metabolism in insulin-resistant men. *Diabetologia* **51**, 1466-1474, doi:10.1007/s00125-008-1040-x (2008).
140 Vice, E., Privette, J. D., Hickner, R. C. & Barakat, H. A. Ketone body metabolism in lean and obese women. *Metabolism* **54**, 1542-1545, doi:10.1016/j.metabol.2005.05.023 (2005).
141 Gors, S., Kucia, M., Langhammer, M., Junghans, P. & Metges, C. C. Technical note: Milk composition in mice--methodological aspects and effects of mouse strain and lactation day. *J Dairy Sci* **92**, 632-637, doi:10.3168/jds.2008-1563 (2009).
142 Nassir, F., Adewole, O. L., Brunt, E. M. & Abumrad, N. A. CD36 deletion reduces VLDL secretion, modulates liver prostaglandins, and exacerbates hepatic steatosis in ob/ob mice. *J Lipid Res* **54**, 2988-2997, doi:10.1194/jlr.M037812 (2013).
143 Sass, J. O. Inborn errors of ketogenesis and ketone body utilization. *J Inherit Metab Dis* **35**, 23-28, doi:10.1007/s10545-011-9324-6 (2012).
144 Hori, T. *et al.* Inborn errors of ketone body utilization. *Pediatr Int* **57**, 41-48, doi:10.1111/ped.12585 (2015).
145 Grunert, S. C. & Sass, J. O. 3-hydroxy-3-methylglutaryl-coenzyme A lyase deficiency: one disease - many faces. *Orphanet J Rare Dis* **15**, 48, doi:10.1186/s13023-020-1319-7 (2020).
146 Dasouki, M., Buchanan, D., Mercer, N., Gibson, K. M. & Thoene, J. 3-Hydroxy-3-methylglutaric aciduria: response to carnitine therapy and fat and leucine restriction. *J Inherit Metab Dis* **10**, 142-146, doi:10.1007/BF01800039 (1987).
147 Kritzer, A., Tarrant, S., Sussman-Karten, K. & Barbas, K. Use of skimmed breast milk for an infant with a long-chain fatty acid oxidation disorder: A novel therapeutic intervention. *JIMD Rep* **55**, 44-50, doi:10.1002/jmd2.12152 (2020).
148 Ballard, O. & Morrow, A. L. Human milk composition: nutrients and bioactive factors. *Pediatr Clin North Am* **60**, 49-74, doi:10.1016/j.pcl.2012.10.002 (2013).
149 Jackson, B. A., Gregg, B. E., Tutor, S. D., Bermick, J. R. & Stanley, K. P. Human Milk Retains Important Immunologic Properties After Defatting. *JPEN J Parenter Enteral Nutr* **44**, 904-911, doi:10.1002/jpen.1722 (2020).

150 Van Hove, J. L. *et al.* D,L-3-hydroxybutyrate treatment of multiple acyl-CoA dehydrogenase deficiency (MADD). *Lancet* **361**, 1433-1435, doi:10.1016/S0140-6736(03)13105-4 (2003).
151 van Rijt, W. J. *et al.* Efficacy and safety of D,L-3-hydroxybutyrate (D,L-3-HB) treatment in multiple acyl-CoA dehydrogenase deficiency. *Genet Med* **22**, 908-916, doi:10.1038/s41436-019-0739-z (2020).
152 Bhattacharya, K. *et al.* The use of sodium DL-3-Hydroxybutyrate in severe acute neuro-metabolic compromise in patients with inherited ketone body synthetic disorders. *Orphanet J Rare Dis* **15**, 53, doi:10.1186/s13023-020-1316-x (2020).
153 Younossi, Z. M. Non-alcoholic fatty liver disease - A global public health perspective. *J Hepatol* **70**, 531-544, doi:10.1016/j.jhep.2018.10.033 (2019).
154 Bertolotti, M. *et al.* Nonalcoholic fatty liver disease and aging: epidemiology to management. *World J Gastroenterol* **20**, 14185-14204, doi:10.3748/wjg.v20.i39.14185 (2014).
155 Wang, Y. H., Liu, C. L., Chiu, W. C., Twu, Y. C. & Liao, Y. J. HMGCS2 Mediates Ketone Production and Regulates the Proliferation and Metastasis of Hepatocellular Carcinoma. *Cancers (Basel)* **11**, doi:10.3390/cancers11121876 (2019).
156 Ding, R. *et al.* HMGCS2 in metabolic pathways was associated with overall survival in hepatocellular carcinoma: A LASSO-derived study. *Sci Prog* **104**, 368504211031749, doi:10.1177/00368504211031749 (2021).
157 Su, S. G. *et al.* miR-107-mediated decrease of HMGCS2 indicates poor outcomes and promotes cell migration in hepatocellular carcinoma. *Int J Biochem Cell Biol* **91**, 53-59, doi:10.1016/j.biocel.2017.08.016 (2017).
158 Haukeland, J. W. *et al.* Metformin in patients with non-alcoholic fatty liver disease: a randomized, controlled trial. *Scand J Gastroenterol* **44**, 853-860, doi:10.1080/00365520902845268 (2009).
159 Mantovani, A. *et al.* Glucagon-Like Peptide-1 Receptor Agonists for Treatment of Nonalcoholic Fatty Liver Disease and Nonalcoholic Steatohepatitis: An Updated Meta-Analysis of Randomized Controlled Trials. *Metabolites* **11**, doi:10.3390/metabo11020073 (2021).
160 Wang, Y. H., Suk, F. M. & Liao, Y. J. Loss of HMGCS2 Enhances Lipogenesis and Attenuates the Protective Effect of the Ketogenic Diet in Liver Cancer. *Cancers (Basel)* **12**, doi:10.3390/cancers12071797 (2020).
161 Tokutake, Y. *et al.* Effect of diet composition on coenzyme A and its thioester pools in various rat tissues. *Biochem Biophys Res Commun* **423**, 781-784, doi:10.1016/j.bbrc.2012.06.037 (2012).
162 Leonardi, R., Rehg, J. E., Rock, C. O. & Jackowski, S. Pantothenate kinase 1 is required to support the metabolic transition from the fed to the fasted state. *PLoS One* **5**, e11107, doi:10.1371/journal.pone.0011107 (2010).
163 Sunny, N. E., Parks, E. J., Browning, J. D. & Burgess, S. C. Excessive hepatic mitochondrial TCA cycle and gluconeogenesis in humans with nonalcoholic fatty liver disease. *Cell Metab* **14**, 804-810, doi:10.1016/j.cmet.2011.11.004 (2011).
164 Sanyal, A. J. *et al.* Nonalcoholic steatohepatitis: association of insulin resistance and mitochondrial abnormalities. *Gastroenterology* **120**, 1183-1192, doi:10.1053/gast.2001.23256 (2001).
165 Puchalska, P. *et al.* Hepatocyte-Macrophage Acetoacetate Shuttle Protects against Tissue Fibrosis. *Cell Metab* **29**, 383-398 e387, doi:10.1016/j.cmet.2018.10.015 (2019).

166 Stankova, P. *et al.* Western Diet Decreases the Liver Mitochondrial Oxidative Flux of Succinate: Insight from a Murine NAFLD Model. *Int J Mol Sci* **22**, doi:10.3390/ijms22136908 (2021).
167 Stankova, P. *et al.* Adaptation of Mitochondrial Substrate Flux in a Mouse Model of Nonalcoholic Fatty Liver Disease. *Int J Mol Sci* **21**, doi:10.3390/ijms21031101 (2020).
168 Safer, B. The Metabolic Significance of the Malate-Aspartate Cycle in Heart. *Circ Res* **37**, 527-533, doi:10.1161/01.res.37.5.527 (1975).
169 Cappel, D. A. *et al.* Pyruvate-Carboxylase-Mediated Anaplerosis Promotes Antioxidant Capacity by Sustaining TCA Cycle and Redox Metabolism in Liver. *Cell Metab* **29**, 1291-1305 e1298, doi:10.1016/j.cmet.2019.03.014 (2019).
170 Scholz, R. *et al.* The effect of fatty acids on the regulation of pyruvate dehydrogenase in perfused rat liver. *Eur J Biochem* **86**, 519-530, doi:10.1111/j.1432-1033.1978.tb12335.x (1978).
171 Zwiebel, F. M., Schwabe, U., Olson, M. S. & Scholz, R. Role of pyruvate transporter in the regulation of the pyruvate dehydrogenase multienzyme complex in perfused rat liver. *Biochemistry* **21**, 346-353, doi:10.1021/bi00531a023 (1982).
172 Newsholme, P., Stenson, L., Sulvucci, M., Sumayao, R. & Krause, M. in *Comprehensive Biotechnology* 3-14 (2011).
173 Chiang, J. in *Pathobiology of Human Disease* 1770-1782 (2014).
174 Zhang, Y., Baker, S. S., Baker, R. D., Zhu, R. & Zhu, L. Systematic analysis of the gene expression in the livers of nonalcoholic steatohepatitis: implications on potential biomarkers and molecular pathological mechanism. *PLoS One* **7**, e51131, doi:10.1371/journal.pone.0051131 (2012).
175 Lee, D. Y. & Kim, E. H. Therapeutic Effects of Amino Acids in Liver Diseases: Current Studies and Future Perspectives. *J Cancer Prev* **24**, 72-78, doi:10.15430/JCP.2019.24.2.72 (2019).
176 Moreno-Fernandez, M. E. *et al.* Peroxisomal beta-oxidation regulates whole body metabolism, inflammatory vigor, and pathogenesis of nonalcoholic fatty liver disease. *JCI Insight* **3**, doi:10.1172/jci.insight.93626 (2018).
177 Noland, R. C. *et al.* Carnitine insufficiency caused by aging and overnutrition compromises mitochondrial performance and metabolic control. *J Biol Chem* **284**, 22840-22852, doi:10.1074/jbc.M109.032888 (2009).
178 Koves, T. R. *et al.* Mitochondrial overload and incomplete fatty acid oxidation contribute to skeletal muscle insulin resistance. *Cell Metab* **7**, 45-56, doi:10.1016/j.cmet.2007.10.013 (2008).
179 Le, T. T. *et al.* Disruption of uridine homeostasis links liver pyrimidine metabolism to lipid accumulation. *J Lipid Res* **54**, 1044-1057, doi:10.1194/jlr.M034249 (2013).
180 Aichler, M. *et al.* N-acyl Taurines and Acylcarnitines Cause an Imbalance in Insulin Synthesis and Secretion Provoking beta Cell Dysfunction in Type 2 Diabetes. *Cell Metab* **25**, 1334-1347 e1334, doi:10.1016/j.cmet.2017.04.012 (2017).

CONTRIBUTIONS

The following is a detailed list of contributions made by my supervisor, lab members, collaborators, and myself in this project – Thank you all.

I performed H&E and PSR staining and anti-Plin2 immunohistochemistry (**Fig. 3A, Fig. 6D, Fig. 9C, Fig. 10, Fig. 14B, Fig. 17C**), gene expression analysis (**Fig. 4B, Fig. 5C, Fig. 6E, Fig. 7, Fig. 8B, Fig. 11, Fig. 15B-C, Fig. 17D-E, Fig. 18F, Fig. 19B-C**), body weight and body composition measurements (**Fig. 5E, Fig. 8D-F, Fig. 16A-C**), western blot quantification (**Fig. 4C, Fig. 18C**), metabolomics data analysis (**Fig. 20-21, Table 4**), and genotyping of *Hmgcs2*-KO mice (**Fig. 2B**).

Our previous post-doctoral fellow, Dr. Riyoun Kim, performed western blot (**Fig. 5A**); coordinated *in vivo HMGCS2* adenovirus intravenous injection (with the technical support from Dan de Vette at the ACVS); conducted *in vitro HMGCS2* overexpression experiments, including cell culture, virus infection, Oil-red-O staining, and lipid quantification in HepG2 cells (**Fig. 18A, D-E**); and performed plasma β-hydroxybutyrate measurement of *in vivo HMGCS2*-OE (**Fig. 15D**).

Dr. Riyoun Kim and I performed liver tissue extraction for metabolomics study (**Fig. 20-21, Table 4**).

Dr. Kyoung-Han Kim conducted metabolic measurements of *Hmgcs2*-HET mice (**Fig. 12-13**) and body weight and composition measurements of p14 *Hmgcs2*-KO mice (**Fig. 5F**).

Dr. Kyoung-Han Kim and I performed glucose/ketone measurements (**Fig. 3B-C, Fig. 5D, Fig. 8C**) and tissue collection (**Fig. 6A-C, Fig. Fig. 9A-B**).

Dr. Kyoung-Han Kim, Dr. Riyoun Kim and I performed GTT/ITTs and tissue collections of *HMGCS2*-OE mice (**Fig. 16D-E, Fig. 17A-B**).

Thet Fatica, our laboratory technician, performed western blots (**Fig. 4C, Fig. 18C**).

David Patten and Shama Naz, from the University of Ottawa Metabolomics Core Facility, performed LC-MS metabolomics quantification of liver metabolites. Using the raw data, I performed multivariate statistical analysis, generating a PLS-DA scores plot, heatmap, and quantitative pathway enrichment dot plot (**Fig. 20**).

Xiaoling Zhao, a histopathology technologist at the University of Ottawa Heart Institute, performed all liver tissue processing and assisted in the training of histological experiments including immunohistochemistry protocol optimization.

Dr. Kyoung-Han Kim generated the C57BL/6NCrl-*Hmgcs2*$^{em1(IMPC)Tcp}$/Cmmr mice with the support from The Canadian Mouse Mutant Repository at The Centre for Phenogenomics.

SHAZA ASIF

EDUCATIONAL BACKGROUND

University of Ottawa, Ottawa, ON, Canada *2019 – Present*
M.Sc. in Cellular and Molecular Medicine (CMM)

University of Ottawa, Ottawa, ON, Canada *2017 – 2019*
Honour's B.Sc. in Translational and Molecular Medicine (TMM)

University of Ottawa, Ottawa, ON, Canada *2015 – 2017*
Honour's B.Sc. in Biomedical Science

Bell High School, Ottawa, ON, Canada *2011 – 2015*
Ontario Secondary School Degree

SCHOLARSHIPS & AWARDS

Scholarships

- **Queen Elizabeth II Graduate Scholarship in Science and Technology (QEII-GSST),** University of Ottawa ($15, 000 /year). Jan 2021 – Present.
- **Excellence Scholarship MSc**, University of Ottawa ($2,500 /term). May 2020 –Present.
- **Frederick Banting and Charles Best Canada Graduate Scholarship-Master's (CGS M)**, University of Ottawa ($17, 500 /year). May – Dec 2020.
- **Admission Scholarship MSc**, University of Ottawa ($2,500 /term). Sept 2019 – April 2020.
- **Merit Scholarship**, University of Ottawa ($2,000). 2018 – 2019.
- **Admission Scholarship BSc**, University of Ottawa ($4,500). 2017 – 2019.
- **Work in Biomedical Research (WIBR) Scholarship**, University of Ottawa ($7,500) May – Aug 2018.

Awards

- **Trainee Recognition Award**, University of Ottawa Heart Institute (UOHI). Dec 2020.
- **Award of Excellence in Graduate Studies,** Cellular and Molecular Medicine (CMM), University of Ottawa ($250). Dec 2020.
- **University of Ottawa Journal of Medicine (UOJM) Reviewer Award**, University of Ottawa ($100). June 2020.
- **Honourable Mention,** CMM Seminar Day, University of Ottawa ($100). Feb 2020.
- **Honourable Mention**, UOHI Summer Student Research Day. July 2019.
- **Dean's Honour List**, University of Ottawa. 2017 – 2019.
- **Honor Roll Society**, Bell High School. 2011 – 2015.
- **Academic Excellence in Science**, Bell High School. 2012 – 2013.
- **Silver Medal in Academic Excellence**, Bell High School. 2011 – 2013.

JOURNAL PUBLICATIONS

- **Asif S**, Kim RY, Kim KH. *Sex-dependent and independent effects of intermittent fasting against diet-induced obesity and fatty liver diseases* (in preparation).
- ***Asif S**, *Kim RY, Fatica T, Naz S, Zhao X, Patten D, Mulvihill EE**,** Kim KH. *The role of Hmgcs2-mediated ketogenesis in the development of non-alcoholic fatty liver disease* (submitted to *Molecular Metabolism*).
- ***Asif S**, *Morrow M, Mulvihill E, Kim KH. *Understanding Dietary Intervention-Mediated Epigenetic Modifications in Metabolic Diseases.* Frontiers in Genetics. 2020 Oct 15. https://doi.org/10.3389/fgene.2020.590369

**Indicates equal author contribution*

CONFERENCE PUBLICATIONS

- ***Asif S**, *Kim R, Kim KH. *Understanding the role of ketogenesis in NAFLD development and treatment.* **University of Ottawa Faculty of Medicine Research Day 2021.** September 2021 (*poster presentation*).
- ***Asif S**, Kim R, Kim KH. *Investigating the role of ketogenesis in NAFLD development and treatment.* **2021 Ottawa Cardiovascular Research Day.** May 2021 (*poster presentation*).
- ***Asif S**, *Kim R, Kim KH. *Investigating the metabolic benefits of intermittent fasting-induced ketogenesis in a non-alcoholic fatty liver disease mouse model.* **2020 Canadian Vascular and Lipid Summit**. October 16, 2020 (*selected for oral presentation*).
- ***Asif S**, Kim R, Oh Y, Kim KH. *Delineating the role of Ankrd11 in the development of patent ductus arteriosus through the use of novel mouse models of KBG syndrome.* **2020 Ottawa Cardiovascular Research Day.** May 2020 (*selected for poster presentation*).
- ***Asif S**, *Kim R, Kim KH. *Investigating the metabolic benefits of intermittent fasting-induced ketogenesis in a non-alcoholic fatty liver disease model.* **CMM Poster Day**. February 25, 2020 (***Honourable mention**, seminar presentation*).
- ***Asif S**, *Kim R, Kim KH. *Investigating the metabolic benefits of intermittent fasting-induced ketogenesis in a NAFLD model.* **CMM Seminar Day**. May 5, 2020 (*poster presentation*).
- **Asif S**, Kim R, Oh Y, Kim KH. *Cardiac-specific Ankrd11-KO as a novel mouse model of patent ductus arteriosus in KBG syndrome*. **CMM/NSC Research Day.** October 24, 2019 *(rapid fire presentation).*
- **Asif S**, Kim R, Oh Y, Kim KH. *Cardiac-specific Ankrd11-KO as a novel mouse model of patent ductus arteriosus in KBG syndrome*. **Southern Ontario Cardiovascular Research Association (SOCRA) 2nd Annual Conference.** October 18, 2019 *(poster presentation).*
- **Asif S**, Kim R, Oh Y, Kim KH. *Cardiac-specific Ankrd11 knockout mice present with patent ductus arteriosus*. **1st Annual Faculty of Medicine Research Day.** September 25, 2019 *(poster presentation).*
- **Asif S**, Kim R, Oh Y, Kim KH. *Cardiac-specific Ankrd11 knockout mice present with patent ductus arteriosus*. **UOHI Summer Student Research Day (SSRD).** July 26, 2019 *(**Honourable mention**, seminar presentation).*

- **Asif S**, Kim R, Oh Y, Kim KH. *Investigating a phenotype associated with KBG syndrome using Ankrd11 loss-of-function mouse models*. **2nd- Annual TMM Honours Seminar Symposium.** Mar 29, 2019 *(seminar presentation).*
- **Asif S**, Kim R, Oh Y, Kim KH. *Novel mouse model of patent ductus arteriosus in KBG syndrome using Ankrd11 cardiac-specific knockout*. **2nd- Annual TMM Honours Poster Symposium.** Jan 11, 2019 *(poster presentation)*.
- **Asif S,** Mak-Washburn E, Robichaud S, Ouimet M. *Determining the role of ORP6 in cholesterol homeostasis of the brain.* **2nd- Annual TMM Rotation Seminar Symposium.** April 11, 2018 *(seminar presentation).*
- **Asif S**, Parent S, Davis DR. *Human explant-derived cardiac stem cells genetically engineered to over-expression of KCNN4 on myocardial function after ischemic injury.* **2nd-Annual TMM Rotation Poster Symposium.** Feb 16, 2018 *(poster presentation).*

**Indicates equal author contribution*

RESEARCH EXPERIENCE

Graduate research student *May 2019 – Present*

- *Functional Genetics and Metabolism Laboratory, University of Ottawa Heart Institute*
- Supervisor: Dr. Kyoung-Han Kim
- Project: Investigating ketogenesis in the development and treatment of non-alcoholic fatty liver disease (NAFLD)

- Examining genetic mouse models of fatty liver disease development and treatment (i.e., whole-body CRISPR/Cas9 gene knockout and adenovirus overexpression)
- Maintaining mouse colonies (i.e., setting up breeding, checking plugs, genotyping, and weaning litters)
- Monitoring gross metabolic changes in mice through regular body weight, food intake and body composition measurements
- Performing glucose and insulin tolerance tests for determination of glucose homeostasis in mice
- Collecting and processing mouse metabolic tissues (i.e., adipose, liver, heart, pancreas) for molecular analysis
- Utilizing molecular (i.e., qPCR, western blots) and metabolomic techniques to understand differences in gene and protein expression and metabolite levels in mice
- Performing histological analysis of mouse liver tissue through Haematoxylin & Eosin (H&E), picrosirius red (PSR), and immunohistochemical staining methods
- Presented project findings at local (i.e., Ottawa Cardiovascular Research Day) and national (i.e., Canadian Vascular and Lipid Summit) conference(s)

Undergraduate research student *May 2018 – April 2019*

- *Functional Genetics and Metabolism Laboratory, University of Ottawa Heart Institute*
- Supervisor: Dr. Kyoung-Han Kim
- Project: Investigating the role of transcription factor Ankrd11 in the development of cardiac and skeletal symptoms of KBG syndrome

- Established genetic mouse models of KBG syndrome and cell-lineage tracing (i.e., cardiac and neural crest cell-specific conditional gene knockout utilizing Cre/lox system)

- Setup timed matings for collection of embryos (E) and postnatal (P) mice at different developmental timepoints (i.e., E10.5-E18.5, P0-P5)
- Validated mouse models through molecular techniques (i.e., epifluorescent microscope imaging, genotyping, qPCR)
- Performed echocardiographic and histological analysis (i.e., H&E staining) to investigate cardiac function and structure, respectively, in mice
- Performed phenotypic analysis for determination of skeletal deformities (i.e., skeletal measurements and staining with alizarin red and alcian blue dye) in mice
- Presented project findings in poster(s), oral seminar(s) and thesis report

Undergraduate research student *February – March 2018*
- *Cardiovascular Metabolism and Cell Biology Laboratory, University of Ottawa Heart Institute*
- Supervisor: Dr. Mireille Ouimet
- Research Project: Investigating the role of ORP6 in cholesterol homeostasis of the brain
    - Extracted and quantified the mRNA expression of ORP6 in brain tissue and microglia and astroglia cell lines through molecular techniques (i.e., qPCR, gel electrophoresis)
    - Presented project findings at the University of Ottawa TMM Rotation Seminar Symposium

Undergraduate research student *January – February 2018*
- *Cardiac Translational Research Laboratory, University of Ottawa Heart Institute*
- Supervisor: Dr. Darryl Davis
- Research Project: Investigating the effects of KCNN4-overexpression in cardiac stem cells on post-myocardial infarction cardiac regeneration
    - Performed immunohistochemical analysis for detection of neo-vascularization within myocardial infarct region of KCNN4-treated mice
    - Quantified percent viable tissue within risk region of Masson-trichrome stained heart sections of KCNN4-treated mice
    - Presented project findings at the University of Ottawa TMM Rotation Poster Symposium

SUPERVISORY/TRAINING EXPERIENCE

Hyejin Lee *January 2021 – Present*
Research student, University of Ottawa Heart Institute
- Techniques: Metabolic tissue (i.e., adipose, liver, kidney) collection and fixation, paraffin embedding and sectioning of metabolic tissue and embryos, and Haematoxylin & Eosin staining.

Shruthi Karthikeyan *January – February 2020*
Undergraduate research student, University of Ottawa
- Project: Investigating Ankrd11 in cardiovascular development using a novel mouse model of KBG Syndrome
- Techniques: Embryo and postnatal mouse collection, paraffin embedding and sectioning, Haematoxylin & Eosin staining, ZEISS epifluorescent microscope imaging
- Presented project findings at the University of Ottawa TMM Rotation Poster Symposium

Elayna Tian *May – August 2019*
Summer research student, University of Ottawa

- Project: Investigating the metabolic effects of intermittent fasting between males and females
- Techniques: Body weight, food intake, and body composition measurement of mice. Paraffin embedding and sectioning of mouse metabolic tissues (i.e., liver, adipose tissue).
- Presented project findings in an oral seminar at the University of Ottawa Heart Institute Summer Student Research Day (SSRD)

RESEARCH TECHNIQUES

- **Molecular and biochemical techniques:** DNA/RNA isolation, PCR, qPCR, western blot, immunostaining
- **Histological techniques:** paraffin embedding and sectioning tissue (i.e., liver, heart, embryo), Hematoxylin & Eosin staining, PSR staining, ZEISS epifluorescent microscope imaging
- **Metabolic study techniques:** glucose and insulin tolerance tests (GTT/ITT), EchoMRI, CLAMS metabolic cage
- **Other:** echocardiography, embryo collection, skeletal staining (alizarin red, alcian blue), mouse colony management (i.e., genotyping, weaning)

ACADEMIC ACTIVITIES

Section Editor, *University of Ottawa Journal of Medicine (UOJM)* *Oct 2019 – Aug 2021*

- Performed an initial review of submitted manuscripts to assess eligibility
- Assigned manuscript revision from 2-3 reviewers
- Compiled revisions, made final decisions regarding submission and conveyed feedback and decision with the author
- Participated as a reviewer of 6 submissions for the UOJM National Commentaries Contest
- Received **UOJM Reviewer Award 2020**

LTS Volunteer, *Let's Talk Science Outreach, Ottawa, Canada* *Sept 2017 – June 2021*

- Visited elementary classrooms (Grade 1 & 3, ~20-25 students) in-person and/or virtual to deliver curriculum-aligned hands-on science activities/workshops for students
- Helped students to develop an interest in the field of science by sharing career options and opportunities in STEM
- Evaluated and judged student grant applications for the Ottawa Science Innovation Challenge (OSIC)

UOHI laboratory activity, *LTS Encounters with Canada* *Oct. 23rd, 2019*

- Presented to a group of 20 high school students (Grade 11-12) on the topic of embryonic development
- Prepared and lead a hands-on-activity in which students rotated stations to view embryos at different developmental timepoints
- Answered any questions pertaining to the topic and my research

Promotional Coordinator, *TMM Student Association* *Sept 2018 – April 2019*

- Organized and arranged for fundraising and promotional events
- Designed and marketed apparel and other promotional material
- Created and designed promotional posters

Student Mentor, *TMM Mentoring Program* *Sept 2018 – April 2019*

- Guided the mentee through the TMM Program
- Provided practical experience and advice to the mentee
- Assisted the mentee in discovering research and networking opportunities and exploring future career choices

IgNITE Science Case Competition Mentor, *University of Ottawa* *Feb 2019*

- Mentored students by providing direction and support in their project
- Organized workshops to assist in project planning and presentation
- Revised and edited the work of the mentees

NON-ACADEMIC ACTIVITIES

Project Manager, *Empower'em, Ottawa, Canada* *Sept 2018 – Present*

- Plan and coordinate events centered around empowering women of colour (WOC)
- **'Our Way Forward' mentorship program (January – May 2021)**: A mentorship program designed for WOC to build confidence in their personal and/or professional areas of life. Created information document, mentee and mentor application forms, newsletter, workbook for mentees, guidebook for mentors, and feedback surveys. Interviewed potential mentors and mentees and finalized 10 mentor/mentee pairs for pilot program.
- **'Happy HERlidays' donation drive (December 2018):** A women's donation drive for the holidays. Collected donation items (i.e., woman hygiene products, socks) from university campus, workplaces, community centres and acquaintances for St. Joe's Women's Centre.

Pharmacy Assistant
Shoppers Drug Mart, Ottawa, ON, Canada *July 2013 – July 2020*

- Entered and dispensed prescriptions according to physician-prescribed instructions
- Applied insurance plans and dealt with drug coverage-related problems
- Maintained on-shelf medicinal inventory and managed expired medications for disposal
- Completed administrative duties including faxing refill requests, filing documents, answering patient calls, and placing drug orders

Volunteer, *Queensway Carleton Hospital, Ottawa, Canada* *June 2013 – May 2019*

- **Information Desk**: Directed patients and visitors to various hospital facilities and departments as well as answered questions regarding patient room inquiries
- **Surgical Inpatient Units**: Provided refreshments and company to patients as well as assisted hospital staff in minor errands
- **Infection Prevention and Control (IPAC)**: Conducted direct observation of hand hygiene practices as a hand hygiene auditor using electronic CKM auditing tool
- **Gift Shop**: Maintained store inventory and managed cash register